INVESTIGATION ON FLOW CHARACTERISTICS OF JETS EMANATING FROM ROUND AND RECTANGULAR NOZZLES WITH AND WITHOUT BEVEL

A THESIS

Submitted by

SANDHYA M.

for the award of the degree

of

DOCTOR OF PHILOSOPHY

DIVISION OF MECHANICAL ENGINEERING
SCHOOL OF ENGINEERING
COCHIN UNIVERSITY OF SCIENCE AND TECHNOLOGY, KOCHI

DECEMBER 2017

DIVISION OF MECHANICAL ENGINEERING
SCHOOL OF ENGINEERING
COCHIN UNIVERSITY OF SCIENCE AND TECHNOLOGY

CERTIFICATE

This is to certify that the work presented in this thesis entitled **"Investigation on Flow Characteristics of Jets Emanating from Round and Rectangular Nozzles with and without Bevel"** is based on the authentic record of research done by **Sandhya M** under my guidance towards the partial fulfilment of the requirements for the award of the degree of **Doctor of Philosophy** of the Cochin University of Science and Technology and has not been included in any other thesis submitted for the award of any degree.

Dr. Tide P. S.
(Supervising Guide)
Professor
Division of Mechanical Engineering
School of Engineering
Cochin University of Science and Technology

DIVISION OF MECHANICAL ENGINEERING
SCHOOL OF ENGINEERING
COCHIN UNIVERSITY OF SCIENCE AND TECHNOLOGY

CERTIFICATE

This is to certify that all the relevant corrections and modifications suggested by the audience during the pre-synopsis seminar and recommended by the Doctoral Committee of Sandhya **M** have been incorporated in the thesis entitled **"Investigation on Flow Characteristics of Jets Emanating from Round and Rectangular Nozzles with and without Bevel".**

Dr. Tide P. S.
(Supervising Guide)
Professor
Division of Mechanical Engineering
School of Engineering
Cochin University of Science and Technology

DECLARATION

I hereby declare that the work presented in this thesis entitled **"Investigation on Flow Characteristics of Jets Emanating from Round and Rectangular Nozzles with and without Bevel"** is based on the original research work carried out by me under the supervision and guidance of **Dr. Tide P. S.**, Professor, Division of Mechanical Engineering, School of Engineering, Cochin University of Science and Technology, Kochi-22 and has not been included in any other thesis submitted previously for the award of any degree.

Kochi   **Sandhya M.**
20th December 2017

ACKNOWLEDGMENT

ABSTRACT

A major contributor of noise pollution near airports during take-off is the propelling jet. The mixing of jet flow with the ambient air creates a noisy turbulent flow. The turbulent structures responsible for the noise can be evaluated numerically by RANS calculations together with standard turbulence models. Numerical investigation of compressible subsonic jets emanating from new designs in the nozzle geometry intended to reduce the noise level were performed by employing RANS model as it is capable of accounting for the subtle effects of design innovations on the turbulent structures responsible for noise generation.

Numerical simulations of a turbulent compressible subsonic jet from round and bevelled nozzles were carried out using commercial CFD software. The Mach number at exit for the above nozzles was 0.75. Simulations were performed in a three dimensional computational domain using steady RANS equations and SST k-ω turbulence model. Default values for all model constants and second order accurate discretization for all variables were used. The computational domain was discretized using hexahedral / tetrahedral mesh with approximately 2 million cells. The flow was investigated for axial and radial profiles of velocity components, shear layer thickness, self preserving nature, turbulent intensity, turbulent viscosity and Reynolds's stresses. The bevelled nozzle was found to attain self similarity beyond an axial distance equal to four times the diameter of the jet. The results were found to be in reasonable agreement with the available experimental data in the literature. It was observed that the bevelling of nozzle can significantly change both flow pattern and turbulence structures of the jet and thus considered as an efficient passive method for jet noise reduction.

Rectangular turbulent jets have been investigated more extensively than any other non circular jets over the past few decades. As compared to axi-symmetric nozzles, rectangular nozzle geometries are more beneficial to noise reduction by enhanced mixing. Numerical simulations of turbulent compressible subsonic jet from baseline rectangular nozzles with aspect ratios of 2:1, 4:1, 8:1 and its bevelled nozzles of two bevel length ratios were carried out using steady RANS equations and SST k-ω turbulence model. The Mach number at exit for the above nozzles was 0.9. Simulations were performed in a three dimensional computational domain. A hybrid mesh with approximately 2.5 million hexahedral / tetrahedral cells was used to discretize the computational domain. The flow was investigated for the velocity fields, mean and variance of axial velocity, the jet spread rate, boundary layer characteristics at the nozzle exit and jet core turbulence. The impact of aspect ratio and bevel length on these parameters was analyzed. The results were found to be in reasonable agreement with the available experimental data in the literature. It was observed that both aspect ratio and bevel length ratio have significant effects on jet entrainment, mixing and turbulence production. Acoustic calculations were performed using FW-H acoustic analogy after computing the acoustic source data obtained from the unsteady RANS calculations. The pressure fluctuations were determined for all forward and aft receivers (30° to 150°) which were located outside the computational domain. The acoustic predictions show that rectangular bevel nozzles have better acoustic benefit when compared with plain round and rectangular nozzles.

CONTENTS

LIST OF TABLES

LIST OF FIGURES

LIST OF ABBREVIATIONS

AR	Aspect Ratio
ASM	Algebraic Stress Model
BLR	Bevel Length Ratio
CAA	Computational Aero Acoustics
CD	Convergent Divergent
CFD	Computational Fluid Dynamics
DES	Detached Eddy Simulation
DNS	Direct Numerical Simulation
DSM	Dynamic Smagorinski Model
ERN	Extensible Rectangular Nozzle
FFT	Fast Fourier Transform
FWH	Ffowcs Williams- Hawkings
LES	Large Eddy Simulation
NPR	Nozzle Pressure Ratio
OASPL	Overall Sound Pressure Level
PIV	Particle Image Velocimetry
RANS	Reynolds Averaged Navier-Stokes
RSM	Reynolds Stress Model
SGS	Subgrid Scale
SPL	Sound Pressure Level
SST	Shear Stress Transport
URANS	Unsteady Reynolds Averaged Navier-Stokes

NOMENCLATURE

a_∞	Ambient Speed of sound
D_j	Equivalent diameter of jet
e	Energy
h	Short dimension of rectangular nozzle
H	Shape factor
k	Kinetic energy
L	Length of bevel beyond exit of plain nozzle
M_a	Acoustic Mach number
p	Pressure
p_∞	Ambient pressure
Re_D	Jet Reynolds number
r	Radial coordinates
t	Time
T_j	Jet static temperature (ideally expanded)
T_{0j}	Jet stagnation temperature
T_∞	Ambient temperature
u, v, w	Velocity components in Cartesian coordinates
u', v', w'	Fluctuating velocity components in Cartesian coordinates
U_j	Jet exit velocity (ideally expanded)
U_∞	Free stream velocity
U_c	Mean stream wise velocity along the centreline
U_0	Mean stream wise velocity at the centre of nozzle exit
u_i	Cartesian components of velocity vector
uu	Mean square of fluctuating velocity (variance of axial component of velocity)for rectangular nozzle.

vv	Mean square of fluctuating velocity (variance of radial component of velocity) for rectangular nozzle
$\overline{u'u'}$.	Mean square of fluctuating velocity (variance of axial component of velocity)for round and bevel nozzle
$\overline{v'v'}$	Mean square of fluctuating velocity (variance of radial component of velocity)for round and bevel nozzle
x_i	Cartesian coordinate vector component
x_0	Virtual origin
$y_{0.5}$	Jet half width for round and bevel nozzle.
y	Radial distance measured along the Y axis
$Y_{1/2}$	Jet half width for rectangular nozzle in the XY plane
$Z_{1/2}$	Jet half width for rectangular nozzle in the XZ plane
ρ	Density
μ	Dynamic viscosity
μ_t	Turbulent viscosity
δ_{ij}	Kronecker delta
δ	Displacement thickness
θ	Momentum thickness
τ	Shear stress
v	Kinematic viscosity
ω	Specific rate of dissipation of turbulent kinetic energy.

CHAPTER - 1

INTRODUCTION

1.1   MOTIVATION

Environmental concerns and stringent noise regulations in the vicinity of airports have made 'the suppression of jet noise and its prediction' a subject of ongoing intensive research. Jet noise is one of the major concerns, especially when aircrafts are taking off with maximum thrust. At take-off, the main sources of noise are the propelling jet and the engine fan, of which the jet exhaust is usually the strongest noise source at full power. Jet mixing noise in aircrafts can cause permanent hearing damage to human ear. The flow field and hence the noise generation is dominated entirely by turbulent mixing in the case of ideally expanded subsonic and supersonic axi-symmetric jets. Investigations on both the mean flow and turbulent characteristics of jet are highly significant as they play a vital role in the jet noise predictions.

As such, jet flow properties are difficult to measure or predict analytically. The fluctuating quantities can be determined experimentally, but highly expensive and time consuming. Difficulty in the prediction of the effect of turbulence is due to the wide range of length and time scales of motion even in flows with very simple boundary conditions. Modelling of the noise sources need tremendous details of the jet flow characteristics. Numerical simulation of low speed jets using standard turbulence models provide better knowledge on the flow field which is essential for the computation of jet mixing noise. New designs in nozzle geometries such as plain round nozzles with bevel and chevrons, noncircular nozzles such as elliptical, triangular, square, and rectangular nozzles at different nozzle conditions such as Mach

number, temperature, Reynolds's number, nozzle diameter, bevel angle, aspect ratio etc., which improve the turbulent characteristics of the jet were widely emerged. These configurations were seen to alter the jet mixing noise significantly and hence accepted as techniques for jet noise reduction in aircrafts for the last few decades.

Among the different methods employed by researchers to calculate the flow field and the radiated sound of jets emanating from nozzles, LES appears to be the most preferred one. Although LES predictions are quite accurate for simple geometries with proper grid resolution, it is computationally very expensive. The new designs in the nozzle geometry intended to reduce the noise level from the jet can more easily be evaluated using computationally less expensive RANS simulation. Even though RANS methods could only provide time-averaged turbulent information, it can capture the trends exhibited by experiments reasonably well, while altering the geometry or flow conditions. The flow and turbulent characteristics of the jet using unsteady RANS calculations may be used to model the acoustic sources and predict noise by enabling acoustic analogy.

Current jet noise research highlights on three main areas like improvement in noise prediction tools, the better understanding of the primary noise generating mechanisms and noise reduction devices like chevrons, bevel nozzles, lobed mixers, micro jets etc. The Computational Aero Acoustic (CAA) methods demand for extreme numerical accuracy and high computational resources for the accurate prediction of noise. Even though LES meets the accuracy requirement for jet noise prediction, it requires higher order numerical schemes and high resolution mesh which do not lend themselves well to complicated grid topologies. To evaluate the performance of new concepts a more reliable method for modelling the source mechanism is essential.

Demand for noise reduction in jets from plain circular nozzle brought the idea of bevelled nozzles. The circular nozzle is bevelled at an angle to give an inclination to the jet axis in the upward direction so that the noise footprints on the ground can be reduced. It was experimentally proved that bevelled nozzle produce same or greater absolute thrust than the round nozzle. The bevelled nozzles specifically reduce the noise in the peak polar radiation angles and the maximum noise benefit is observed in the azimuthal direction of the longer lip (Viswanathan and Czech, 2011). Bevel angle is another design parameter as the extent of sound reduction in a bevel nozzle depends on the inclination of the jet. Jet flow with different bevel angles was simulated by earlier researchers (Rice and Raman (1993), Viswanathan *et al*. (2005), Viswanathan *et al*. (2008)) and it was observed that bevelling the jet by 20° offered better acoustic benefit. Numerical simulation of a jet emanating from bevelled nozzle using RANS calculations with a standard turbulence model can provide reasonably accurate flow field data for better acoustic prediction. This enables the designers to compare the acoustic benefits of various bevelled nozzle configurations with respect to the baseline round nozzle. The influence of various design parameters on the flow field and the noise generation can also be analyzed with limited computational resources. The complex interactions between azimuthal and stream wise vortices resulted in increased entrainment characteristics and better fine-scale mixing of noncircular jets compared to the round nozzle of the same nozzle exit area and the rectangular jets were proved to be the best (Mi *et al*., 2000). Nozzle aspect ratio is a significant parameter as it strongly influences the dimensionality of the velocity fields of jets issuing from rectangular nozzles. The major drawback with the rectangular nozzle design was losses found in the subsonic internal flow transition from a circular to a rectangular profile. The transition from a circular to a rectangular cross-section upstream of the nozzle exit plane has a great role in the character of the vortical

structures generated in the corners of the rectangular flow-path. This problem was resolved in the Extensible Rectangular Nozzle (*ERN*) model system in which the flow transition ducts have been designed for transition from round piping to a rectangular cross-section using flat wrap methodology to minimize the flow non uniformities at the nozzle exit (Frate and Bridges, 2011). Extensible rectangular nozzles (both plain rectangular and rectangular nozzle with bevel) of aspect ratio 2, 4 and 8 were constructed and tested for acoustic measurements by Bridges (2012). Bridges and Wernet (2015) experimentally investigated above nozzles for mean and turbulent flow characteristics. Particle Image Velocimetry (PIV) measurement data were reported in a view for the researchers to validate the predictions of their numerical calculations and also to prepare the database for the development of acoustic prediction codes. The present research basically focuses on aerodynamic and aero-acoustic characteristics of jets emanating from rectangular nozzles with and without bevel.

1.2   OBJECTIVES OF THE STUDY

The main objectives of the work can be summarized as follows:

1. To perform computational studies of the aerodynamics of compressible subsonic jet emanating from a plain round nozzle and to validate the RANS simulation with the experimental data reported in literature.

2. To conduct numerical simulation for circular bevelled nozzle and to investigate the flow characteristics such as the axial and radial velocity variation along centreline/rake, shear layer thickness, self preserving nature, turbulent intensity, turbulent viscosity and Reynolds's stresses of the emanating jet and to compare the predictions with that of the plain round nozzle.

3. To perform numerical simulations of plain rectangular nozzles for different Aspect Ratios and to study the variation of mean and variance of axial velocity along the centreline and also along the major and minor axis lip lines of the rectangular nozzles and then to compare the results with the experimental data reported in the literature.

4. To carry out numerical simulations of rectangular bevelled nozzles for different Aspect Ratios and Bevel Length Ratios and to analyze the variation of mean and variance of axial velocity.

5. To investigate the flow characteristics like Jet spread rate, Exit boundary layer characteristics and Jet core turbulence for both rectangular plain and bevel nozzles.

6. To perform Aero-Acoustic calculations for determining the Overall Sound Pressure Level (OASPL) and compare the acoustic benefit attained for Round and Rectangular nozzles with and without bevel.

1.3 THESIS OUTLINE

Chapter 1 discusses with the background and motivation of the present work. Current status of researches in the field of computational aerodynamics and aeroacoustics are described briefly and finally the objectives of the present work are outlined.

A detailed review of the available literature on experimental and numerical investigation of compressible subsonic jet for the jet aerodynamics and aeroacoustics is presented in Chapter 2.The review is based on different parameters such as

configurations of the nozzle geometry, Reynold's number, temperature of the jet, and the simulation method used etc.

Chapter 3 describes the turbulent jet flows and turbulent free jets from round and rectangular nozzles. Both the mean and turbulent flow characteristics of a turbulent free jet are explained.

Numerical modelling is explained in Chapter 4, starting from the governing equation, turbulence modelling and finally the aeroacoustic modelling.

The computational procedure like domain and mesh, boundary conditions, the numerical scheme etc. are explained in Chapter 5.

The flow characteristics obtained from the numerical simulation of round and bevel nozzle and also rectangular and rectangular bevel nozzle are presented in Chapter 6 and 7 respectively.

Chapter 8 presents the overall conclusion and also the scope for future work.

CHAPTER - 2

LITERATURE REVIEW

Aircraft noise is a serious environmental concern for people living in the vicinity of the airports. The dominant source of aircraft noise especially during takeoff is the propelling jet. Jet mixing noise in aircrafts can cause permanent hearing damage to human ear. The reduction of jet noise has become a topic of ongoing intense research due to stringent noise regulations around airports. A review of the available literature on experimental and numerical investigation of compressible subsonic jet for the jet aerodynamics and aeroacoustics is presented in this chapter. The review is based on different parameters like the inflow and boundary conditions, the simulation method used etc.

The field of aeroacoustics have begun with the first theory on jet noise by Sir James Ligthill (Lighthill, 1952). This theory was developed to predict the intensity of noise produced by turbulent jets. To describe the acoustic waves, Lighthill reformulated the equations of fluid motion as a wave equation and is now referred to as Lighthill's acoustic analogy. An experimental investigation to establish the relationship between instability waves and jet noise was conducted by Moore (1977). It was observed that the instability waves were not a direct source of noise but in a subsonic jet it modifies the downstream turbulence. Thus it was concluded that the accurate prediction of downstream turbulence could lead to an accurate jet noise model. Then the focus of research had been placed on flow characteristics that are directly influencing the jet flow development and mixing process and thereby the jet noise produced. This was possible either through changing the nozzle conditions or by influencing the instability waves in the shear layer. Boersma *et al*. (1998) confirmed

that altering the nozzle condition can not only control the mixing region but can influence the turbulent properties downstream of the initial mixing region. Thus new concepts and designs in the nozzle geometry were established as methods for jet noise reduction.

Computational aeroacoustics (CAA) has undergone spectacular progress with the rapid development of computer resources during the last three decades. Direct Numerical Simulation (DNS), Large Eddy Simulation (LES) and Unsteady RANS simulations are the simulation methods generally used in computational aeroacoustics. In these methods, the acoustic information can be obtained directly by solving the compressible flow equations or in a secondary step. Various methods like FW-H analogy (Di Francescantonio, 1997; Ffowcs Williams and Hawkings, 1969) and the Kirchoff formulation (Lyrintzis, 1994) have been developed for compressible simulations which extend the acoustic waves outside the simulation domain. Several numerical studies have been carried out in Computational Aero Acoustics (CAA) to investigate the sound radiated from a jet with different initial conditions like nozzle geometries, Reynold's number, temperature conditions etc.

2.1   NOZZLE CONFIGURATIONS

Many of the previous works show that the jet mixing aero dynamics is highly dependent on the nozzle exit shape (Ho and Gutmark, 1987; Gutmark *et al*., 1989; Hussain and Husain, 1989; Quinn, 1989; Miller *et al*., 1995). Devices like chevrons, bevel nozzles, lobed mixers, micro jets etc. has been established as a method for jet noise reduction since last few decades. The complex interactions between azimuthal and stream wise vortices resulted in increased entrainment characteristics and better fine-scale mixing of noncircular jets compared to the round nozzle of the same nozzle

exit area (Mi *et al.*, 2000). By altering the mean and turbulent flow characteristics through the variation in nozzle geometries a reduction in jet noise can be achieved. In the subsequent subsections, the review on the compressible jet flow based on the shape of the jet at the nozzle exit is analysed for the following nozzles.

- Round nozzle
- Circular bevelled nozzle
- Noncircular nozzles
- Rectangular plain nozzle
- Rectangular bevelled nozzle

2.1.1 Round Nozzle

Anderson *et al.* (2003, 2005) investigated the flow field and the radiated sound of an isothermal Mach 0.75 compressible jet with Reynolds number 50000 using Large Eddy Simulation and Kirchhoff surface integration. The Favre filtered Navier Stokes Equations were solved using cell centred finite volume method solver. For the solution of convective fluxes a low dissipation third order upwind scheme and for the viscous fluxes, a second order centred difference approach was applied. A three stage second order Runge-Kutta method was used for time marching. The sub grid scale stresses were computed using Smagorinsky's sub grid scale model. The computational domain contained boundary fitted block structured mesh with a total of 3 million cells. At the inlet of the nozzle, total pressure and total enthalpy were specified and at outlet static pressure was specified. At all free boundaries, absorbing boundary conditions were used. Sound pressure levels in the far-field were evaluated with a hybrid approach. Kirchhoff surface integration was utilized for the propagation of sound to far-field locations. Instantaneous pressure on the Kirchhoff surface obtained from the LES predicted sound pressure levels which were in excellent agreement with

measured values. The aerodynamic results and the sound pressure levels were validated against the experimental data reported by Jordan *et al*. (2002) and were found in good agreement except for the initial jet spreading and the potential core length.

Large Eddy Simulation of two compressible jets, one an isothermal jet and other a hot jet were carried out by Anderson *et al*. (2004) for a Mach number of 0.75. It was found that heating of the jets results in a higher mixing and hence a shorter potential core region. Heated jet was found to be narrower than the isothermal jet. The aerodynamic results and the sound pressure levels were validated against the experimental data reported by Jordan *et al*. (2002, 2003). Initial jet spreading and potential core length were not predicted correctly owing to the presence of coarse region in the nozzle outlet. A higher Sound Pressure Level (SPL) was obtained with heated jet in both experimental and numerical work. However, the increase was not sufficient to make any conclusion regarding the relation between the temperature ratio and SPL.

Boersma and Lele (1999) carried out the Large Eddy Simulation of a compressible 0.9 Mach jet, one at a moderate Reynolds number 36×10^3 and other at a high Reynolds number 100×10^3. They used a model based on the Boussinesq hypothesis. Navier-Stokes equations were rewritten in a cylindrical coordinate system, with x, r, and θ as the axial, radial, and azimuthal coordinate directions, respectively. In the numerical scheme used, spatial derivatives in axial and radial direction were taken with 6th order compact finite differences. In the azimuthal direction a Fourier method with approximate idealising was used. The time integration was carried out with a fourth order Runge-Kutta scheme. The number of grid points used in

simulations for moderate Reynolds numbers was less when compared to the fine grids employed for high Reynolds numbers. The centre line velocity, axial velocity, Reynolds stresses, potential core, density profiles, time series of pressure and power spectra were analysed in these range of Reynolds number.

Bogey *et al.* (2003) carried out a three-dimensional circular jet simulation with a Mach number of 0.9 and Reynolds number of 65000 using LES to study both flow field and acoustic radiation. The validation of the computation is then carried out by comparing both flow properties and the radiated sound field with experimental data available in the literature. The full three-dimensional Navier-Stokes equations written in a conservative form were solved. To compute sound wave with more accuracy a low dispersive and low dissipative numerical algorithm was used. To accommodate different discretization in the flow field and in the acoustic far field a Cartesian and non-uniform mesh was used. Though Large Eddy Simulation (LES) can be performed for simulating flows at higher Reynolds number, by computing only the larger scales and by taking into account the effects of unresolved ones through a sub grid scale model, the Smagorinsky model was applied to make the problem simpler. The physical part of the computational domain was extended axially up to 20 times the radius of the jet for the flow field, and up to 30 times radius for the acoustic field. The computational domain was discretized with varying mesh sizes, minimum near to the centreline and increasing in the radially outward direction. The simulated flow field showed that the potential core length obtained was consistent with the experimental value. Flow properties, namely flow development, mean flow parameters and turbulent intensities, were in good agreement with measurements. The sound field provided by LES compared well with experimental results in terms of directivity,

spectra and levels. The sound sources in the jet were found around the end of the potential core and were similar to the experimental observations.

Most of the experimental studies on the influence of initial conditions on the jet flow have been conducted for jets with Reynolds numbers about $10^5 < Re_D < 5 \times 10^5$. In this range, the exit shear layer is expected to be transitional, but the use of tripping devices in the nozzle can make it go fully turbulent. Bogey and Bailly (2005) investigated the effect of inflow conditions on the flow development and sound field of 0.9 Mach circular jet with Reynolds number 4×10^5. The investigated parameters were the forcing amplitude, the initial shear-layer thickness and the use of the first four azimuthal modes when synthesizing the forcing disturbances. The filtered compressible Navier–Stokes equations were solved using highly accurate numerical schemes with low dispersion and low dissipation properties. A 13-point finite difference scheme was used for spatial discretization, whereas an explicit six-stage Runge–Kutta algorithm was applied for time integration. The mean profiles of velocities, pressure, and density were imposed at the inflow boundary. Both the flow development and the emitted sound were shown to depend appreciably on the initial parameters chosen to model the inflow of the transitional jet.

Bodony and Lele (2004, 2005) performed Large Eddy Simulation of three cold and hot jets ($T_j / T_\infty = 1.8$, 2.3 and 2.7) at Mach numbers 0.5, 0.9 and 1.5. In the first part of calculation a near-field large-eddy simulation that captures the sound-generating turbulent field and the radiated noise, and in the second part a region that continues the radiated sound to distances far away from the jet plume was adopted. The azimuthal derivatives were evaluated using Fourier bases. The acoustic far field was related to the near field through a Kirchhoff surface in the form of a right circular

cylinder that encloses the jet. Pressure fluctuations on the surface of the cylinder were collected as functions of time and of the axial and azimuthal directions. Predictions of flow parameter were found to be in good agreement with experimental data. The ability of LES to accurately predict the radiated sound was found to be strongly dependent on the jet operating conditions. The noise from the heated jet simulations were found to be over-predicted and the unheated jet sound predictions were in better agreement with the experimental data.

A high order accurate three dimensional LES code was developed and tested by Uzun *et al.* (2003) utilizing a robust dynamic subgrid-scale (SGS) model for a turbulent isothermal jet at a Reynolds number 10^5. A sponge zone that was attached downstream of the physical domain, damps out the disturbances before the spurious waves reach the outflow boundary. To predict the far field noise accurately they coupled the near field data provided by LES with the Ffowcs Williams-Hawkings method for computing noise propagation to the far field. Favre-filtered unsteady, compressible, non-dimensionalized Navier-Stokes equations formulated in curvilinear coordinates were solved. To compute the spatial derivatives at interior grid points away from the boundaries, a non-dissipative sixth-order compact scheme was employed. Implicit spatial filtering was employed to get rid of the high frequency oscillations resulting from the unresolved scales. The mean flow parameters calculated were found to be in good agreement with the experimental results.

Lew *et al.* (2005) carried out 3D Large Eddy Simulation of two turbulent hot jets with temperature ratios T_j/T_1=1.76 and T_j/T_1=2.70. The 3D LES code used in this study was dynamic Smagorinsky (DSM) subgrid-scale model. The unsteady, Favre-

filtered, compressible, non-dimensional LES equations were solved. In order to eliminate numerical instabilities that can arise from the boundary conditions, the sixth-order tri-diagonal spatial filter and for time advancement, the explicit fourth-order Runge-Kutta scheme was used. LES methodology was applied at a fixed ambient Mach number of *M*= 0.9 for jet noise prediction without any heating. To study the far-field noise, the porous Ffowcs Williams-Hawkings (FWH) surface integral acoustic formulation was employed. Single point statistics such as jet growth rates, centreline decay and turbulence intensities compared reasonably well with experimental data.

Bogey *et al*. (2007) experimentally investigated a round, isothermal and cold jet of diameter 38 mm and Mach number between 0.6 to 1.6 and $Re_D \geq 5 \times 10^5$. Properties of near-field jet noise particularly at 7.5 diameters from the jet centre line were documented which differ appreciably from properties of far-field noise. The results were presented to form a database that can be used for the validation of the acoustic fields determined numerically by compressible Navier-Stokes computations.

Tide and Babu (2009*a*) performed an unsteady RANS simulation with the Shear Stress Transport (SST *k-ω*) model for cold and hot jets. Nozzle of 50 mm diameter was used to study the baseline round configuration and 6 lobed chevron configurations with 0^0 and 5^0 taper angles along the nozzle edge. The computational domain used for the three-dimensional simulation was 180^0 semi-circular cross section. The domain extended $50D_j$ downstream of the nozzle exit, $10D_j$ at inlet, $20D_j$ at outlet and the length of the buffer zone was $40D_j$. Favre averaged Navier–Stokes equations along with the SST *k–ω* turbulence model equations were solved. The nozzle inlet was modelled as a pressure inlet with static and stagnation pressure

specified. The rest of the domain inlet and the upper semi-circular entrainment surface were modelled as pressure inlets at the ambient pressure and temperature. The domain outlet was taken to be a pressure outlet at the ambient pressure. The bottom boundary was treated as a symmetry surface. All solid surfaces were treated as adiabatic surfaces and standard wall functions were used. It was found that heating of the jets results in a higher mixing and hence a shorter potential core region. Heated jet was found to be narrower than the isothermal jet. Comparison of mean actual velocity and fluctuating components showed good agreement with the LES results.

The effect of chevrons on noise was also investigated by Tide and Babu (2009*b*) for *M*=0.75 hot and cold jets. Noise predictions using unsteady RANS calculation was improved by applying periodic boundary conditions and improving the near wall resolution. The 3D calculations were carried out on a hexahedral mesh with 1.1 million cells in a 30°pie sector for the baseline round nozzle. Hybrid meshes of 1.5 million cells were used for simulations with chevron lobes in a view to keep the wall *y*+ less than 10. Overall sound pressure levels at far-field observer locations were calculated using Ffowcs Williams-Hawkings equation. Numerical prediction of stagnation pressure, stagnation temperature, turbulent kinetic energy and 90°observer spectral trends were compared with experimental data.

Freund *et al.* (2001) computed the mean flow development and the radiated sound of a 0.9 Mach circular jet by using DNS. Karabasov *et al.*(2010) developed a hybrid methodology for jet noise prediction using optimised modelling and numerical techniques. Acoustic propagation wa**s** modelled by solution of a system of adjoint Linear Euler Equations, capturing convective and refraction effects using a spatially developing jet mean flow provided by a RANS CFD solution. Goldstein's acoustic

analogy, including a Gaussian function model for the two-point cross-correlation of the fourth-order velocity fluctuations in the acoustic source was used for modelling sound generation.

Uzun and Hussaini (2010) carried out LES for a round nozzle with overset grid capability to compute the jet flow in detail and the effect of inflow conditions on the jet flow field and far field noise. Simulation of a baseline round nozzle for the flow inside the nozzle and the free jet flow outside were performed simultaneously by a high-order accurate, multi-block, large eddy simulation (LES) code with overset grid capability. For the round nozzle jet the governing equations were solved on a very fine mesh with approximately 370 million grid points.

2.1.2 Circular Bevelled Nozzle

New designs on the baseline round nozzle configuration were evaluated experimentally and numerically after analysing the thrust penalty, noise generation, suppression and propagation coupled with these nozzle profiles (Figure 2.1). Viswanathan *et al*. (2005) simulated the flow field and the noise generated by round and bevelled nozzles (45^0 and 33^0). Results from both RANS and LES computations were presented. The aerodynamic predictions from RANS were in good agreement with experimental measurements. Paliath and Morris (2005) presented the jet noise prediction from a circular bevelled nozzle using Detached Eddy Simulation (DES). DES allows a transition from URANS to LES. Viswanathan *et al.* (2008) carried out simulations of the flow field and noise of single and staggered dual, round, and bevelled nozzles with the goal of gaining insights into the flow features that are responsible for noise generation. The geometry of the nozzles must be satisfactory, for both aerodynamic and acoustic performance, especially for propulsive devices. A

two-step Reynolds Averaged Navier Stokes/Large Eddy Simulation methodology was developed and applied to several nozzle geometries, allowing a new level of complexity in the geometry. The predictions of the gross thrust by RANS computations were in good agreement with experimental measurements. The spectral predictions from LES were also in good agreement with measured data, for a wide range of jet conditions. The measured azimuthal variations in the noise field from bevelled nozzles were reproduced by LES.

Tide and Srinivasan (2009*c*) conducted experimental study on bevelled nozzle and measured the overall sound pressure level, acoustic spectra and directivity over a range of nozzle pressure ratio from 1.5 to 5. To assess the effects of geometric variations on jet plume evolution and radiated noise in dual stream nozzles, (Viswanathan *et al.,* 2012) performed a joint computational and experimental program with different combinations of primary and secondary nozzle geometries like round and bevelled and their modifications. Rice and Raman (1993) experimentally investigated a supersonic jet issued from a series of both convergent and convergent divergent nozzles with single bevel, double bevel and without bevel. They performed experiments to study the effect of nozzle exit geometry on jet noise and found that all bevelled geometries exhibited a screech noise reduction for under expended jets and for the double bevelled C-D nozzle a significant reduction in noise was observed when operating at design conditions.
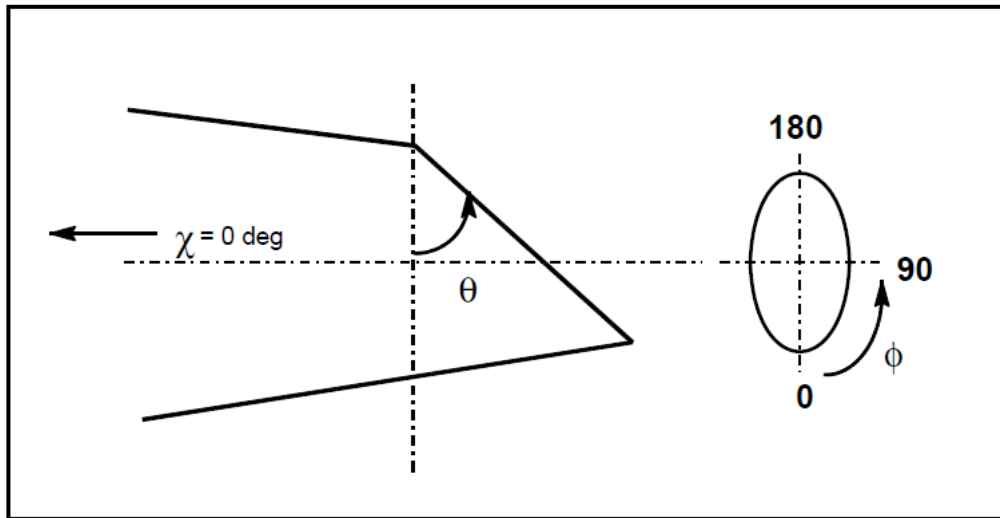
Fig. 2.1　　Conceptual sketch of a bevelled nozzle and the　measurement convention for polar angle (χ), bevel angle(θ) and the azimuthal angle (ϕ) (Viswanathan and Czech, 2011)

2.1.3　Non Circular Nozzles

More extensive research have been proceeding on noncircular jets for the past few decades due to their potential to provide increased mixing rates relative to the circular jet. Experimental study on the spreading characteristics of free jets from various asymmetric nozzles was conducted by Zaman (1996*a*). The results were compared with that of a circular nozzle. The nozzles included in the comparative study are shown in Figure 2.2.
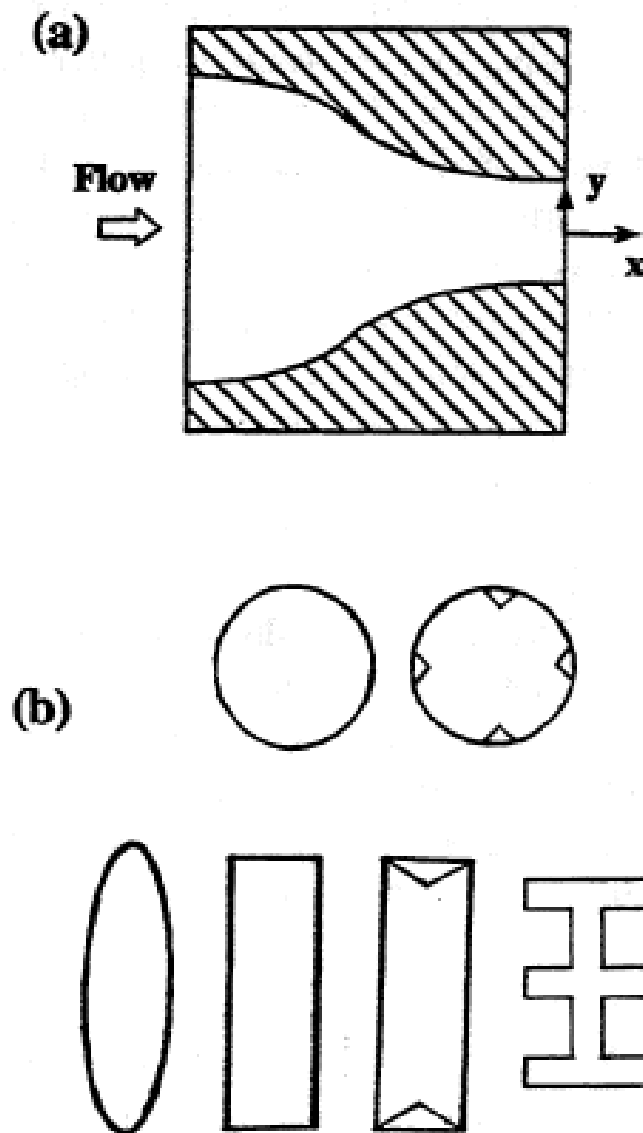
Fig. 2.2 Schematics of (a) Nozzle interior and (b) Nozzle
exit shapes. Source: Zaman(1996*a*)
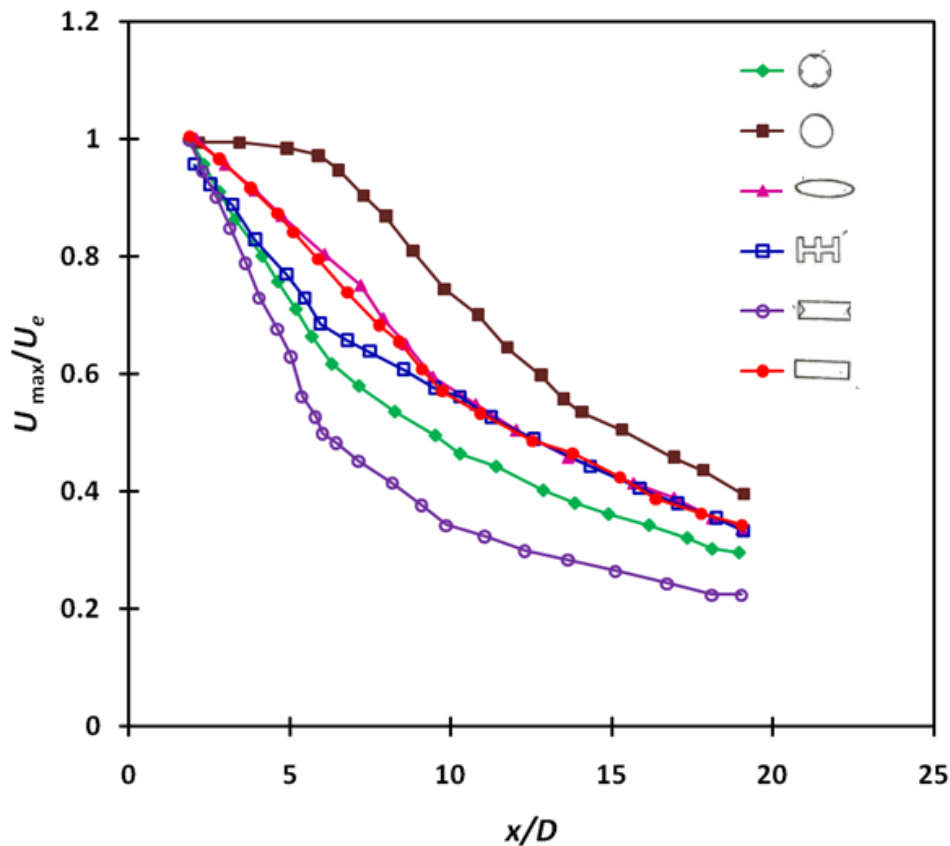
Fig. 2.3   Stream wise variation of maximum mean velocity with different nozzle exit shapes (Source: Zaman, 1996*a*)

The study involved circular, rectangular and elliptic nozzles, rectangular nozzle fitted with two tabs on the narrow edges and the circular nozzle fitted with four equally spaced tabs. Measurements covered incompressible subsonic conditions to under expanded supersonic conditions up to a jet Mach number of 1.96. The spreading of the asymmetric jets was found to be marginally higher than that of the circular jet at subsonic conditions. However, it was found to be significantly higher at supersonic conditions during screech. Jet spreading for the two tab configuration was found to be the largest among all the cases for both subsonic and supersonic regimes. The stream wise variation of maximum velocity for the different nozzles at the subsonic conditions is shown in Figure 2.3. The velocity decay was found to be the fastest for the rectangular jet with two tabs and the slowest for the circular jet without tabs.

Gutmark and Grinstein (1999) reviewed the experimental, theoretical, and numerical results obtained for flow field and the mechanisms of jet flow development in non circular jets. The effects of geometrical configurations such as the nozzle eccentricity in elliptic and rectangular jets, sharp corners of rectangular and triangular jets and axial vorticity generators at nozzle exit in circular and non circular jets were investigated. Several issues related to axis switching and the variation of the shear layer spreading rate in the azimuthal direction and turbulence production were commonly established to all noncircular shapes. The complex interactions between azimuthal and streamwise vortices resulted in increased entrainment characteristics and better fine-scale mixing of noncircular jets.

Mi *et al.* (2000) investigated centre line mean flow and turbulence characteristics of different jets issuing from different nozzle types (i.e. circular, elliptical, triangular, square, rectangular, cross-shaped and star-shaped) as shown in Figure 2.4. The study was conducted to establish the true influence of jet exit shape. The centreline velocities in nine jets issuing from differently shaped nozzles were measured using identical facilities and nominally identical experimental conditions. The experimental results of centreline variation of maximum velocity for all the nozzles were plotted as shown in Figure 2.5. As compared to axi-symmetric nozzles, rectangular nozzle geometries are more beneficial to noise reduction due to enhanced mixing. Increased mixing levels for the noncircular nozzle configurations were observed, particularly for the triangular and rectangular shapes.
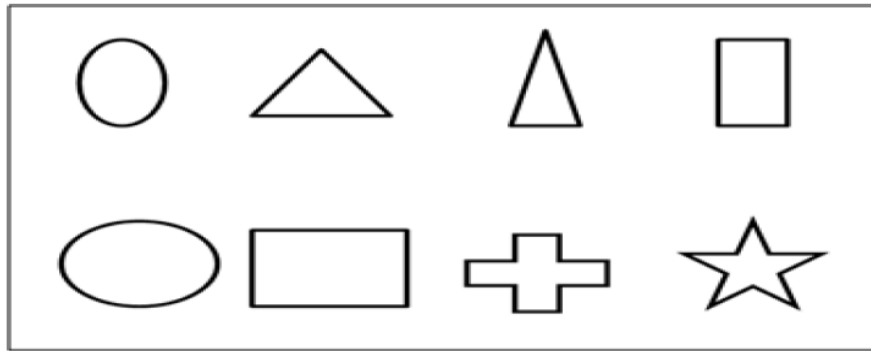
Fig. 2.4 Orifice shapes used by Mi*et al.* (2000)
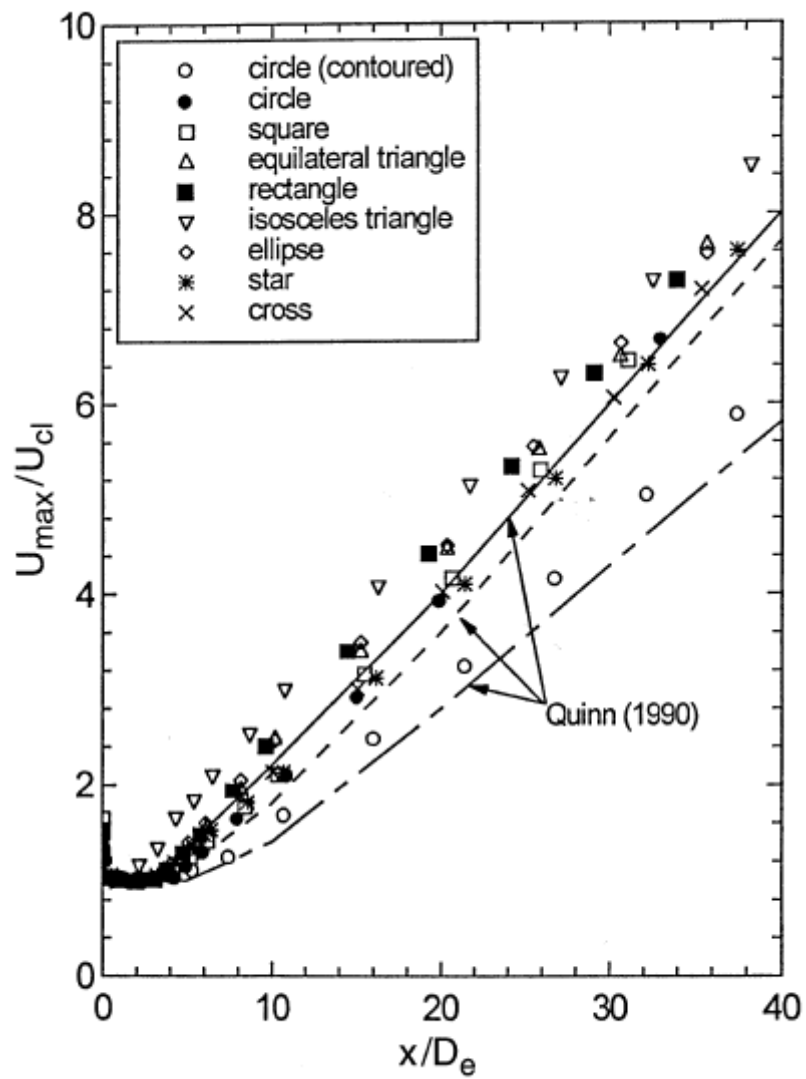
Fig. 2.5   Centre line variation of maximum mean velocity (Mi *et al.*, 2000)

Kim and Park (2013) carried out numerical simulation of circular, square and triangular jet to investigate the effect of non circular inlets on the flow structures in turbulent jets using Reynolds Stress Model. The variation of jet half-width, vorticity thickness and secondary flows for non-circular jets were compared with that of a circular jet. The parameters like jet half-width and vorticity thickness of noncircular jets were reported to develop much faster than that of a circular jet.

2.1.4 Rectangular Plain Nozzle

Experimental investigations on jets emanating from two types of rectangular nozzles (rectangular slot with sharp edge and rectangular channel) were conducted by Sfeir (1979). The mean and turbulent flow field characteristics of the jet issuing from rectangular channel were having a two dimensional region which extended further downstream when compared to the other jet. Mi *et al*. (2004) carried out an experimental study of jets issuing from a circular and a notched rectangular orifice with same opening areas. The near-field mixing characteristics showed that the notched jet entrains the ambient fluid at a higher rate than the circular jet and hence it decays and spreads faster yielding a shorter potential core. In the case of notched jet, the phenomenon of axis switching occurs at an axial distance approximately equal to 3.15 times the equivalent diameter of the jet. 'Axis-switching' is the exchange of orientation of major and minor axes of the jet plume from the original nozzle orientation as the plume develops downstream.

Krothapalli *et al*. (1980) experimentally investigated a rectangular jet ($AR = 16.7$) and an array of rectangular jets equally spaced with 8 times the smaller dimension of the lobe. The mean and turbulent flow characteristics of the jet with a mean velocity of 60 m/s at the nozzle exit and Reynolds number equal to 1.2×10^4

based on the width of the lobe were studied. In the case of a single rectangular jet, the flow was characterized by the presence of three distinct regions. These regions were the potential core region, a two-dimensional type region, and an axisymmetric region. In the case of array of rectangular jets, the mutual interaction between the jets results in a lower turbulence level when compared to a single jet at corresponding locations. Nozzle aspect ratio is an important parameter that strongly influences the dimensionality of the velocity fields of jets issuing from rectangular nozzles (Mi *et al.,* 2005). Significant information on the effects of nozzle aspect ratio on downstream development was reported for turbulent jets issuing from rectangular nozzles.

Krothapalli *et al*. (1981) measured mean velocities and turbulent shear stresses of a low subsonic rectangular jet emanating from nozzles with Aspect Ratio (*AR*) between 5.5 and 16.7. It was reported that for nozzles with *AR* less than 10, no two dimensional plane jet region was identified and the initial decay rate was dependent on nozzle geometry. The appearance of saddle-shaped major axis profiles was seen to be related to the three dimensional vortex rings shed from the nozzle lip.

Gurunath *et al*. (2014) conducted a computational study on a low speed rectangular jet to investigate the effects of jet mixing, jet decay and jet spread. The numerical simulation of the jet was performed with cross section as 20×120 mm at the exit, velocity of the jet as 50 m/s and Reynolds number based on the nozzle width as 45000. Velocity profiles of rectangular jet were compared with that of a circular jet and a 4.3% increase in jet decay at an axial distance of eight times the equivalent diameter was observed.

Von Glahn (1989) developed a numerical model for a jet from a rectangular nozzle to predict the axial and transverse velocity characteristics and the model was demonstrated for a subsonic cold jet from a rectangular nozzle with *AR* 6. Empirical correlations were developed for plume axial velocity decay and transverse spreading in static conditions. The axial distance from the nozzle exit to transform the jet plume cross section from rectangular to circular is modelled in terms of the nozzle aspect ratio and the jet flow conditions.

Vouros *et al*. (2014) conducted an experimental study on the three dimensional development of a jet emanating from a sharp edged rectangular orifice with aspect ratio 10:1. Two special features of rectangular jet like the saddle back mean and axial velocity profile and the dumb bell shaped velocity contours were considered for further analysis. The vorticity distribution in the transverse plane of the jet was found to scientifically influence the saddleback shape, while the dumbbell was explained by the two terms in the axial mean vorticity transport equation that diffuse fluid from the centre of the jet towards its periphery. The flow field was seen to resemble an axisymmetric jet beyond an axial distance of 30 times slot width from the jet exit. Uchiyama *et al*. (2013) carried out a computational study on a jet issuing from a rectangular nozzle with *AR* of 15. Direct numerical simulation using vortex in cell method was employed for the numerical calculation of mean and turbulent flow characteristics of the jet. The DNS results were found successfully agreeing with the experimental values. Numerical investigation on supersonic jet from CD nozzles with rectangular exit geometry with different aspect ratios was carried out by Kumaraswamy *et al*. (2015). The study was conducted in under expanded and over expanded conditions to determine how aspect ratio of a rectangular cross section

influences the jet mixing and jet spread characteristics. The results showed that as the aspect ratio of rectangular nozzle increases, the static pressure and the rate of total pressure decay increases resulting in decreasing shock strength which in turn increases jet mixing and reduces noise.

Computational results of acoustic prediction using Large Eddy Simulation of a jet issuing from a rectangular nozzle with aspect ratio 1:5 were presented by Rembold and Kleiser (2004). Using the Lighthill's acoustic analogy the role of the spurious waves and deconvolution in the far-field noise was examined and it was concluded that the LES based acoustic prediction is accurate only up to an estimated cut off frequency. Experimental study was conducted by Tsuchiya and Horikoshi (1986) on rectangular jets from nozzles with different aspect ratio of 5 and less. The study was concentrated to see the influence of nozzle exit geometry, aspect ratio and Reynolds number on the flow field near the nozzle exit. The stream-wise turbulent intensity was seen to be significantly influenced by the above parameters.

Sundararaj and Elangovan (2013) numerically investigated the effect of internal grooves on rectangular nozzles on the jet flow development. The computational study was carried out on a nozzle with square grooves of 4 mm side and 5 mm axial depth cut in different orientations like on major axis only, on minor axis only and on both major and minor axis. The grooves had no influence on the jet growth within the potential core region. A decrease in the jet centreline velocity decay and thereby a reduction in the jet mixing was found due to the presence of grooves. However, grooves had significant influence on jet decay in the far field and negligible effect on the near field.

Alnahhal and Panidis (2009, 2011) experimentally investigated the influence of sidewalls, endplates and both sidewalls and end plates in a rectangular nozzle of *AR*=15 on the turbulent jet flow field. An increase of the mean stream wise velocity at the edge of the jet was observed in the presence of the sidewalls but no effect with the end plates. The presence of endplate and sidewalls resulted in the highest decay rates at all Reynolds number tested and was found to strongly affect the turbulent field of the rectangular jet at *Re*=20,000. Behrouzi and McGuirk (2015) studied experimentally the effect of an aft deck in the lower wall of a high aspect ratio rectangular nozzle on supersonic jet plume behaviour. The aft deck created asymmetry in the entrainment characteristics within the shear layers and also induced a net transverse pressure force on the plume by altering the inviscid shock cell structure. The net pressure force exerted on the jet is altered by the aft-deck surface and lead to upward or downward transverse deflection of the jet depending on NPR. The separation and reattachment of the plume from the aft deck wall was observed for sufficiently high NPR, and a sufficiently long aft-deck. The addition of an aft deck reduced turbulence levels in the plume near field with extended potential core.

2.1.5   Rectangular Bevelled Nozzle

Aiming improved nozzle performance and reduced acoustic emissions Frate and Bridges (2011) introduced a new rectangular nozzle design called Extensible Rectangular Nozzle (*ERN*) model system. They have created 3D fabrication ready computer solid models for a family of rectangular convergent nozzles like the baseline round nozzle, chevron, bevel, side wall cutback/extended edge and chevron combination nozzles. All these nozzle geometries were designed for an equivalent diameter 2.13" and three aspect ratios say 2, 4, and 8. The transition from a circular to

a rectangular cross-section upstream of the nozzle exit plane has a great role in the character of the vortical structures generated in the corners of the rectangular flow path. An optimum design of the nozzle should minimize losses found in the subsonic internal flow transition from a circular to a rectangular profile. In *ERN* model, the flow transition ducts have been designed to transition from round piping to a rectangular cross-section using flat wrap methodology to minimize the flow non uniformities at the nozzle exit.
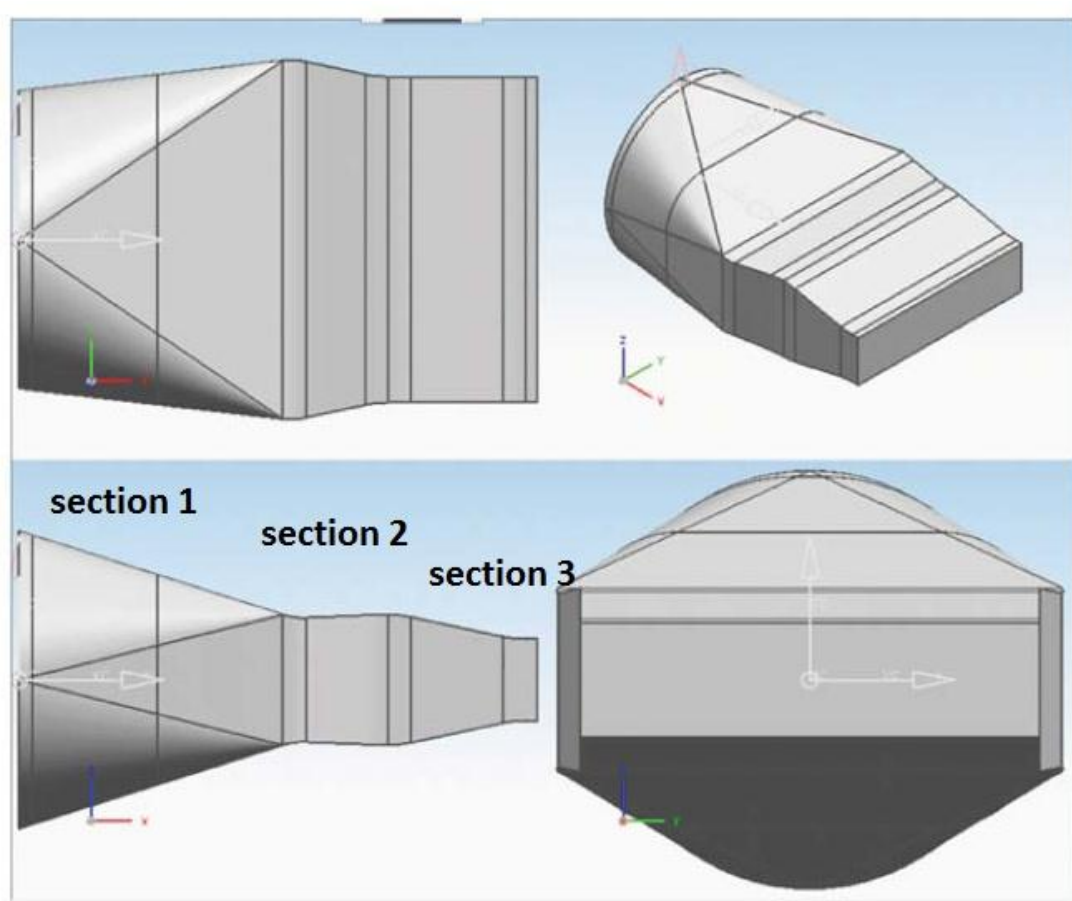
Fig. 2.6   Sectional view of rectangular nozzle geometry with AR = 4
            Source: Frate and Bridges, (2011)

A sectioned view of extensible rectangular nozzle with aspect ratio 4 from Frate and Bridges (2011) is shown in Figure 2.6. From the circular pipe subsonic inflow to the choked rectangular nozzle exit was divided into three sections.

- Section 1: Flow area is decreased using flat-wrap methodology, from a circular to a rectangular cross-section.

- Section 2: Rectangular flow area is decreased using constant minor axis while sidewalls approach centre-plane. Interface plane is at the end of section 2.

- Section 3: Rectangular flow area is decreased using constant major axis while moving top/bottom walls in, towards the centre-plane to a final area where top/bottom walls become parallel to the flow direction as well.

Extensible rectangular nozzles (both base line and bevel) of aspect ratio 2, 4 and 8 were constructed and tested for acoustic measurements by Bridges (2012).The experiments were conducted in a high subsonic flow condition and the results were compared with that of a round nozzle (2" diameter) which was also constructed and tested under the same conditions. With increase in aspect ratio, a reduction in the peak aft noise and an increase in high frequency noise in the broader side of the nozzle was observed. Azimuthally, noise reduction was observed on the narrow side of the nozzle and an increase on the wide side. With extended bevel length, the noise increased everywhere. Bridges (2014) carried out testing of the acoustic impact of the aft deck surface of rectangular nozzles with aspect ratio 2, 4 and 8 and compared the results with that of bevelled rectangular nozzles. Noise increased with deck length in the case of nozzle with aft deck whereas it increased with increasing aspect ratio for bevelled nozzle.

Bridges (2015) conducted acoustic measurements of rectangular nozzle with aspect ratio 8 and its variations in geometry such as bevel, slants, single board chevrons and notches in a high subsonic flow regime. The bevel nozzle increased the noise in all directions whereas the slant caused less increase in noise compared to bevel and the increase was only in the direction of longer side. A single chevron with zero penetration to the wide edge of the rectangular nozzle made no acoustic impact whereas inverting the chevron to create a single wide notch on the broad side of the nozzle increased the noise by several dB. However, adding internal vanes to the rectangular nozzle produced a reduction in noise at low frequencies, along with a directional shedding tone off at the trailing edges. Bridges and Wernet (2015) experimentally investigated a set of Extensible Rectangular Nozzles (*ERN*) with aspect ratio 2, 4 and 8 for the mean and turbulent flow characteristics. Particle Image Velocimetry (PIV) measurement data were documented for the velocity fields, mean and variance, from the round, rectangular, and bevelled rectangular nozzles of equivalent jet diameter 2.14" at high subsonic speeds of   M = 0.9. Bevelled rectangular nozzles were characterised by triangular side walls formed by extending the lower lip of the rectangular nozzles and the sides aligned by the minor axis meeting this lip for all the three aspect ratios. The extension length (*L*) of the lower edge of the bevelled nozzles was made in increments to the shorter dimension (*h*) of the rectangular nozzle. The design features of plain and rectangular bevel nozzles are shown in Figure 2.7. All three components of the turbulence, their relationships and distributions were also presented for rectangular nozzles and contrasted with the same measurements in a round jet. It was concluded that on increasing the aspect ratio, turbulence and mixing is increased and thereby the length of the potential core is decreased. The anisotropy in turbulence was found to be concentrated mainly in the

minor axis causing an azimuthal dependence in noise production. The PIV data were presented to validate the results of numerical models which may be useful in the development of acoustic prediction codes.

Basic nozzle, 2:1, 1.34"x2.68"	NA2Z	
Basic nozzle, 4:1, 0.948"x3.79"	NA4Z	
Basic nozzle, 8:1, 0.671"x5.36"	NA8Z	
Bevel nozzle, 2:1, 1.3" ext (L/h = 1) (L/D_j = 0.625)	NA2B1	
Bevel nozzle, 2:1, 2.7" ext (L/h = 2) (L/D_j = 1.25)	NA2B2	
Bevel nozzle, 4:1, 1.3" ext (L/h = 1.4) (L/D_j = 0.625)	NA4B1	
Bevel nozzle, 4:1, 2.7" ext (L/h = 2.8) (L/D_j = 1.25)	NA4B2	
Bevel nozzle, 8:1, 1.3" ext (L/h = 2) (L/D_j = 0.625)	NA8B1	
Bevel nozzle, 8:1, 2.7" ext (L/h = 4) (L/D_j = 1.25)	NA8B2	
Round nozzle, 5° contraction	SMC000	
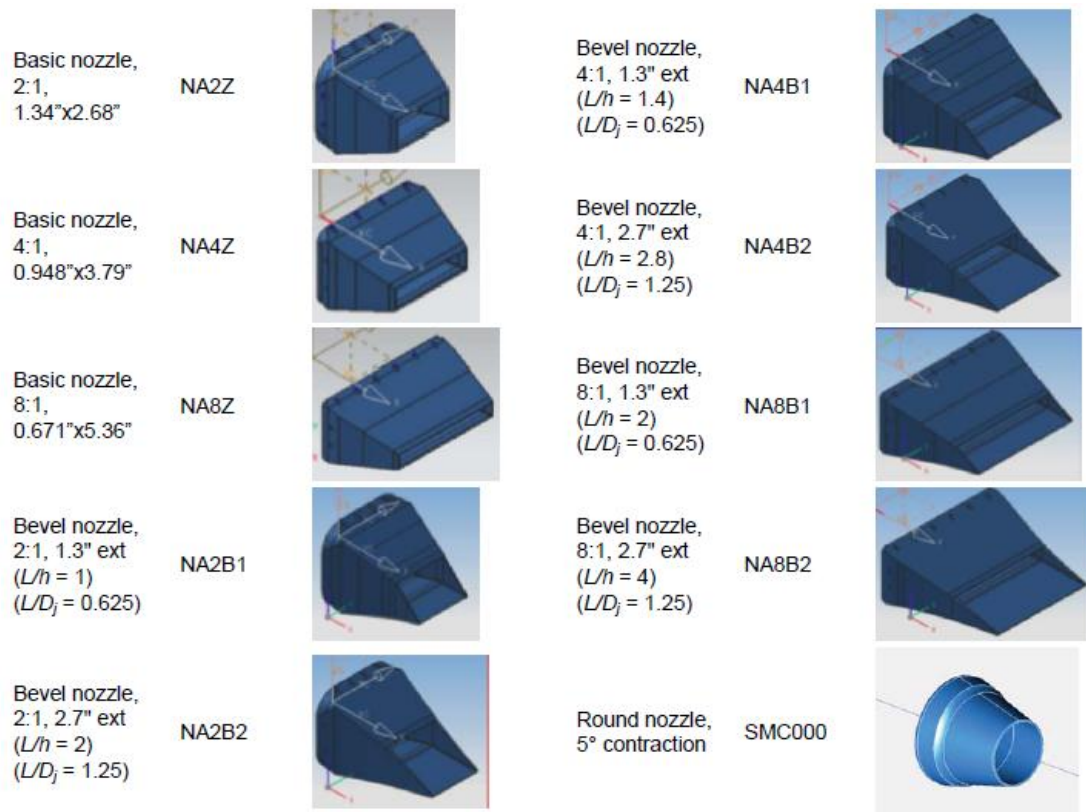
Fig. 2.7   Design features of nozzle hardware (Bridges and Wernet, 2015)

2.2   SIMULATION METHODS

The application of Direct Numerical Simulation (DNS) and Large Eddy Simulation (LES) are more feasible to jet noise prediction methodologies with the recent improvements in the processing speed of computers. The first DNS of a turbulent jet was carried out by Freund *et al* (2000) for a supersonic jet at Mach number 1.92 with Reynolds number 2000. At similar convective Mach numbers, the computed overall sound pressure levels were found to be in good agreement with

experimental data. Freund (2001) simulated a Mach 0.9 turbulent jet using 25.6 million grid points with a Reynolds number of 3,600. The predictions of mean flow and radiated sound showed excellent agreement with experiment data provided by Stormberg (1980). Moore (2007) performed DNS of a low Reynolds number jet at three temperature ratios. Analysis of turbulent kinetic energy contours showed that heating of the jet can reduce jet noise. Even though the results proved DNS to be best choice for jet noise problem, it still restricted to low Reynolds number and simple geometries. This is because of the wide range of length and time scales which necessitates high resolution requirements that are far beyond the reach of computational facilities available. Since most of problems with practical interest have high Reynolds number, an alternative method known as Large Eddy Simulation (LES) was developed.

Large Eddy Simulation has been used extensively to compute the flow field of turbulent jets. LES is having less computational cost compared to DNS and suitable for doing simulations for problems of practical interest. In LES the large scales are directly resolved and the effect of the small scales or the subgrid scales on the large scales are modelled. Many successful LES computations for different types of flows have been performed to date by various researchers [Boersma and Lele, 1999; Anderson *et al*. (2003, 2004, 2005); Bogey *et al*. (2001, 2003, 2007); Bogey and Bailly, 2005; Bodony and Lele (2004, 2005); Lew *et al.,* 2005; Shur *et al*., 2007; Rembold and Kleiser, 2004; Uzun and Hussaini, 2010; Tucker, 2008; Viswanathan *et al*. (2005, 2008)]. One of the first attempts in using LES as a tool for jet noise prediction was carried out by Mankbadi *et al*. (1994). A high order numerical scheme was employed to perform LES of a supersonic jet flow. The simulation captured the

time-dependent flow structure and Lighthill's theory was applied to calculate the far field noise. De Bonis (2006) made a review on the current state of Large Eddy Simulation (LES) for nozzle flows and reported the issues which currently limit its application. LES requires high order numerical schemes which do not lend themselves well to complicated grid topologies.

Although Reynolds Averaged Navier Stokes (RANS) calculations greatly depend on turbulence models to model all relevant scales of turbulence, the application of RANS based methods to jet noise prediction is also a subject of ongoing research (Khavaran, 1999; Hunter, 2003). The mean flow properties provided by a RANS solver is used for the noise predictions. Since noise generation is a multi-scale problem that involves a wide range of length and time scales, it appears the success of RANS based prediction methods will remain limited unless excellent turbulence models capable of accurately modelling a wide range of turbulence scales are developed and implemented into existing RANS solvers.

Nallasami (1999) presented a review of turbulence models that are significant for the jet noise computations. Flow solutions obtained with k-ε model, algebraic Reynold's stress model and Reynold's stress transport equations were reviewed. Algebraic stress model (ASM) and Reynolds stress transport model were implemented in flow solvers to compute the Reynolds stress components. Three dimensional Navier-Stokes code PAB3D was developed by Pao and Hamid (1996) to obtain numerical solutions to the Reynolds averaged Navier-Stokes equations in three-dimensional spatial domain. A unified method for subsonic and supersonic jet analysis was reported. The Navier-Stokes code was used to obtain solutions for axisymmetric jets with (i) on-design operating conditions at Mach numbers ranging

from 0.6 to 3.0, (ii) supersonic jets containing weak shocks and Mach disks and (iii) supersonic jets with non-axisymmetric nozzle exit geometries. Even though the jet flow contains a variety of complex flow physics, the RANS calculations require only the initial and boundary conditions to be specified. Detailed flow physics developments in the jet were predicted well by the RANS based methods. A more accurate aerodynamic and aeroacoustic prediction tool for high speed high temperature 3D jet flows was provided by Hamid *et al.* (2003) making modifications to the k-Ɛ model. A new temperature gradient correction to the eddy viscosity term was introduced and validated which proved to be a great promise in predicting high and low temperature jet flows. Hamid *et al.* (2006) reviewed the computational methods, code implementation and computed results for a wide range of nozzle configurations at various operating conditions and made comparisons with the available experimental data.

The capabilities of numerical methods applied to compute the underlying turbulent jet fluid dynamics were overviewed by Georgiadis and De Bonis (2006). The article was primarily divided between RANS modelling and unsteady modelling methods like LES. The comparison between RANS based models and LES using practical examples reveal certain issues in flow simulations. Unlike LES, RANS based models can provide only time-averaged information. However, it can easily capture the trends measured in experiments for different nozzle configurations and flow conditions with lesser computational resources. It is obvious that RANS based models are capable of fast evaluation of new nozzle designs and hence immensely used by the designers and manufacturers for better shapes and profiles.

2.3 SUMMARY

- Among the different methods employed by researchers to calculate the flow field and the radiated sound of jets emanating from nozzles, LES appears to be the most preferred one. The small scales of turbulence can be accurately captured using LES, only if proper grid resolution is employed.

- LES methods require high-order numerical schemes and high resolution mesh which do not lend themselves well to complicated grid topologies. LES is computationally very expensive which in turn make it difficult to utilise for the fast evaluation of new designs.

- Even though RANS based methods could only provide time-averaged turbulent information it can capture the trends exhibited by experiments well while altering the geometry or flow conditions of the nozzles. This statement coupled with the fact that RANS solutions are relatively computationally less expensive indicates that RANS based methods still have a place for better nozzle configurations.

- As a method to reduce jet mixing noise, new bevel designs on the baseline round nozzle were investigated. The numerical modelling to predict the aerodynamic and aeroacoustic characteristics of jets from bevel nozzles are seen to be very few in the literature, especially for different bevel angles, lengths and nozzle pressure ratios.

- Extensive research is progressing on noncircular jets which enhances the turbulent mixing characteristics and hence noise suppression. Rectangular jets were found to be more beneficial than all other noncircular nozzle geometries.

- In rectangular nozzle the transition from a circular to a rectangular cross-section upstream of the nozzle exit plane have a great role in the character of the vortical structures generated in the corners of the rectangular flow path. Extensible Rectangular Nozzle (*ERN*) has been designed to minimize losses induced due to the subsonic internal flow transition from a circular to a rectangular profile and also the non uniformities in the flow at the nozzle exit.

- Rectangular nozzles with and without bevel with different aspect ratios were experimentally investigated for the flow field and the measured data published for the validation of numerical models for predicting turbulence that can be used to develop better acoustic prediction codes.

CHAPTER - 3

TURBULENT JET FLOWS

Turbulent flows can be found in many engineering and technological applications such as jet pumps, ejectors, jet propulsion devices, combustors etc. The flow is said to be turbulent when it becomes unsteady, irregular, random, chaotic and the motion of every eddy is unpredictable (Pope, 2002). If the flow is free to develop without any effects from solid boundaries it is a free shear flow. The four types of free shear flows are jet flow, mixing layer, wake, and boundary layer.

3.1   TURBULENT FREE JET

A jet is a coherent stream of fluid that is projected into a surrounding medium, usually from a nozzle configuration. The stream of fluid may be initially laminar or turbulent, while the surrounding medium may be stationary with respect to the nozzle, or moving, in which case it is said to be a co-flow. In a flow initially emanating as a laminar jet to the surrounding medium, there exists a layer called the shear layer across which the properties of the flow change sharply from the jet to the surrounding medium. This shear layer is usually unstable, and wave-like disturbances may form and grow outwards from the nozzle which disrupts the regular laminar behaviour. The turbulent free jet is a free shear flow with mean flow gradients that develop in the absence of boundaries (George, 2000). This kind of flow is characterized by a main flow direction in which the velocity is significantly greater than in the transverse direction whereas the gradients in the transversal direction are much larger than those in the main direction. Figure 3.1 shows the development of a single-stream jet. High velocity fluid is continuously added through a nozzle into stagnant surroundings. As it

exits the nozzle, the flow of the high-velocity fluid is fully aligned with the nozzle wall, and a core region of potential flow is formed. The shear layer is generated between the high-velocity fluid and its surroundings. The thickness of this shear layer depends on the thickness of the boundary layer at the nozzle exit. The shear layer develops in size downstream the flow due to entrainment of the ambient fluid. As the width of the shear layer increases, the radial extent of the potential core region decreases and more and more region of the flow becomes turbulent. The entire jet is turbulent and thus fully developed soon after the potential core closure. The jet becomes self-preserving or self-similar in the fully developed region. This means that profiles of mean flow quantities can be collapsed by proper scaling. It has long been assumed that these self similar profiles are independent of initial conditions for all quantities and therefore universal for all jets. Typically, the interaction of turbulent eddies with each other and with the shear layer, may produce acoustic waves.
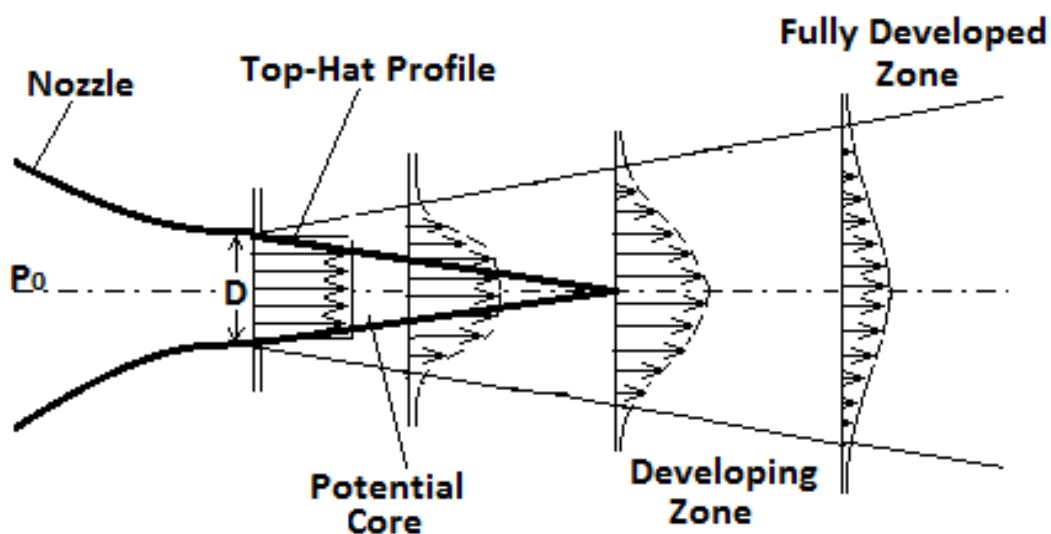
Fig. 3.1   Flow regions in a developing jet

3.1.1   Turbulent Rectangular Jet

The flow field of a rectangular jet presented by Krothapalli *et al*. (1981) is shown in Figure 3.2. The variation of $\ln\left(\frac{U_c}{U_0}\right)^2$ with $\ln\left(\frac{X}{D}\right)$, where U_c is the mean axial velocity along the centreline of the jet and U_0 is the mean velocity at the centre of the nozzle exit and $\frac{X}{D}$ is the axial distance nondimensionalised with the diameter of the jet is also shown in the same figure. The flow is characterized by the presence of three distinct regions. These regions are: (i) the potential core region in which the axial component of velocity remains a constant (ii) a two-dimensional type region AB in which velocity decays roughly at the same rate as that of a planar jet and (iii) an axisymmetric region, which is downstream of B where the velocity decay is almost same as that of a axisymmetric jet.
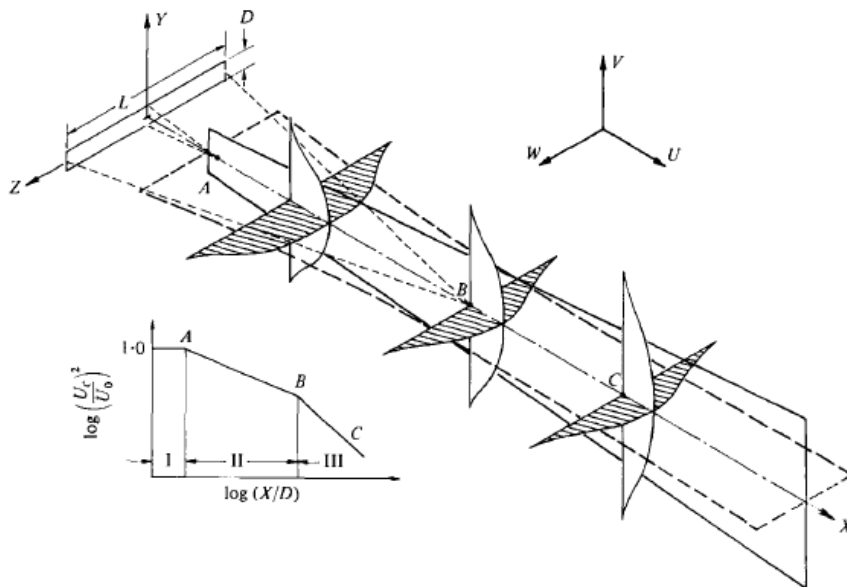
Fig. 3.2   Schematic representation of the flow field of a rectangular jet
(Krothapalli *et al*., 1981)

A rectangular jet may approximate the behaviour of a plane jet, if the aspect ratio is large enough to minimize the importance of entrainment in the span wise *z*

direction and hence establish a statistically two-dimensional flow (Pope, 2002). The initial and boundary conditions strongly affect the development of turbulent jets issuing from rectangular nozzles. Many experimental investigations have found that the flow fields of rectangular jets are strongly influenced by Reynolds number (Deo *et al.*, 2008; Suresh *et al.*, 2008) and also aspect ratio (Quinn,1992; Mi *et al.*, 2005; Deo *et al.*, 2007a). As the aspect ratio decreases, Krothapalli *et al.* (1981) reported that the location where the jet first assumes axisymmetric behaviour goes upstream toward the exit of the nozzle.

3.2   FLOW CHARACTERISTICS OF TURBULENT JET

3.2.1   Mean Velocity Field

The mean velocity field of a three dimensional flow is described by the velocity components *u, v* and *w* in the *x, y* and *z* directions. The axial component of mean velocity (u) can be analysed to study the behaviour of the flow at different axial and radial locations of the jet like the rate of mixing, shear layer thickness, self similarity, jet spread rate, boundary layer characteristics etc.

3.2.1.1 Potential Core Length

Potential core length is defined as the axial location where the average axial velocity *u* is 0.95 times the jet velocity at nozzle exit U_j and characterizes as a measure of mixing rate between jet and its surrounding fluid. A higher mixing level is supported by shorter potential core length (Quinn, 1992; Deo *et al.*, 2007). Mean axial velocity *u* is nondimensionalised by the mean velocity of jet at the centre of nozzle exit U_j and the downstream distance from the nozzle exit *x* is nondimensionalised by the diameter or equivalent diameter of the jet D_j for circular and rectangular jets respectively. The variation of u/U_j with x/D_j along the centreline provides an

indication of the potential core length and velocity decay for circular and rectangular jets. In the case of rectangular nozzles variation of u/U_j with x/D_j along the lip lines of major and minor axis indicates the effect of aspect ratio of rectangular nozzles on velocity decay. For the bevel nozzle, variation of u/U_j with x/D_j along the longer and shorter side of the bevel provides the effect of bevel length ratio (*BLR*) on velocity decay. The downstream development of the flow can be visualised from the radial profiles of axial velocity at different axial stations and also from the velocity profiles on stream-wise and cross stream planes.

3.2.1.2 Shear Layer Thickness

Shear layer is the region in which most of the interactions and mixing between the ambient and jet fluids take place. Therefore, understanding the fluid dynamic phenomena in the shear layer during the downstream evolution of a jet is important. Shear layer thickness $\delta = (R_{0.95} - R_{0.1})$, where $R_{0.95}$ and $R_{0.1}$ being the radial locations where $u / U_{centreline} = 0.95$ and 0.1 respectively (Arakeri *et al.*, 2003). A wider shear layer region with increase in x/D_j designates a faster flow development. The virtual origin (x_0) is the point from which the jet appears to be originating and is located at the *x*- intercept of the straight line fit to shear layer thickness δ plotted against x/D_j .

3.2.1.3 Self similarity

The jet flow asymptotically attains the self- similar profile of a round jet at an axial distance far away from the nozzle exit irrespective of the nozzle cross sectional shape. A study on the self similarity of the jets can be obtained by plotting u/U_c against $(y-y_{0.5})/(x-x_0)$ at different axial stations where U_c is the centreline velocity, $y_{0.5}$ is the jet half width and x_0 is the virtual origin (Arakeri *et al.*, 2003). Carazzo *et al.*(2006) explains the influence of initial conditions, nozzle geometry and turbulence structures on the self similarity of the jets. Non identical states of self similarity can

be linked to the turbulent structures. At intermediate distances, large-scale structures appear in the flow. However at large distances, they eventually become permanent and the flow is fully self similar.

3.2.2 Turbulent velocity field
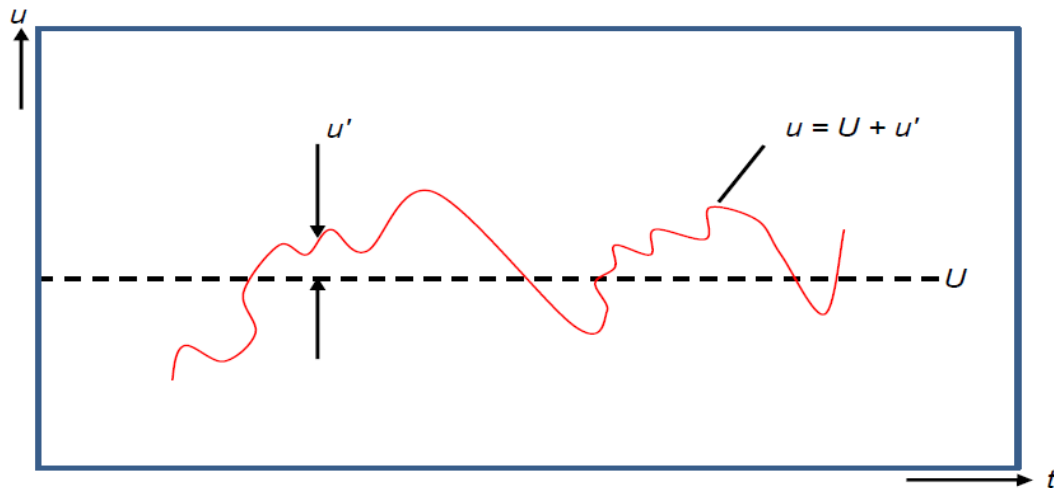
Fig. 3.3 Definition of mean and fluctuating component of velocity (White, 1994)

In turbulent flows, fluctuations will lead the velocity to rapidly vary as a random function of time and space (White, 1994). In a three dimensional flow *u'*, *v'* and *w'* are the fluctuating components corresponding to the respective mean velocity components *u, v* and *w*. The turbulent velocity *u'* in stream wise direction is defined as the deviation of the instantaneous velocity *u* from its mean value *U* (i.e. $u' = u - U$) and is represented in Figure 3.3. The fluctuating components of velocity in the axial (*u'*) and radial (*v'*) directions can be noted to calculate the turbulent flow characteristics such as Reynolds stresses ($\overline{u'u'}$, $\overline{v'v'}$ and $\overline{u'v'}$), turbulence intensity, axial/radial velocity variation along centreline/rake etc. The flow characteristics of jet (especially Reynolds stresses) emanating from nozzles are indispensable to acquire information on the acoustic sources and also on thrust generation. The condition of

the boundary layer at the nozzle exit and the jet core turbulence are also important parameters which has a significant impact on the jet noise

3.2.3 Flow Characteristics of Rectangular Jets

3.2.3.1 Mean and variance of velocity field

The mean and variance of velocities for the analysis of jet emanating from rectangular nozzles are defined as given below (Bridges and Wernet, 2015)

Mean velocity, $\qquad U_i = \frac{1}{t} \int_0^t u_i \, dt$ $\qquad\qquad\qquad$ (3.1)

Variance of velocity, $\qquad u_i u_i = \frac{1}{t} \int_0^t (u_i - U_i)(u_i - U_i) dt$ $\qquad$ (3.2)

Root mean square velocity, $\quad u_i' = \sqrt{u_i u_i}$ $\qquad\qquad\qquad$ (3.3)

where 'i' is equal to 1, 2 and 3 for the x, y and z components of velocity respectively.

3.2.3.2 Spread rate of rectangular jets
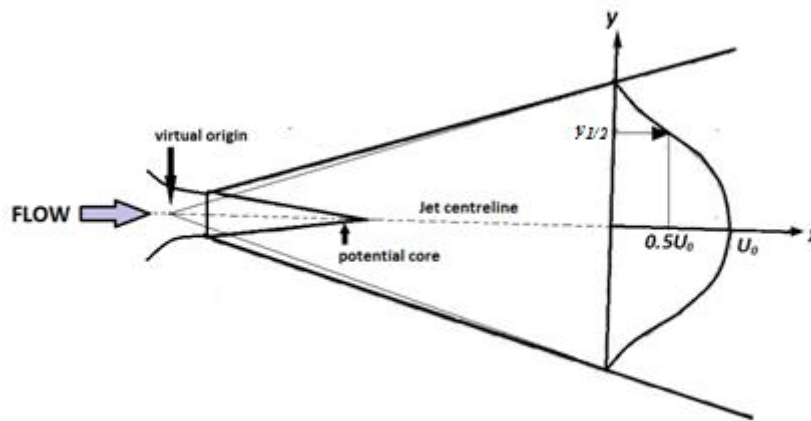
Fig. 3.4   Virtual origin and half width ($y_{1/2}$) of rectangular jet

Jet half width at any axial location is defined as the distance of a transverse plane from the centreline where the mean velocity becomes half of the corresponding centreline velocity. The jet half width in the *XY* plane, i.e. across the shortest dimension of the rectangular nozzle is designated as $Y_{1/2}$ and in the *XZ* plane it is

designated as $Z_{1/2}$. The spreading of turbulent rectangular jets across the smaller dimension of the nozzle is higher than that in the larger dimension.

The jet in the *XY* plane spreads linearly with *X* and with a relation of the form $Y_{1/2}/D_j = A_1[x/D_j + A_2]$, where the slope A_1 is the spread rate and depends on the nozzle geometry, aspect ratio, Reynold's number and side walls. A_2 is the virtual origin of the flow (Alnahhal *et al.*, 2011). Virtual origin is the point from where the jet appears to originate and is shown in figure 3.4.

The variation of the half-width in the *XZ* plane is neither linear nor it increases monotonically (Krothapally *et al.*, 1981). At some intermediate axial locations, the half-widths in the central planes cross over. The distance from the nozzle exit to the cross-over point along the *X* axis increase with aspect ratio.

3.2.3.3 Type of Initial Boundary Layer

The parameters that are usually estimated to assess the jet inflow conditions is the shape factor (*H*) which is the ratio of displacement thickness (δ) to the momentum thickness (θ) (Zaman, 1985, 2012). Conventionally, $H = 2.59$ (Blasius boundary layer) is typical of laminar flows, while $H = 1.3 - 1.4$ is typical of turbulent flows. A value falling in between this range of shape factor means that the boundary layers are transitional in nature. The displacement thickness and momentum thickness can be calculated using the following integration considered for compressible flows, as the present study focuses on high subsonic flows.

Displacement thickness, $\qquad \delta = \int_{y=0}^{y=\infty} \left(1 - \frac{\rho u}{\rho_j U_j}\right) dy \qquad\qquad$ (3.4)

Momentum thickness, $\theta = \int_{y=0}^{y=\infty} \frac{\rho u}{\rho_j U_j}\left(1 - \frac{\rho u}{\rho_j U_j}\right) dy \qquad\qquad$ (3.5)

Shape factor, $H = \frac{\delta}{\theta} \qquad\qquad$ (3.6)

3.3   JET ACOUSTICS

The investigation and understanding of jet noise is associated with the understanding of turbulence as the sources of sound are defined by the turbulent flow itself. Both the fine scales and the larger structures are responsible for the noise that is generated in turbulent jet (Tam, 1998). In jet flows, the sound-generating structures are convected downstream by the mean flow. The moving source radiates more sound in the direction of transportation of the source as shown in Figure 3.5. When the wave front propagates through the jet on the way to the far-field region, its path tends to bend away from the jet axis due to refraction. This is due to the fact that the convection velocity near the centreline is higher compared to the outer region which makes the tilting of an acoustic wave front passing through this region. The refraction effect creates a zone of relative silence downstream of the noise generating region as less sound is propagated in this direction.
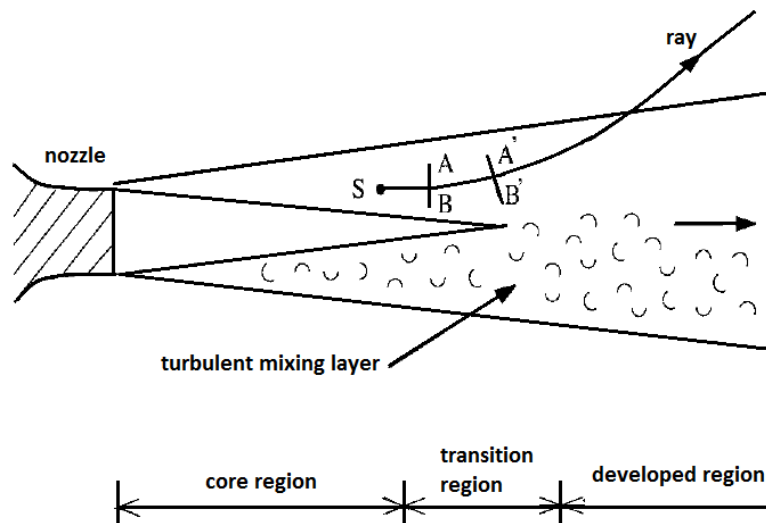
Fig. 3.5 Schematic diagram showing the different regions in a turbulent mixing layer and the movement of a localized noise source (Tam, 1998).

The source of noise generated in a turbulent jet can be monopole noise associated with fluctuating mass inflow, dipole noise with turbulent eddies deforming

near aerodynamic surfaces and quadrupole noise with a pair of turbulent eddies in close proximity deforming each other.

Due to the nonlinearity of the governing equations it is very difficult to predict the sound generation in fluid flows. The fact that the sound field is in some sense a small perturbation of the flow can be used to obtain approximate solutions. Aero-acoustics provides such approximations and at the same time defines the acoustical field as an extrapolation of an ideal reference flow. The difference between the actual flow and the reference flow is identified as a source of sound. This idea was introduced by Lighthill, (1952, 1954) who called this an analogy.

3.4   COMPUTATIONAL AEROACOUSTICS USING UNSTEADY RANS

The acoustic analysis is based on unsteady RANS calculations. The near field flow characteristics obtained from appropriate governing equations are used to predict the sound with the aid of analytically derived integral solutions to wave equations. The acoustic analogy essentially decouples the propagation of sound from its generation by separating the flow solution process from the acoustics analysis. Time accurate solutions of the flow field variables, such as pressure, velocity components, and density on source surfaces obtained from unsteady RANS calculations are required to evaluate the surface integrals for computing the time histories of sound pressure at prescribed receiver locations. The interior surfaces enclosing the jet account for the contributions from the quadrupoles and act as source surfaces. Sound pressure signals thus obtained can be processed using the fast Fourier transform to compute acoustic quantities and power spectra.

CHAPTER - 4

NUMERICAL MODELLING

Jet flow, like other forms of gas and liquid flows, is governed by well known equations that predict the evolution of the properties of the flow in time, from an initially known state. For the purposes here, we are considering jet flows of a gas (such as air) from a nozzle, into an initially quiescent volume of the same kind of gas..

4.1 GOVERNING EQUATIONS

The Navier-Stokes equations are derived by application of Newton's law of conservation of momentum and forces to a fluid in each of the spatial dimensions. These are complemented by an equation derived by consideration of conservation of mass and an equation derived by consideration of conservation of energy. In compressible jet flow solutions, especially high speed flows, the governing equations solved are Favre averaged continuity equation, momentum equations, and energy equation (Versteeg and Malalasekra, 1995). These five equations are able to completely determine the evolution of the five state variables.

The equation for conservation of mass

$$\frac{\partial \overline{\rho}}{\partial t} + div(\overline{\rho}\widetilde{\boldsymbol{U}}) = 0 \tag{4.1}$$

The equation for conservation of momentum

$$\frac{\partial(\overline{\rho}\widetilde{U})}{\partial t} + div(\overline{\rho}\,\widetilde{U}\widetilde{\boldsymbol{U}})$$
$$= -\frac{\partial \overline{P}}{\partial x} + div\left(\mu\,grad\,\widetilde{U}\right) + \left[-\frac{\partial\left(\overline{\overline{\rho}u'^2}\right)}{\partial x} - \frac{\partial\left(\overline{\overline{\rho}u'v'}\right)}{\partial y} - \frac{\partial\left(\overline{\overline{\rho}u'w'}\right)}{\partial z}\right] + S_{Mx} \tag{4.2}$$

$$\frac{\partial(\overline{\rho}\tilde{V})}{\partial t} + div(\overline{\rho}\tilde{V}\boldsymbol{U})$$

$$= -\frac{\partial\overline{P}}{\partial y} + div(\mu \, grad \, \tilde{V}) + \left[-\frac{\partial\left(\overline{\rho u'v'}\right)}{\partial x} - \frac{\partial\left(\overline{\rho v'^2}\right)}{\partial y} - \frac{\partial\left(\overline{\rho v'w'}\right)}{\partial z} \right] + S_{My}$$

$$(4.3)$$

$$\frac{\partial(\overline{\rho}\widetilde{W})}{\partial t} + div(\overline{\rho}\widetilde{W}\boldsymbol{U})$$

$$= -\frac{\partial\overline{P}}{\partial z} + div(\mu \, grad\widetilde{W}) + \left[-\frac{\partial\left(\overline{\rho u'w'}\right)}{\partial x} - \frac{\partial\left(\overline{\rho v'w'}\right)}{\partial y} - \frac{\partial\left(\overline{\rho w'^2}\right)}{\partial z} \right] + S_{Mz}$$

$$(4.4)$$

The equation for conservation of energy

$$\frac{\partial(\overline{\rho}\tilde{e})}{\partial t} + div(\rho\tilde{e}\boldsymbol{U}) = -\overline{P}div\tilde{U} + div(k \, gradT) + \Phi + S_e$$

$$(4.5)$$

4.2   TURBULENCE MODELLING

Turbulence modelling is the construction and use of a numerical model to predict the features of turbulence. A turbulent fluid flow has features on many different length scales, which all interact with each other. A common approach is to average the governing equations of the flow, in order to focus on large-scale and non-fluctuating features of the flow.

4.2.1   Closure Problem in Turbulence

The Navier–Stokes equations govern the velocity and pressure of a fluid flow. In a turbulent flow, each of these quantities may be decomposed into a mean part and a fluctuating part. Averaging the equations gives the Reynolds-averaged Navier–Stokes (RANS) equations, which govern the mean flow. However, the nonlinearity of

the Navier–Stokes equations causes the velocity fluctuations to appear in the RANS equations with the nonlinear term $-\rho\overline{u'_i u'_j}$ from the convective acceleration. This term is known as the Reynolds stress. Its effect on the mean flow is like that of a stress term, such as from pressure or viscosity. To obtain equations containing only the mean velocity and pressure, we need to close the RANS equations by modelling the Reynolds stress term as a function of the mean flow, removing any reference to the fluctuating part of the velocity. This is the closure problem in turbulence.

4.2.2 Boussinesq's Hypothesis

Boussinesq was the first to attack the closure problem, by introducing the concept of eddy viscosity. In 1877 Boussinesq proposed a relation (Equation 4.6) to connect the turbulence stresses to the mean flow to close the system of equations. In the present work, Boussinesq hypothesis is applied to model the Reynolds stress terms with a new proportionality constant μ_t, the turbulence eddy viscosity.

$$-\rho\overline{u'_i u'_j} = \mu_t\left(\frac{\partial U_i}{\partial x_j} + \frac{\partial U_j}{\partial x_i}\right) - \frac{2}{3}\rho k \delta_{ij} \tag{4.6}$$

Where k is the turbulent kinetic energy, $k = \frac{1}{2}\overline{u'_i u'_j}$

and δ_{ij} is Kronecker delta $= \begin{cases} 0, & for\, i \neq j \\ 1, & for\, i\ = j \end{cases}$

4.2.3 SST k-ω Turbulence Model

In computational fluid dynamics, the k–ω turbulence model is a common two equation turbulence model that is used as a closure procedure for the Reynolds-averaged Navier–Stokes (RANS) equations. The model attempts to predict turbulence by two partial differential equations for two variables, k and ω, with the first variable being the turbulence kinetic energy (k) while the second (ω) is the specific rate of

dissipation (conversion of the turbulence kinetic energy *k* into internal thermal energy).

The SST *k-ω* turbulence model (Menter, 1993) is a two-equation eddy-viscosity model which has become very popular. The use of a *k-ω* formulation in the inner parts of the boundary layer makes the model directly usable all the way down to the wall through the viscous sub-layer. Hence SST *k-ω* model can be used as a low Reynolds number turbulence model without any extra damping functions. The SST formulation also switches to *k-ε* behaviour in the free-stream and thereby avoids the common *k-ω* problem that the model is too sensitive to the inlet free-stream turbulence properties. The researchers who use the SST *k-ω* model often merit it for its good behaviour in adverse pressure gradients and separating flows. The SST *k-ω* model does produce a bit too large turbulence levels in regions with large normal strain, like stagnation regions and regions with strong acceleration. This tendency is much less pronounced than with a normal *k-ε* model though.

The two variables calculated are usually interpreted as '*k*' the turbulence kinetic energy and '*ω*' the rate of dissipation of eddies.

Transport equation for *k*

$$\frac{\partial(\rho k)}{\partial t} + div\,(\rho k \boldsymbol{U}) = div\left[\left(\mu + \frac{\mu_t}{\sigma_k}\right)grad(k)\right] + P_k - \beta^* \rho k \omega \tag{4.7}$$

Transport equation for *ω*

$$\frac{\partial(\rho \omega)}{\partial t} + div\,(\rho \omega \boldsymbol{U})$$
$$= div\left[\left(\mu + \frac{\mu_t}{\sigma_{\omega,1}}\right)grad(\omega)\right] + \gamma_2\left(2\rho S_{ij}.S_{ij} - \frac{2}{3}\rho\omega\frac{\partial U_i}{\partial x_j}S_{ij}\right) - \beta_2 \rho \omega^2$$
$$+ 2\frac{\rho}{\sigma_{\omega,2}\omega}\frac{\partial k}{\partial x_k}\frac{\partial \omega}{\partial x_k} \tag{4.8}$$

4.3   AERO ACOUSTICS

4.3.1   Lighthill's Acoustic Analogy

The field of aeroacoustics have begun with the first theory on jet noise by Sir James Ligthill (Lighthill, 1952). This theory was developed to predict the intensity of noise produced by turbulent jets. To describe the acoustic waves, Lighthill reformulated the equations of fluid motion as a wave equation and is now referred to as Lighthill's acoustic analogy.

Wave equation from the Acoustic Analogy Theory is given by

$$\partial^2 \rho / \partial t^2 - a_\alpha^2 \nabla^2 \rho = \partial^2 T_{ij} / \partial x_i \partial x_j \tag{4.9}$$

The left hand side of the equation represents the acoustic wave propagation and the right hand side indicates the source of noise generation.

Lighthill Stress Tensor 'T_{ij}' is given as;

$$T_{ij} = \rho v_i v_j + p - \rho a_\alpha^2 . \delta_{ij} \tag{4.10}$$

The first term in Lighthill's stress Tensor is called Reynolds' stress. The second term is related to the entropy changes in acoustic fields and the third term to the viscous shear stresses caused by gradients of the acoustic particle velocity. The convective velocity terms are all added to the source part of the equation in Lighthill's analogy. Hence it is assumed in the analogy that the static flow velocity is zero outside the source region. The entropy fluctuations and the viscous stresses are also introduced into the source part. Therefore, it is assumed that there are no losses due to the viscosity or the thermal conductivity of the fluid outside the source region, which means that the fluid outside the source region is an ideal fluid.

CHAPTER - 5

COMPUTATIONAL PROCEDURE AND SOLUTION METHODOLOGY

5.1   ROUND AND BEVEL NOZZLE

A 3D simulation of plain round nozzle and a bevelled round nozzle were conducted. The simulation parameters to be considered are the nozzle geometry, the computational domain, the mesh generated within the domain, the boundary conditions applied to the domain boundaries, the flow parameters and numerical schemes used for calculation.

5.1.1   Nozzle Geometry

Simulations have been performed for two jets, one from a round and other from a 20^0 bevelled nozzle (Fig. 5.1). The diameter (D_j) and length of the nozzles were 50 mm and 380 mm respectively. The exit Mach number attained was 0.75.
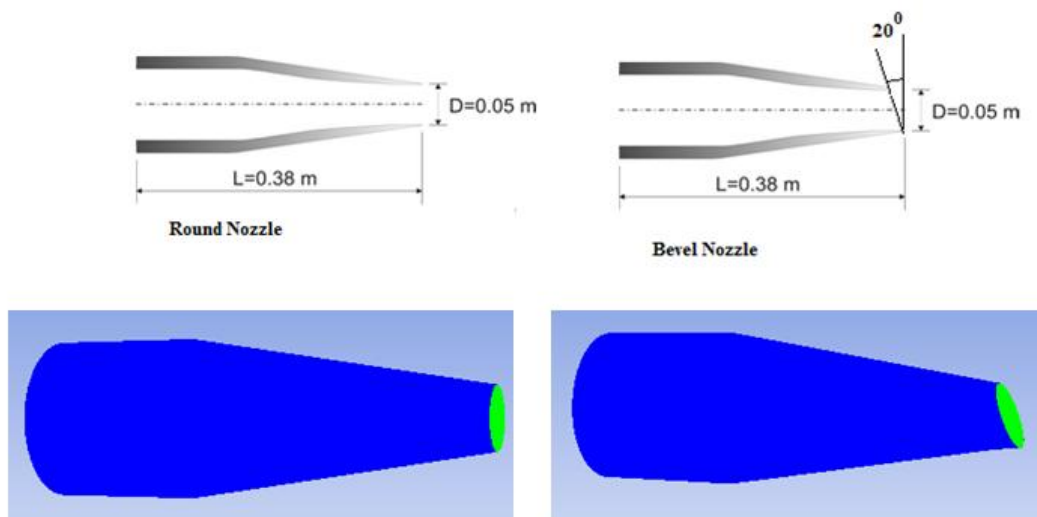

Fig. 5.1 Nozzle geometry for Round and Bevel nozzles

5.1.2   Computational Domain and Mesh

The Computational domain selected for round bevel nozzle is shown in Figure 5.2. Since both the nozzles are having plane symmetry only a half portion of the three dimensional geometry used for calculation is shown. The axial extent of the domain was 50 times the nozzle diameter ($50D_j$) downstream of the nozzle exit. The radial extent of the domain at the inlet was $10D_j$, at the outlet it was $20D_j$ and the length of buffer zone was $40D_j$. The buffer zone was provided to minimize the effect of reflections at the domain outlet on the flow field (Anderson *et al.*, 2004). Domain extent in the axial, radial and azimuthal directions was finalized after inspecting the predicted length and thickness of the potential core and shear layer respectively.

Grid independence study and grid sensitivity analysis were carried out on four grid size, viz. 0.5 million, 1 million, 2 million and 2.5 million cells. It was observed that the variation in the properties were within 1% when grids of 2 and 2.5 million cells were compared. The computational domain has been discretized using hexahedral mesh for the round nozzle and a hybrid mesh (90% hexahedral and 10% tetrahedral) for the bevelled nozzle with approximately two million cells. Computational domain with mesh is shown in Figure 5.3 and the closer view of mesh details at the nozzle exit for both round and bevel nozzle is shown in Figures 5.4 and 5.5 respectively.

Mesh refinement near the no-slip surfaces was such that the area weighted average value of wall y^+ for the inner wall for round and bevel nozzles were approximately 30. For outer wall, the above values were approximately 5.The near wall spacing varies from 5 μm to 10 μm corresponding to this value of wall y^+. It is important to not only resolve the wall regions, but also resolve the flow as well. Very

fine mesh sizes were used near the nozzle exit and along the general vicinity of the

shear layer.Adequate resolution in the axial, radial and azimuthal directions was

maintained by keeping the cell equi-angle skew measure as low as possible. The

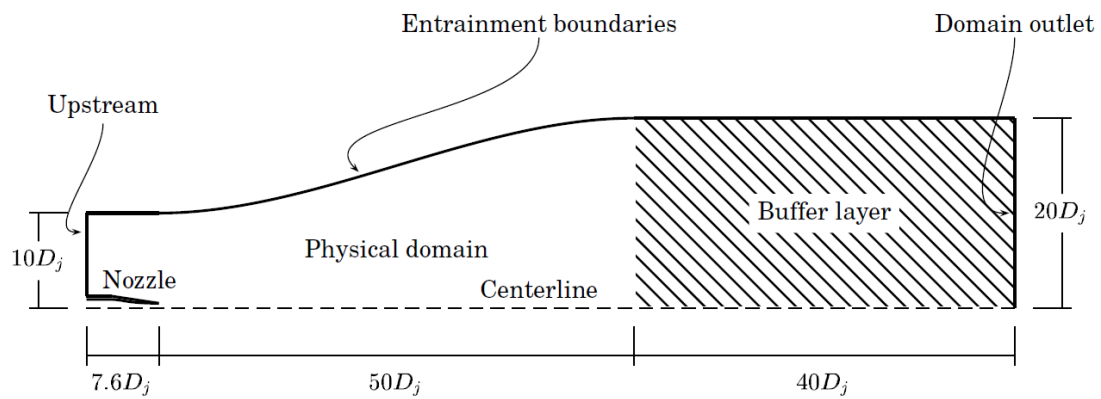maximum volume weighted average of cell equi-angle skew was 0.42.

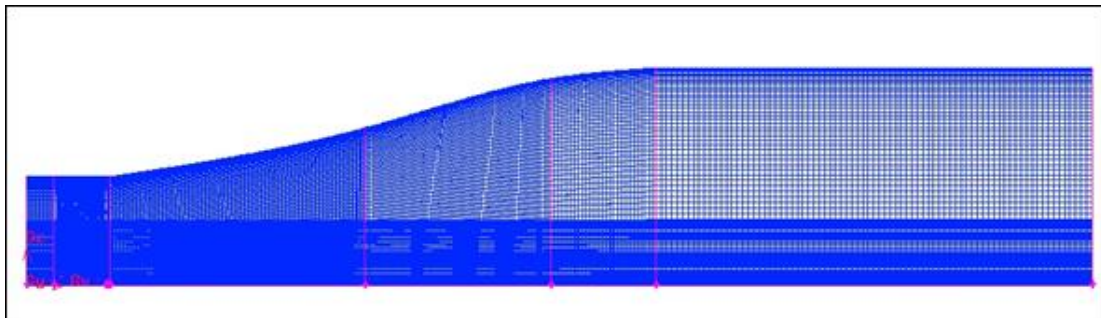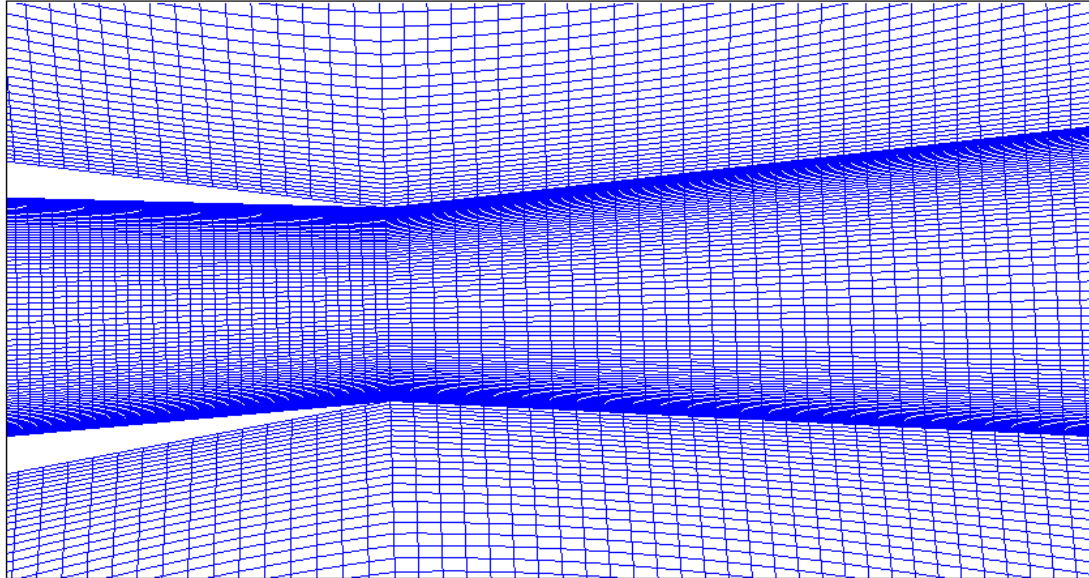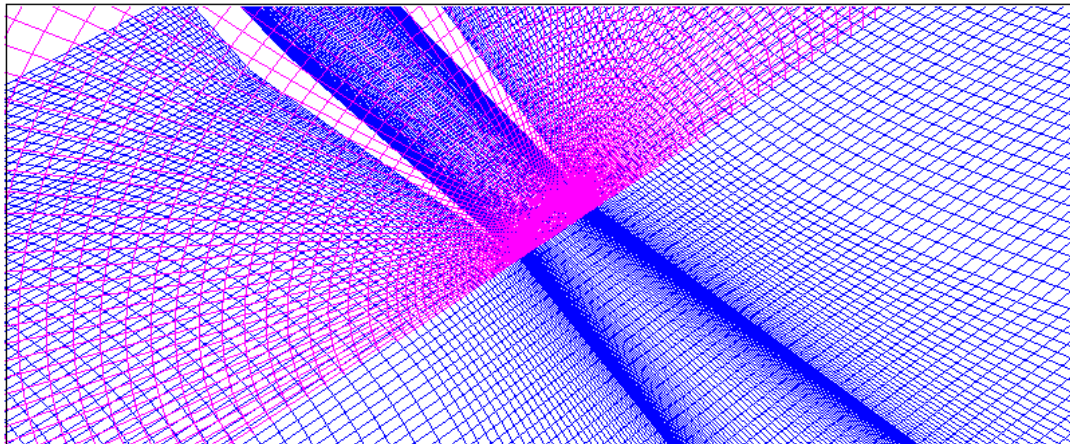Fig. 5.2 Sectional view of computational domain

Fig. 5.3 Computational domain with mesh

(a)

(b)

Fig. 5.4 Mesh details at nozzle exit for round nozzle (a) Plan view in *XZ* plane
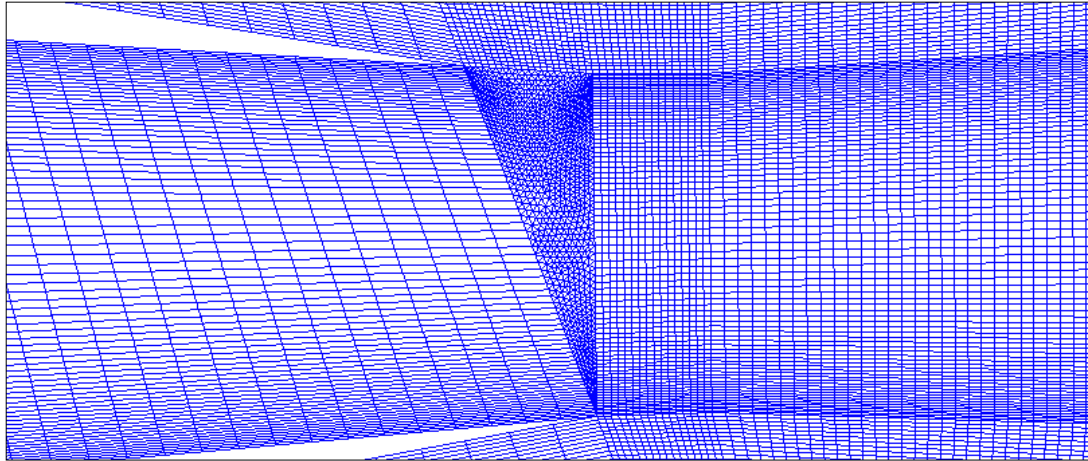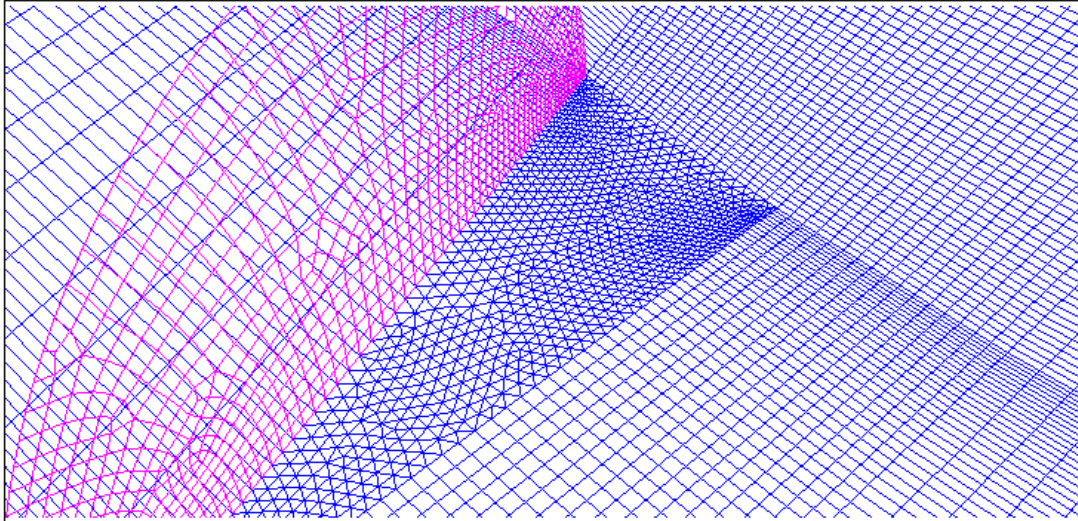   (b) isometric view

(a)

(b)

Fig. 5.5 Mesh details at nozzle exit for bevel nozzle (a) Plan view in *XY*
        plane (b) isometric view

5.1.3 Boundary Conditions

Computational domain indicating the boundary types and boundary conditions is shown in Figure 5.6. The nozzle inlet has been defined with a boundary type 'pressure inlet' and the total pressure and temperature were specified. The domain inlet and the top entrainment surface have also been modelled as pressure inlets at the ambient pressure and temperature. The domain outlet was taken to be a 'pressure outlet' at the ambient pressure. The bottom boundary has been treated as a symmetry surface. All solid surfaces have been treated as adiabatic surfaces and standard wall functions have been used. The RANS based solver has been used for carrying out calculations. Table 5.1 gives the boundary conditions and Table 5.2 gives the flow conditions for the two simulated jets.
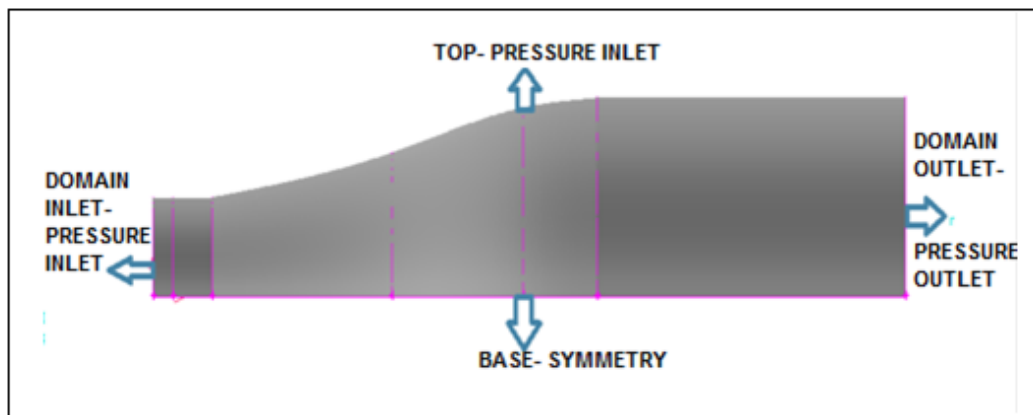

Fig. 5.6 Computational domain with boundary conditions

Table 5.1 : Boundary conditions

Surface	Boundary type	Boundary condition
Nozzle inlet	Pressure inlet	Stagnation pressure and temperature
Domain inlet	Pressure inlet	Ambient pressure and temperature
Top	Pressure inlet	Ambient pressure and temperature
Domain outlet	Pressure outlet	Ambient pressure and temperature
Nozzle wall	Wall	Adiabatic wall
Bottom	Symmetry	Symmetry
All other surfaces	Interior	Interior

Table 5.2 : Flow properties for round and bevel nozzle

Properties	$\dfrac{U_j}{C_\infty}$	$\dfrac{T_j}{T_\infty}$	P_∞ (Pa)	ρ_∞ (kg/m^3)	$C\infty$ (m/s)	U_∞ (m/s)	T_∞ (K)	T_{oj} (K)	Re_D
Values	0.75	1	101300	1.225561	340.174	0	288.0	320.4	5×10^4

5.1.4 Numerical Scheme

Simulations were performed in a three dimensional computational domain using steady RANS calculations. The commercial software used for numerical simulation was ANSYS 14.0. The turbulence model used was SST k-ω with default values for all constants and second order accurate discretization for all variables. The

k-ω model equations do not contain terms which are undefined at the wall, i.e. they can be integrated to the wall without using wall functions. They are accurate and robust for a wide range of boundary layer flows with pressure gradient. The SST k–ω model uses a blending function for gradual transition from the standard k–ω model near the wall to a high Reynolds number version of the k–ε model in the outer portion of the boundary layer. It also contains a modified turbulent viscosity formulation to account for the transport effects of the principal turbulent shear stress.

The SIMPLE method was used for the pressure velocity coupling and the second order upwind scheme for the convection term together with transport equations. Least square cell based method was used for the descretisation of the gradient term and all variables are descretised with second order accuracy. The log-law, which is valid for both, equilibrium boundary layers and fully developed flows, provides upper and lower bounds on the acceptable distance between the cell centroid and the wall, for cells adjacent to the wall. The distance is usually measured in the wall unit y^+. Mesh refinement near the no-slip surfaces was such that the area weighted average value of wall y^+ for the inner wall for round and bevel nozzles were approximately 30. The value of wall y^+ for outer wall was approximately 5 and the near wall spacing was less than 10 μm corresponding to this value. In order to resolve the wall, very fine mesh sizes were used near the nozzle exit and along the shear layer by keeping the cell equi-angle skew measure as low as 0.42. Moreover, the overall mass balance in theentire computational domain was less than 1% of the mass flow rate through the nozzle.

5.2 RECTANGULAR AND BEVELED RECTANGULAR NOZZLE

5.2.1   Geometric Details of Nozzle Profile

The major drawback with the rectangular nozzle design was losses found in the subsonic internal flow transition from a circular to a rectangular profile. The transition from a circular to a rectangular cross-section upstream of the nozzle exit plane has a great role in the character of the vortical structures generated in the corners of the rectangular flow-path. This problem was resolved in the Extensible Rectangular Nozzle (*ERN*) model system in which the flow transition ducts have been designed for transition from round piping to a rectangular cross-section using flat wrap methodology to minimize the non-uniformities in the flow at the nozzle exit (Frate and Bridges, 2011).
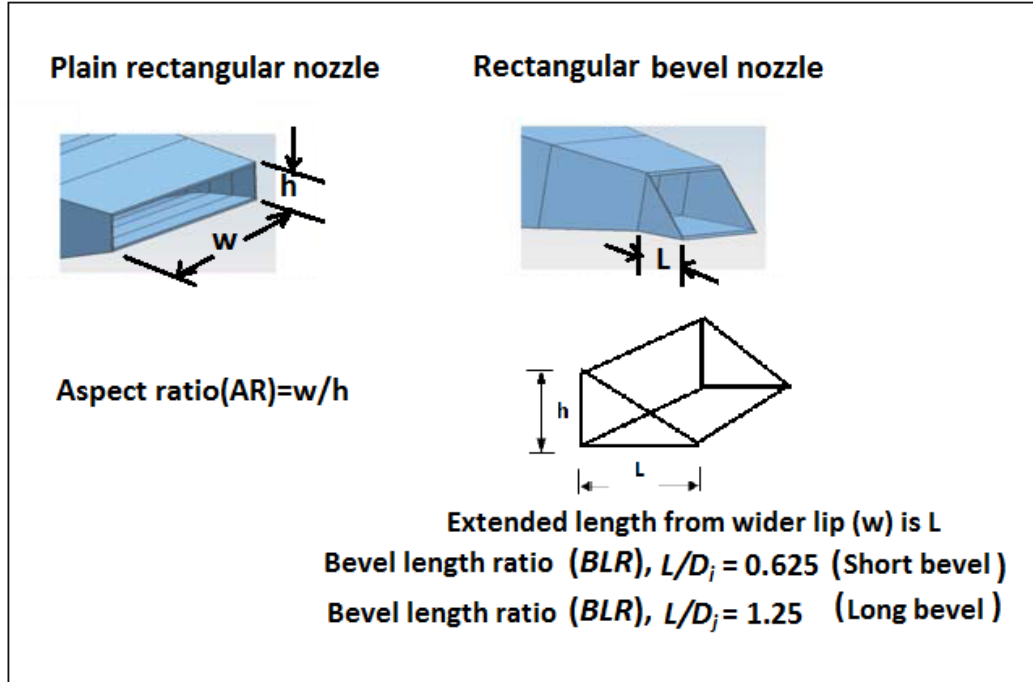

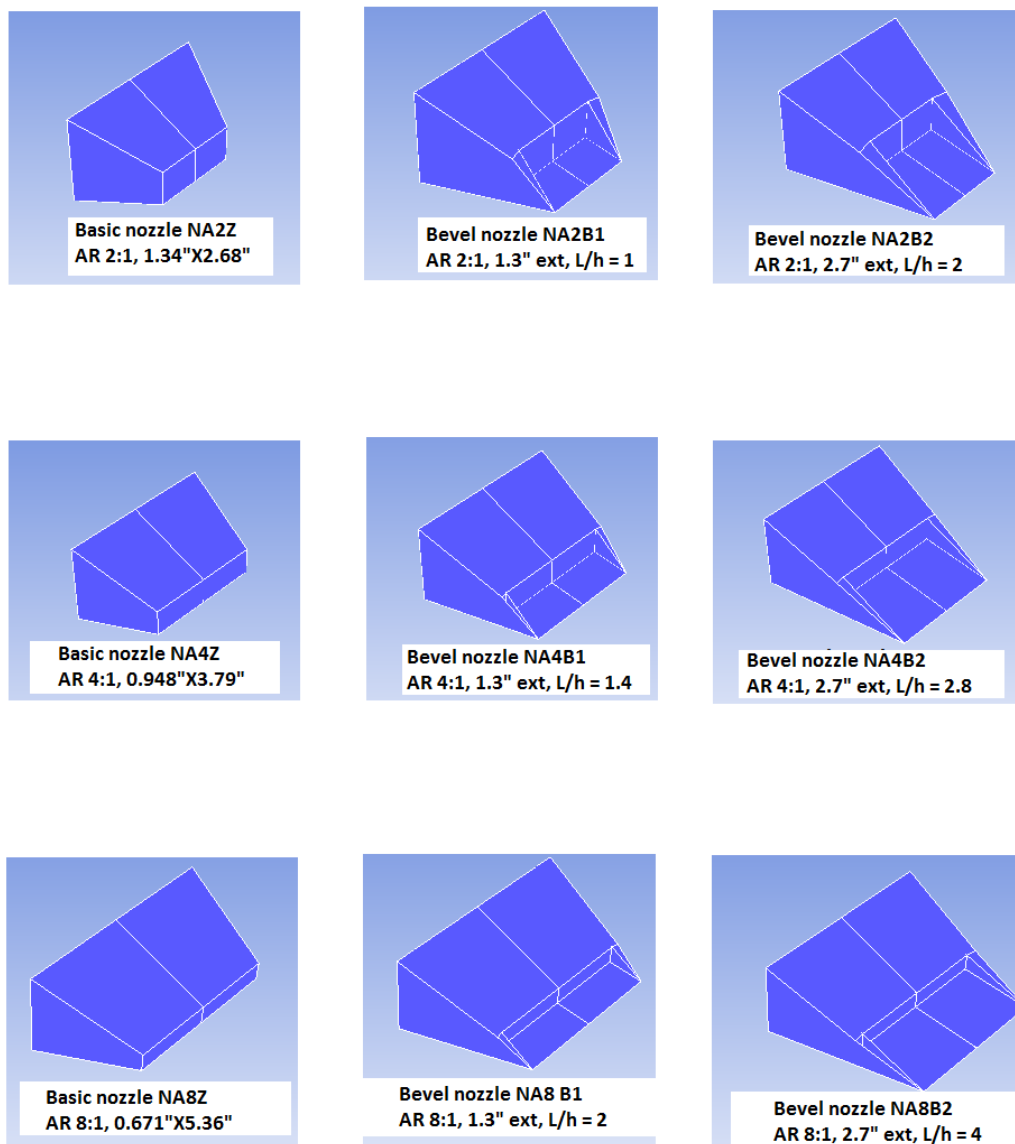Fig. 5.7 Details at nozzle exit, Aspect Ratio (*AR*) and Bevel Length Ratio (*BLR*)

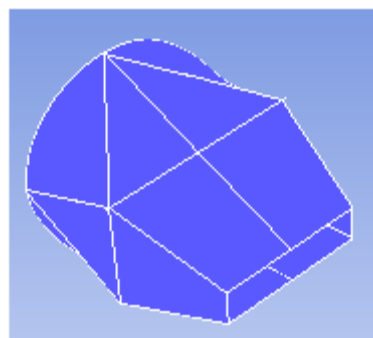Fig. 5.8 Nozzle geometry for Rectangular and Bevel nozzles

Fig. 5.9 Rectangular nozzle full geometry (AR 4, NA4Z)

5.2.2 Gridding Strategy

The jet emanating from a rectangular nozzle does not hold its rectangular profile beyond downstream distance of $x/D_j = 7$ from nozzle exit due to the induced velocities of stream wise vortex pairs which causes the jet to spread and eventually take a circular shape (Zaman, 1996*b*). A cylindrical domain satisfies the above requirement to confine the developing jet completely. The axial extent of the domain was 30 times the nozzle equivalent diameter ($30D_j$) downstream of the nozzle exit and the radial extent of the domain was $10D_j$. Domain extent in the axial, radial and azimuthal directions was finalized after analyzing the predicted length and thickness of the potential core and also the shear layer thickness. Grid independence study was carried out on four grid sizes, viz. 1.2 million, 1.8 million, 2.4 million and 3 million cells. It was observed that the variation in the potential core length were within 1% when grids of 2.4 and 3 million cells were compared and it is shown in Figure 5.10(a). The computational domain has been discretized using a hybrid mesh (90% hexahedral and 10% tetrahedral) with approximately 2.5 million cells as shown in Figure 5.10(b).
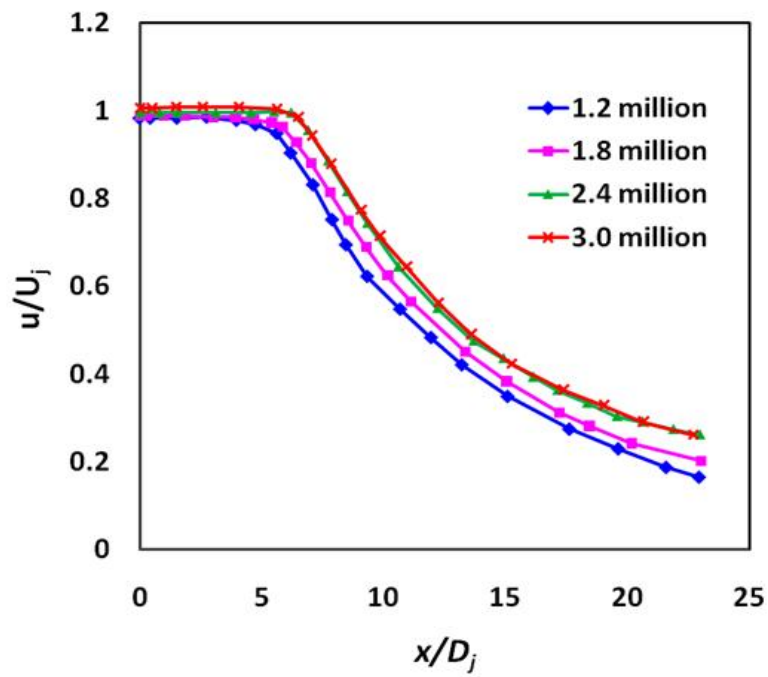
(a)
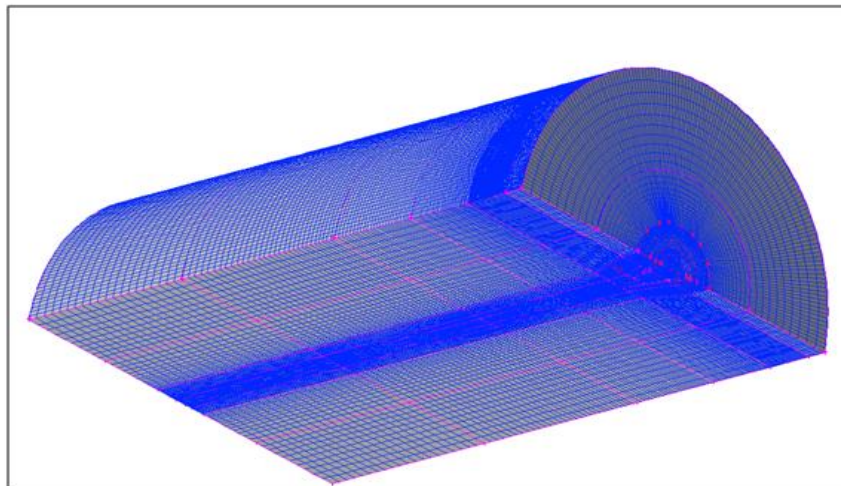
(b)

Fig. 5.10 (a)Comparison of grid resolution (rectangular nozzle NA2Z)
             (b) Computational domain with mesh
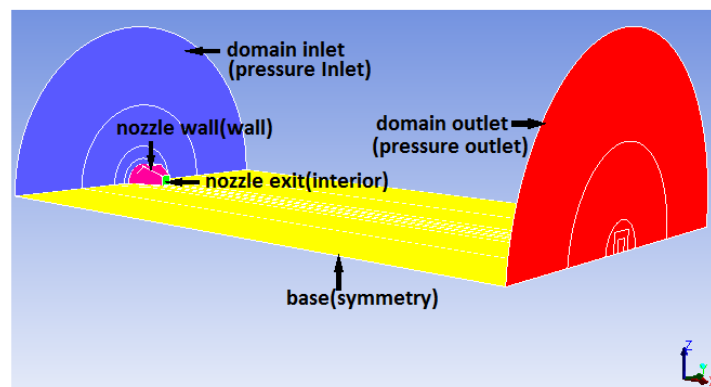
5.2.3 Boundary conditions

Computational domain indicating the boundary types and boundary conditions is shown in figures 5.11 (a) and (b). The nozzle inlet, domain inlet and top entrainment surfaces have been defined as pressure inlet with the total pressure and temperature specified. The domain outlet and bottom boundary were treated as pressure outlet and symmetry surface respectively. The RANS based solver has been used for carrying out calculations with standard wall functions and adiabatic solid surfaces. Table 5.3 represents the inlet conditions for the simulated jets.

Table 5.3 Flow properties for rectangular nozzles.

Properties	Values
M_a	0.9
T_j / T_∞	0.835
P_∞ (Pa)	101325
ρ_∞ (kg/m^3)	1.225561
U_∞ (m/s)	0
T_∞ (K)	303.0
T_0(K)	294
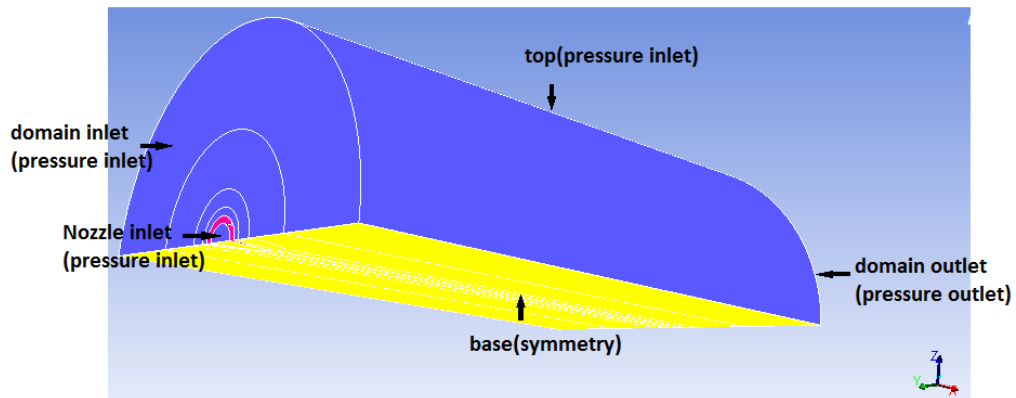
(a)

(b)

Fig. 5.11 Computational domain with boundary conditions (a) outside view showing
    nozzle inlet (b) inside view showing location of nozzle exit relative to
    domain inlet

5.2.4   Numerical Procedure

The RANS simulations were performed on a 3D computational domain using

commercial software, ANSYS 14.0. The turbulence model SST $k\text{-}\omega$ was found to be

accurate and robust for a wide range of boundary layer flows with pressure gradient.

The blending function in this turbulence model allows gradual transition from the

standard k–ω model near the wall to the k–ε model in the outer portion of the boundary layer. The least square cell based method was used for the descretisation, the SIMPLE method for the pressure velocity coupling and the second order upwind scheme for the convection term together with transport equations. In the present simulation, mesh refinement near the no-slip surfaces was such that the near wall spacing was maintained in the range of 5 μm to 10 μm. Adequate resolution in the axial, radial and azimuthal directions was maintained and the calculations were carried out till the residuals for all the governing equations were less than 10^{-5}.

5.3   ACOUSTIC CALCULATIONS

Initially, steady state calculations were run till the overall mass balance in the domain was less than 1% of the mass flow rate through the nozzle. At this point, second order accurate unsteady calculations were started. The time step size was 5 μs and the unsteady calculations were run till there was no change in the predicted values of the overall sound pressure level (SPL). The fluctuating acoustic pressure at the receiver locations were then calculated using the Ffowcs Williams-Hawkings integral method (Lyrintzis, 2003). These receiver locations are the same as the ones used by Andersson *et al.* (2004) for round nozzles (Figure 5.12) and by Bridges (2012) for rectangular nozzles (Figure 5.13). One set of receivers, located at a distance of $30D_j$ from the nozzle exit in the polar plane have been used for the round nozzle where as for the rectangular nozzle the receivers were located both in polar and azimuthalplanes. The time history of the pressure on the FW-H surface is used as the input for the acoustic calculation. This surface is made large enough to enclose all the acoustic sources, in this case, the shear layer and the mixing region. The dimensions of the acoustic surface used here are similar to the one used by Uzun *et al.* (2003). In

the FW-H method, 'Forward-time projection' is used to account for the time-delay between the emission time (the time at which the sound is emitted from the source) and the reception time (the time at which the sound arrives at the receiver location) which in turn is used for computing sound pressure. The overall SPL at a receiverlocation has been calculated using

$$SPL = 20\log_{10}\left(\frac{\sqrt{\langle(P'^2)\rangle}}{P_{ref}}\right) \qquad (5.1)$$

where $P_{ref} = 20 \times 10^{-6}$ Pa. The noise spectra at each receiver location have been obtained using FFT.
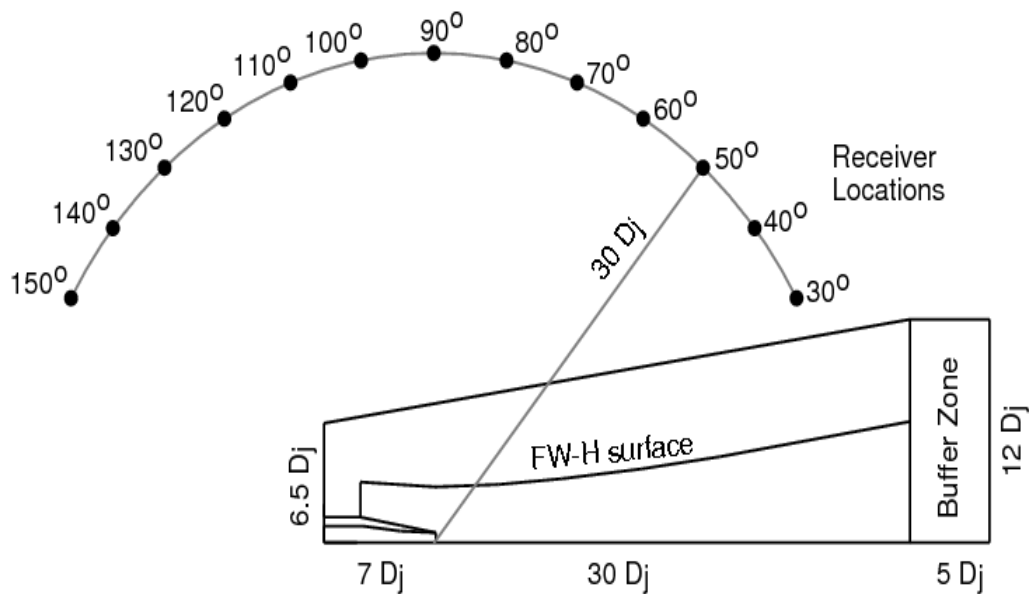

Fig. 5.12   Cross-sectional view of the computational domain along with locations of far field receivers
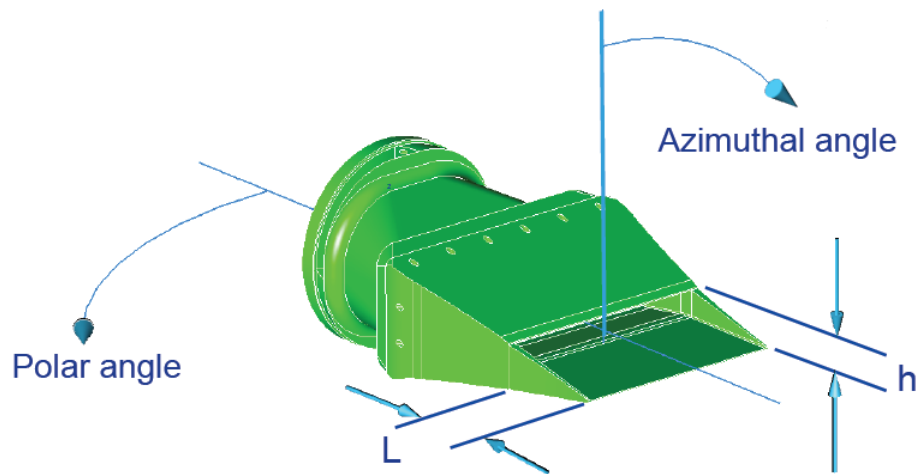
Fig. 5.13 Definition of polar angle and azimuthal angle for rectangular nozzle
(Bridges, 2012)

CHAPTER - 6

FLOW CHARACTERISTICS OF JETS EMANATING FROM ROUND AND BEVEL NOZZLES

6.1   INTRODUCTION

The new designs in the nozzle geometry intended to reduce the noise level from the jet, can more easily be evaluated using computationally less expensive RANS simulation. The flow field and hence the noise generation is dominated entirely by turbulent mixing in subsonic jets. Numerical simulations of a turbulent compressible subsonic jet from round and bevelled nozzles were carried out using ANSYS 14.0. The Mach number at exit for the above nozzles was 0.75. Simulations were performed in a three dimensional computational domain using steady RANS equations and SST k-ω turbulence model. The computational domain was discretized using hexahedral / tetrahedral mesh with approximately 2 million cells. The flow was investigated for axial and radial profiles of velocity components, shear layer thickness, self preserving nature, turbulent intensity, turbulent viscosity and Reynolds's stresses.

6.2   VALIDATION OF NUMERICAL MODEL

The predictions from the circular jet were compared with the experimental data reported by Jordan *et al.* (2002) and LES data reported by Andersson *et al.* (2004), for the purpose of validation. The distribution of centre line velocity (which decides the potential core length) is shown in Figure 6.1 and seen to be in reasonable agreement with experimental data.
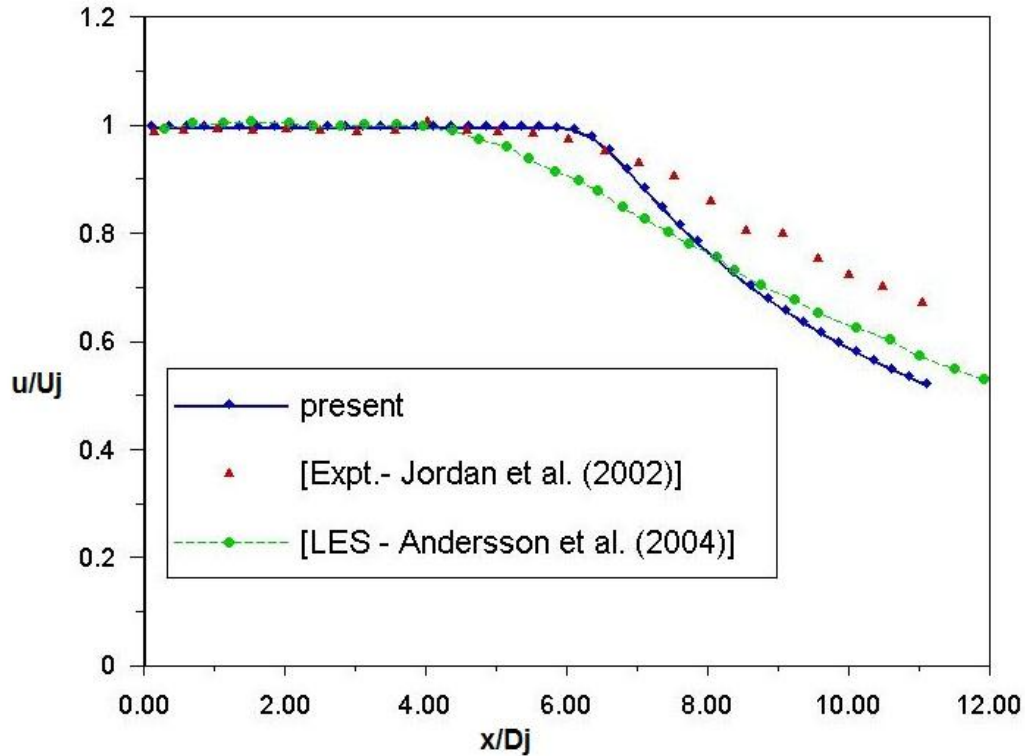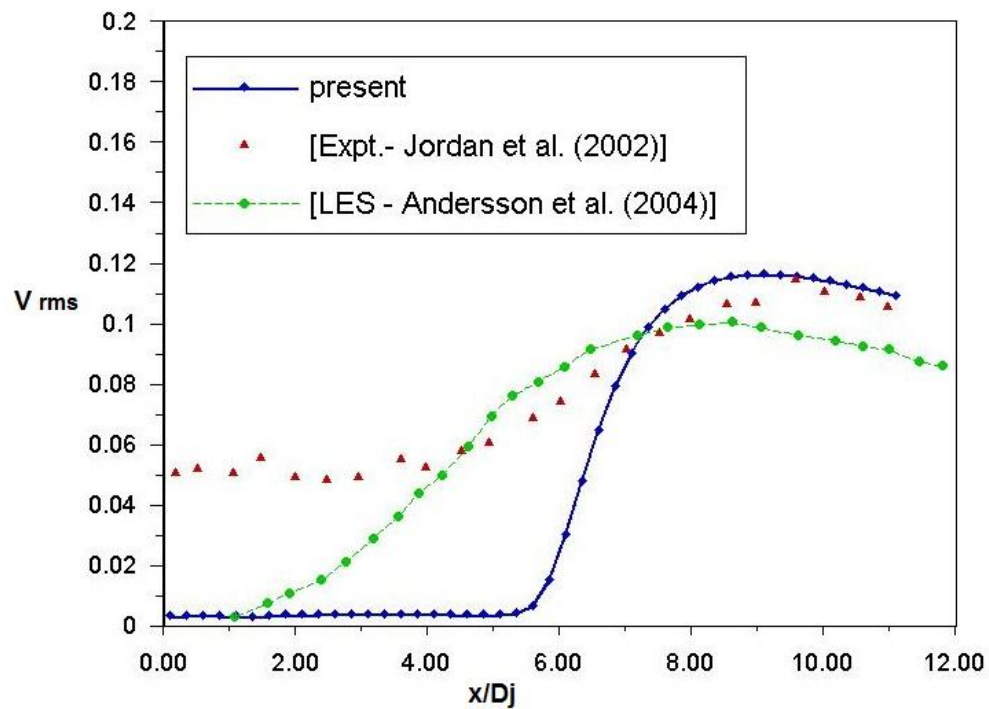
Fig. 6.1 Variation of mean axial velocity along the centreline for round nozzle

The distribution of centre-line turbulent intensity (u_{rms} and v_{rms}) from the present numerical predictions for the circular jet is compared with the experimental data reported by Jordan *et al.* (2002) and LES data reported by Andersson *et al.* (2004) in Figures 6.2 and 6.3. The present numerical predictions particularly for the position and magnitude of the peak turbulent intensity seem to be in reasonable agreement with experimental data. The turbulence anisotropy is captured by the numerical calculations and is indicated by the difference in levels of fluctuating quantities u_{rms} and v_{rms} in Figure 6.4.
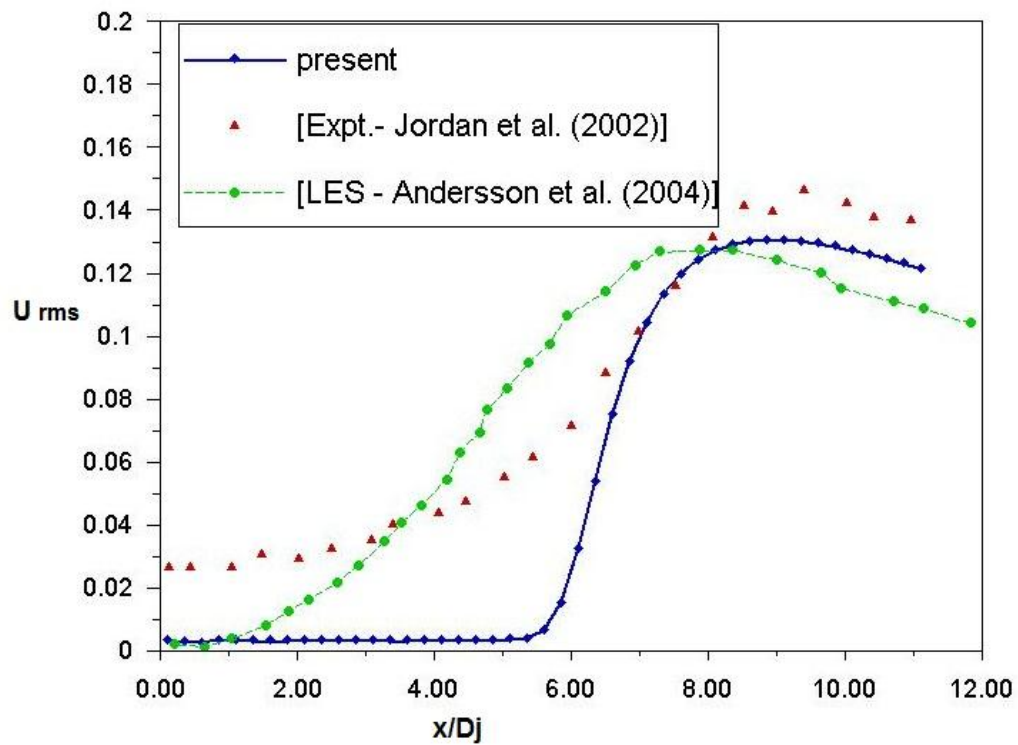
Fig. 6.2 Variation of u $_{rms}$ along the centreline for round nozzle

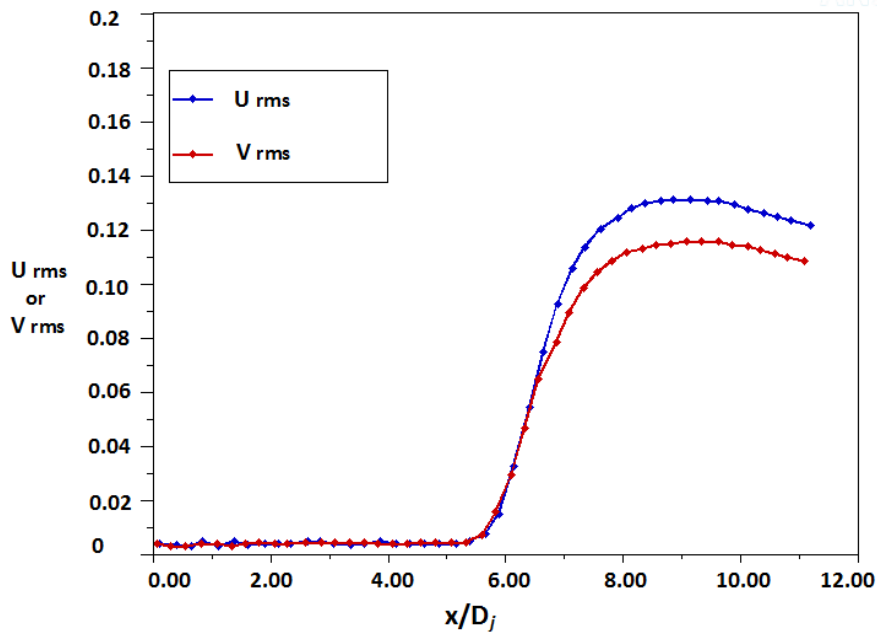Fig. 6.3 Variation of v $_{rms}$ along the centreline for round nozzle

Fig. 6.4 u $_{rms}$ and v $_{rms}$ along the centreline for round nozzle in present simulation.

6.3   RESULTS AND DISCUSSION

6.3.1   Comparison of mean axial velocity

The mean velocity distribution plotted on the central plane for both bevel and round nozzles are presented in Figure 6.5(a) and (b). It clearly shows that the jet plume is deflected towards the shorter lip of the beveled nozzle. It also gives information about the potential core and the downstream flow development. Figure 6.6 shows the comparison of mean axial velocity along the centreline. Potential core length (axial location where the average axial velocity is 0.95 times the jet velocity at nozzle exit U_j) is obtained as $6.5D_j$ for the round nozzle which is similar to the experimental value reported by Jordan *et al.* (2002). The bevel nozzle has a reduced potential core length of $5D_j$. The reduction in potential core length indicates that better turbulent mixing has taken place in bevel nozzle when compared to round nozzle. The radial profiles of axial velocity at   axial locations $x/D_j = 2$ to 12 in steps of 2 are shown in Figure 6.7 (a) and (b), which indicates the down stream development of the flow.
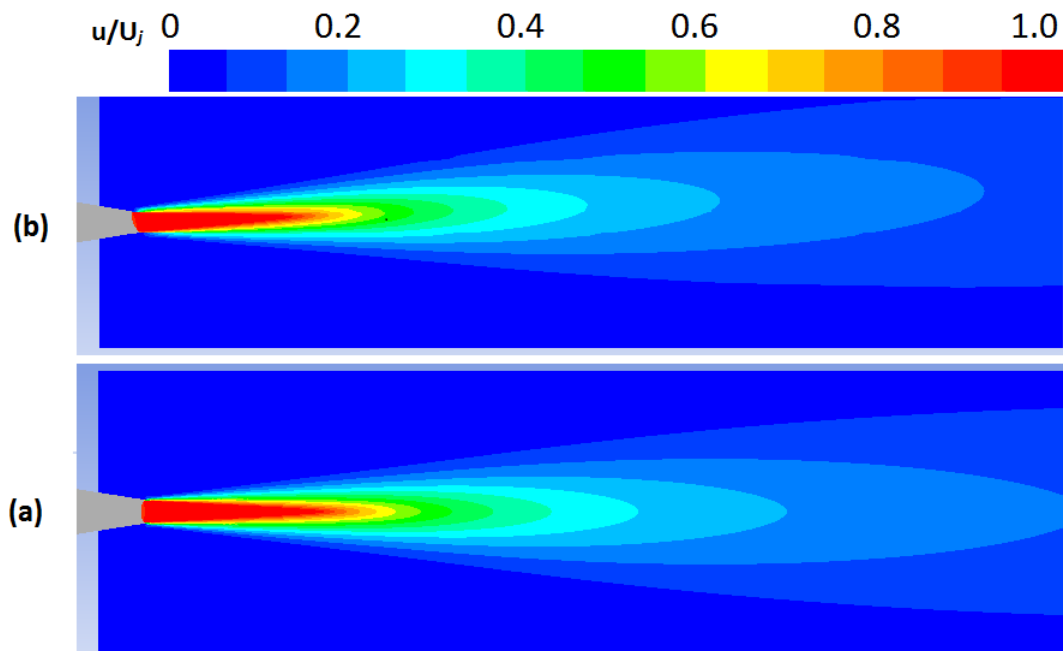
Fig. 6.5 Mean velocity distribution in the central plane (a) Round and (b) Bevel
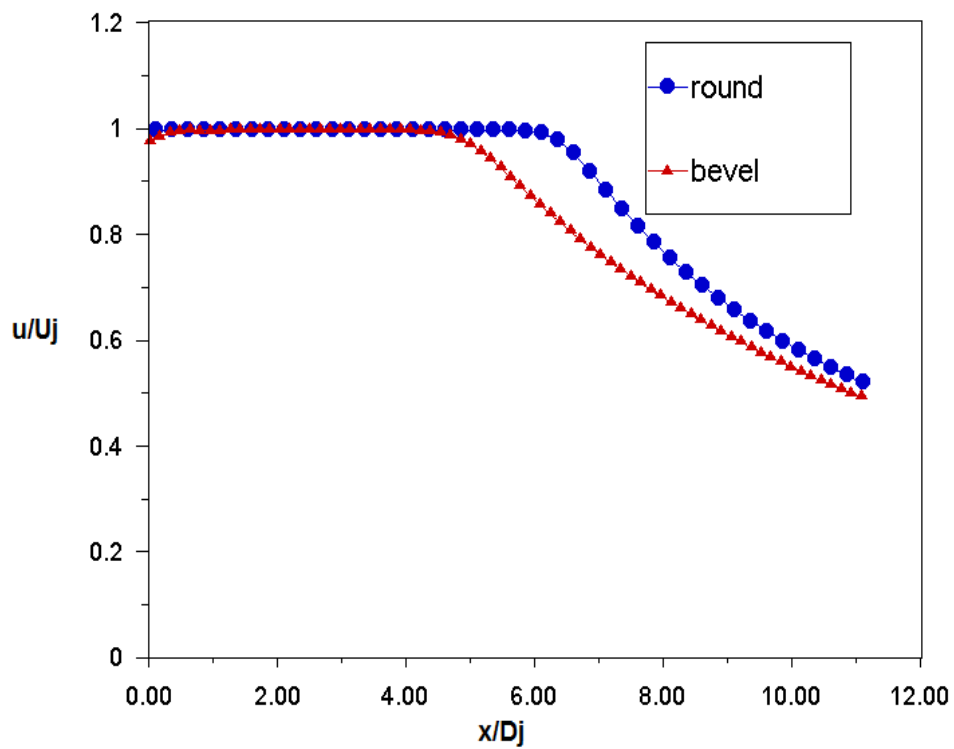

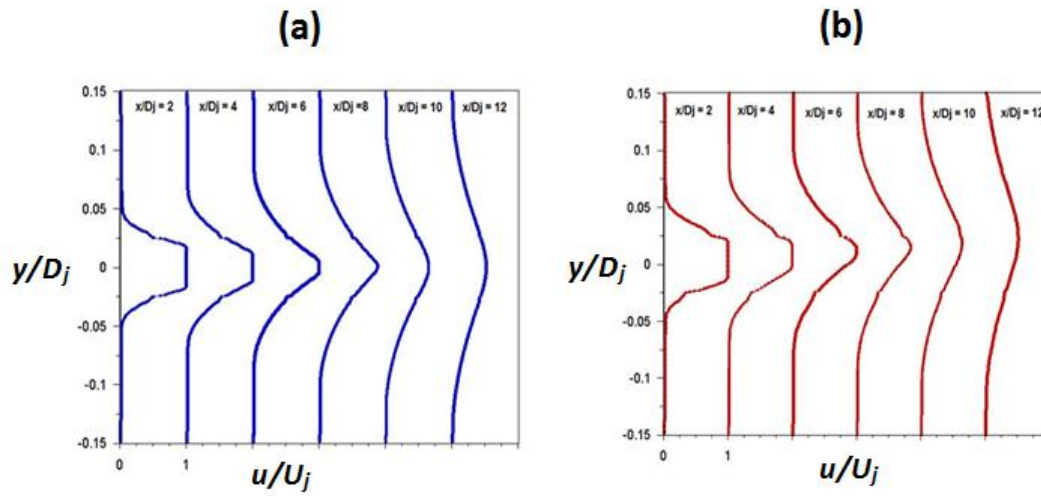Fig. 6.6 Variation of mean axial velocity along the centreline

Fig. 6.7 Radial profile of velocity at different axial stations. (a) Round and (b) Bevel

The comparison of general flow pattern can be visualized from the Mach number contour (Fig.6.8) plotted on radial planes at different axial stations (x/D_j= 1, 2.5 and 5). The beveling of nozzle causes narrowing of the jet in the plane normal to the symmetry plane while the jet widens along the symmetry plane.
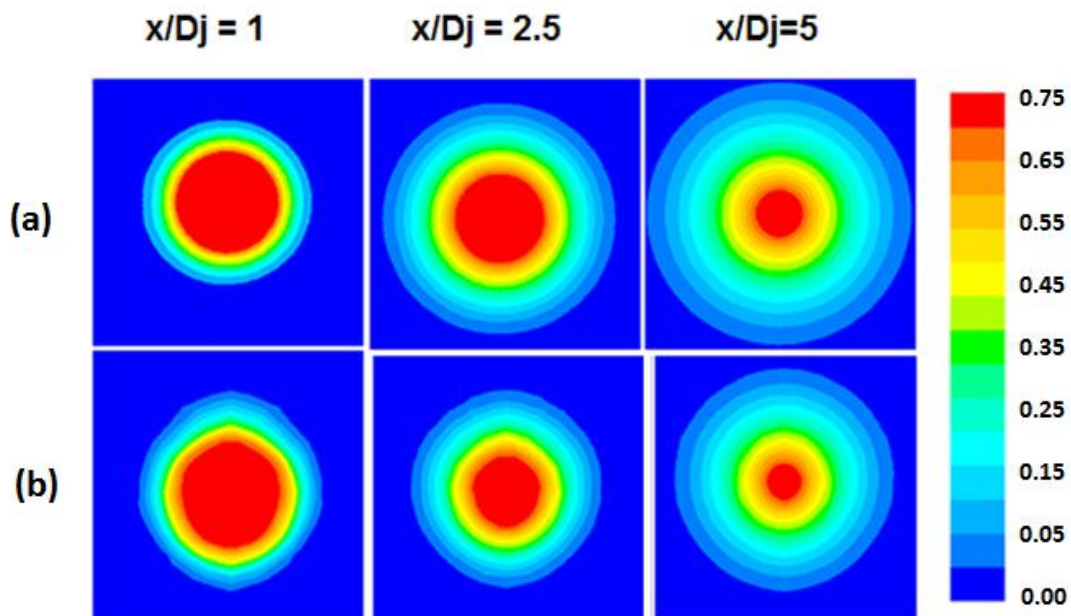

Fig. 6.8 Mach number contours for (a) Round & (b) Bevel

6.3.2   Shear layer thickness

The variation of shear layer thickness as defined by Arakeri *et al.* (2003) is given by $\delta = (R_{0.95} - R_{0.1})$,   where $R_{0.95}$ and $R_{0.1}$ being the radial locations where $u/U_{centreline} = 0.95$ and 0.1 respectively. When compared to round jet, the beveled jet has a wider shear layer region which is consistent with its shorter potential core and faster flow development with increase in x/D_j. The virtual origin is located as the x-intercept of the straight line fit to shear layer thickness (Fig. 6.9) and the value found to be $x_0/D_j =$ -0.92 and -1.1 for round and beveled nozzles respectively.
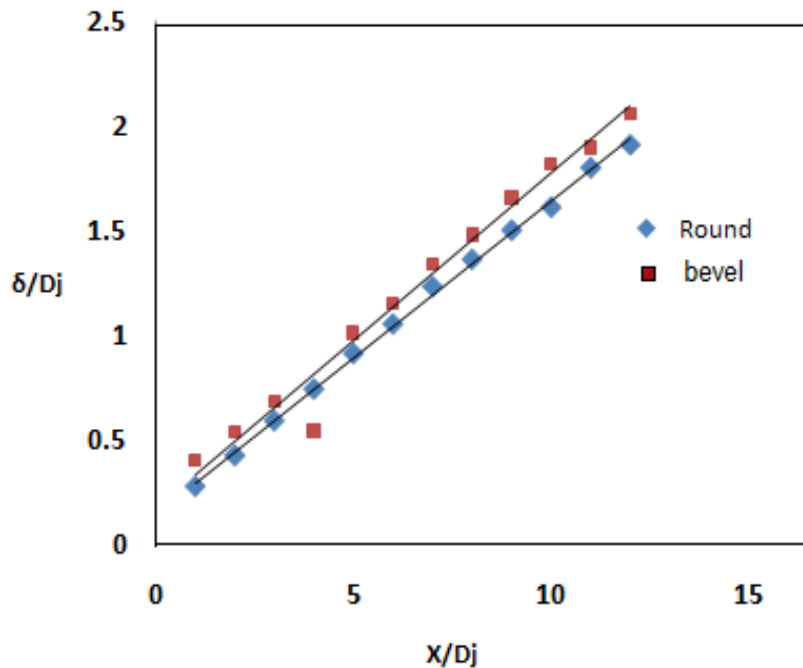

Fig. 6.9 Variation of shear layer thickness

6.3.3   Self similarity

A study on the self similarity of the jets was also performed to see whether the velocity profile collapsed at axial stations downstream of the flow. Self preservation or self-similarity is said to occur when the profiles of velocity can be brought to congruence by simple scale factors which depend on only one transformed coordinate. The study was conducted by plotting u/U_c against $(y-y_{0.5})/(x-x_0)$ at different axial

stations where U_c is the centreline velocity, $y_{0.5}$ is the jet half width and x_0 is the virtual origin. The axial stations were selected from $x/D_j = 2$ to 10 in steps of 2. For the round nozzle the velocity profile at all the downstream axial stations were collapsed and hence the jet is said to be self similar with respect to dimensionless downstream distance which is shown in Figure 6.10(a). For the bevel nozzle there are some deviations upto $x/D_j = 4$ and beyond which it is found to be similar to round nozzle and is clearly visible from Figure 6.10(b). Carazzo *et al.* (2006) have explained the influence of initial conditions, nozzle geometry and turbulence structures on the self similarity of the jets. Non identical states of self similarity can be linked to the turbulent structures and at intermediate distances, large-scale structures appear in the flow. However at large distances from nozzle exit, they eventually become permanent and the flow is fully self similar. Thus, self preservation implies that the flow has reached a kind of equilibrium where all of its dynamical influences evolve together, and no further relative dynamical readjustment is necessary. Self preservation is therefore defined as an asymptotic state attained by a particular flow, after its internal adjustments are completed.
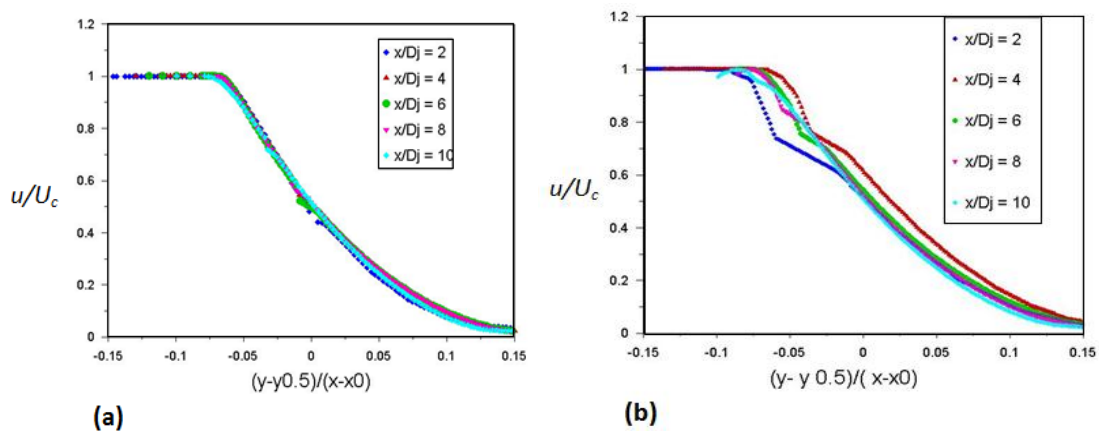

Fig.6.10 Variation of *u /U* centreline with *(y-y$_{0.5}$)/(x-x$_0$)* (a) Round & (b) Bevel

6.3.4 Fluctuating Quantities

The turbulence intensity field along the axial stream wise plane and along the radial planes at different axial locations (x/Dj = 1, 2.5, and 5) for both bevel and round nozzles are presented in Figures 6.11 and 6.12 respectively. From the results it is clear that better initial mixing occurs in the case of bevel nozzle. The variation of fluctuating quantities $\overline{u'u'}^{1/2}$ and $\overline{v'v'}^{1/2}$ along the axis for the round and bevel nozzles are shown in Figures 6.13 and 6.14 respectively. These figures clearly indicate the position and value of maximum turbulence intensity. The turbulence anisotropy is captured by the numerical calculations and is indicated by the difference in levels of fluctuating quantities $\overline{u'u'}^{1/2}$ and $\overline{v'v'}^{1/2}$. The present calculations predicted the position of peak values of turbulence intensity quite well for the round and bevel nozzle. From the plot, it is clear that the turbulence intensity peak is close to the nozzle exit for the beveled nozzle when compared to round nozzle. This is due to higher initial mixing and thereby the reduced potential core length for bevel nozzle is validated. The variation of fluctuating quantities $\overline{u'u'}^{1/2}$ and $\overline{v'v'}^{1/2}$ along radial lines at diffrent axial stations (x/Dj = 1, 2.5, and 5) for the round and bevel nozzles are shown in Figures 6.15 and 6.16. The radial location of the turbulence intensity peak for both the nozzles supports the previous findings and justifications. Axial variation of $\overline{u'v'}$ which indicate the turbulent viscosity for the round and bevel nozzles is shown in Figure 6.17. The values of turbulent viscosity for bevel nozzle seems to be lesser than the round nozzle along the axial direction. The peak values predicted are 0.73 and 0.57 for round and bevel nozzles respectively.
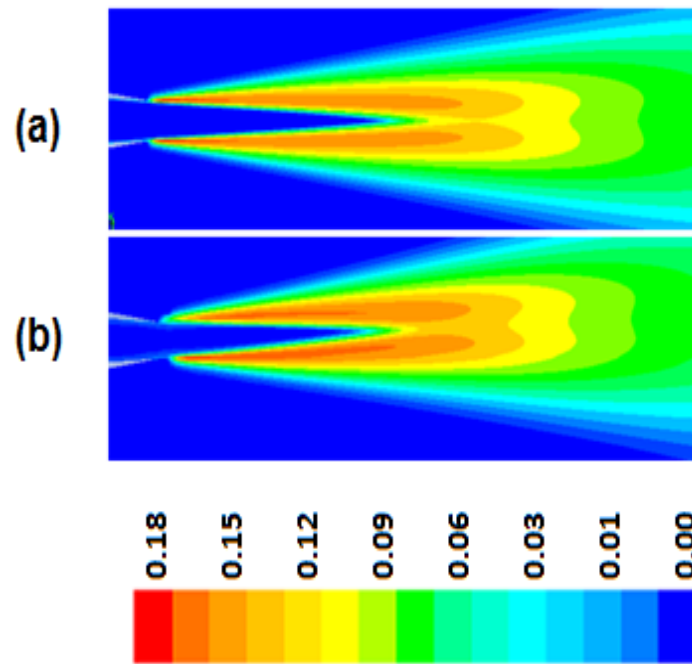
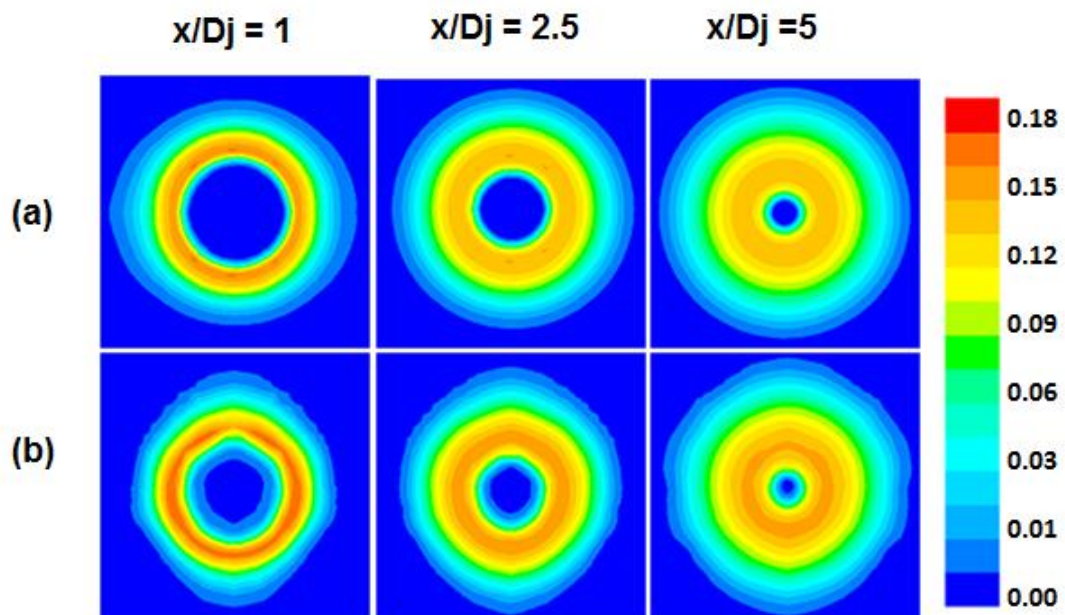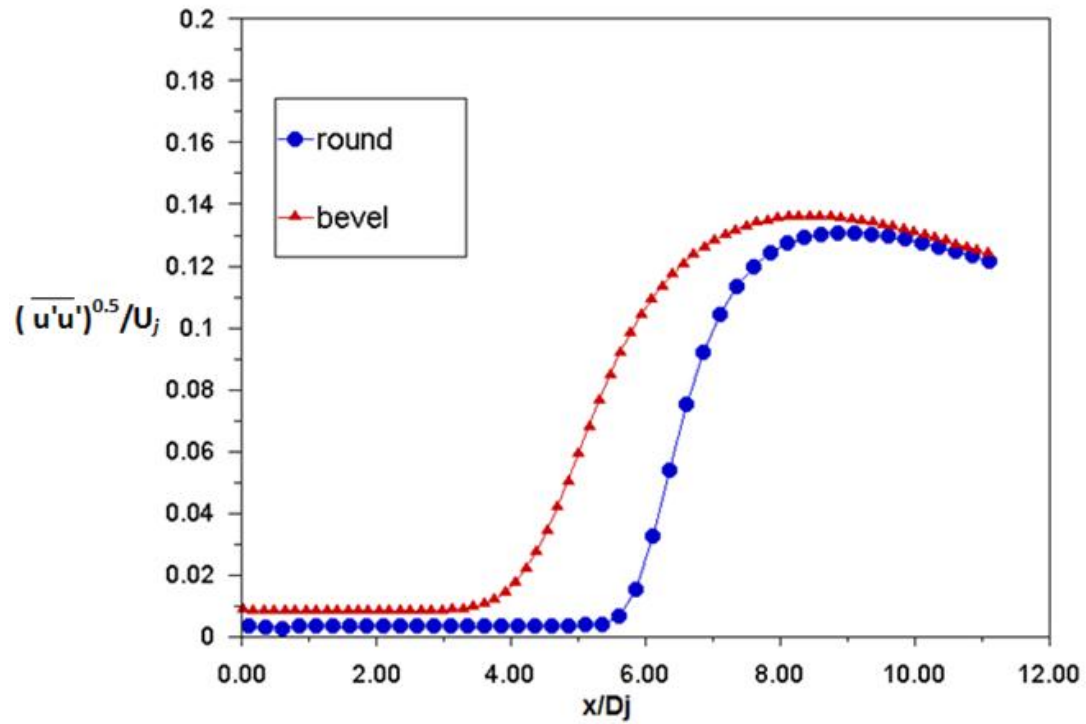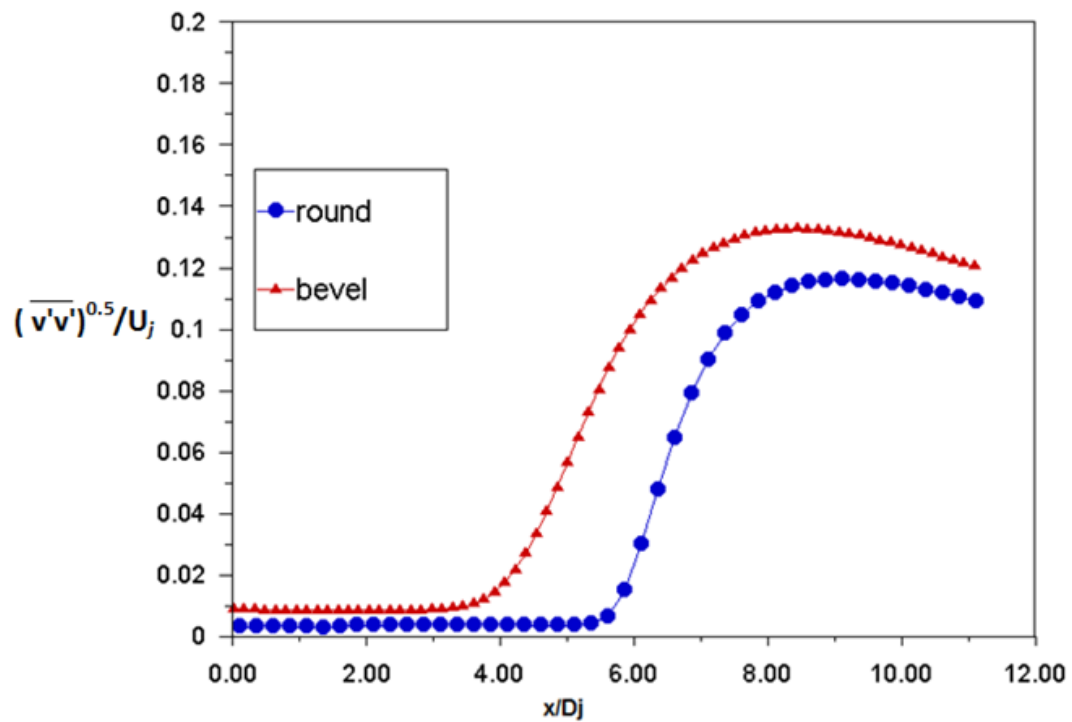Fig. 6.11 Turbulence Intensity distribution in the central plane (a) Round & (b) Bevel
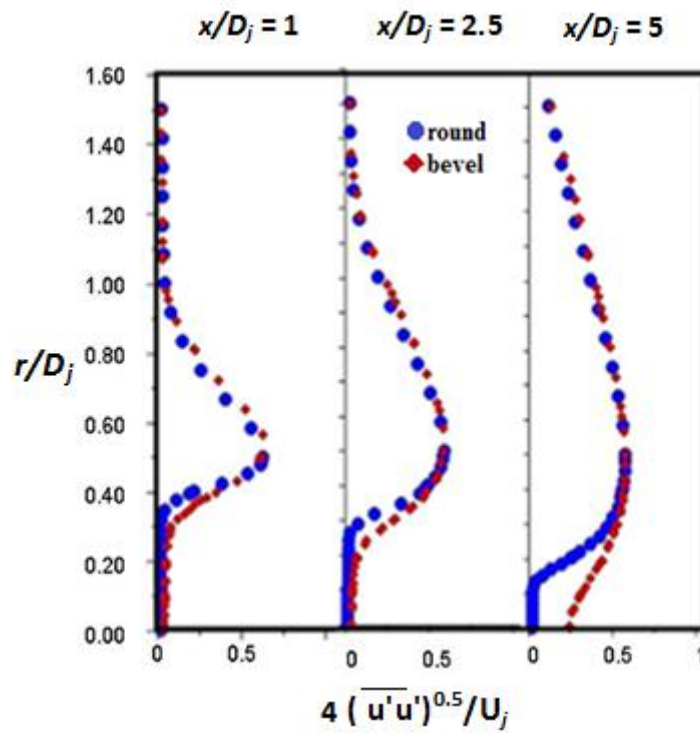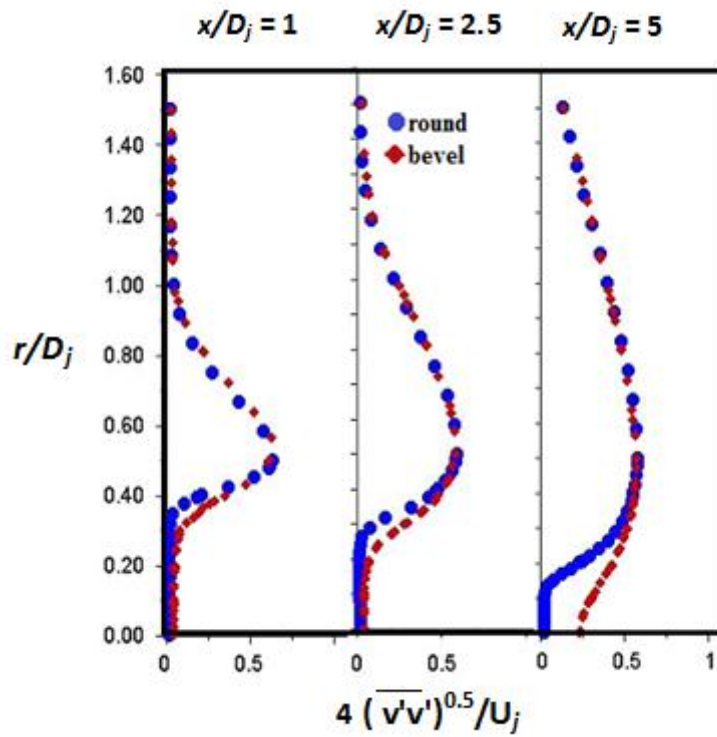

Fig. 6.12 Turbulence Intensity contours for (a) Round & (b) Bevel

Fig. 6.13 Variation of u $_{rms}$ along the centreline

Fig. 6.14 Variation of v $_{rms}$ along the centreline

Fig. 6.15 Radial profile of u $_{rms}$ at different axial stations

Fig. 6.16 Radial profile of v$_{rms}$ at different axial stations

Fig.6.17 Axial variation of peak turbulent viscosity
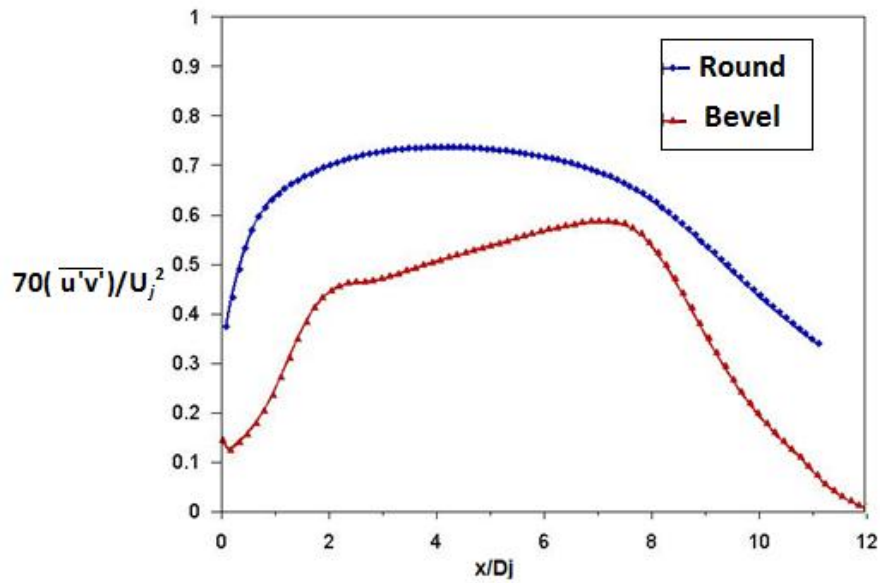
6.3.5 Overall Sound Pressure Level

The overall sound pressure level for the round and bevel nozzles were calculated at different receiver locations as shown in Figure 6.18. At all receiver locations the overall sound pressure level for the bevel nozzle is found to be less when compared to the round nozzle.
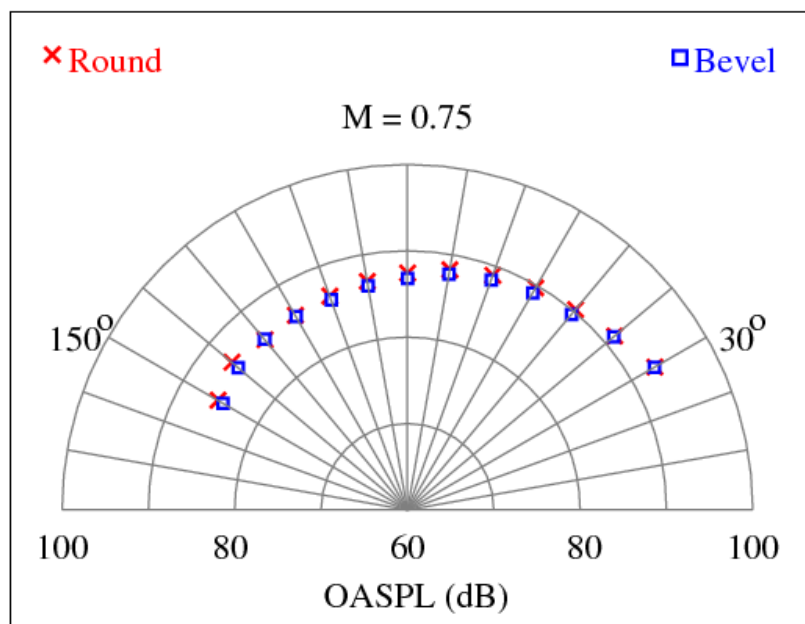

Fig. 6.18 Sound Pressure Level for round and bevel nozzles

6.4   SUMMARY

A computational analysis of a subsonic jet from round and bevelled nozzles has been performed using RANS calculations with SST k-ω turbulence model. The simulations were carried out with a comparatively smaller grid size than that normally used for LES. The predictions seem to be reasonably good for fluctuating quantities such as, $\overline{u'u'}^{1/2}$ and $\overline{v'v'}^{1/2}$ and turbulence viscosity when compared with available experimental data in the literature. Potential core length and shear layer thickness were predicted well in both cases. It was observed that bevel nozzle had a shorter potential core with an enhanced spreading of jet when compared with a round nozzle. The virtual origin was determined and self similarity profiles were plotted. The evaluation of shear layer thickness of bevelled jets also confirmed better spreading and lack of self similarity near to the nozzle exit. The peak values of turbulence intensity together with the turbulence anisotropy were captured accurately. The bevelled nozzle considerably improves turbulent mixing and thereby modifies the turbulent characteristics of the jet. The radial profile of velocities, the contours of Mach number, turbulence intensity and viscosity provide better knowledge on the flow field that is essential for the evaluation of acoustic benefit. The pressure fluctuations were captured at the receiver locations by acoustic analogy and acoustic benefit evaluated. Jet noise reduction was attained for all forward and aft receivers (30° to 150°) which were located outside the computational domain.

CHAPTER - 7

JET DYNAMICS OF FLOW EMANATING FROM PLAIN AND BEVEL RECTANGULAR NOZZLES

7.1   INTRODUCTION

Numerical simulations of subsonic jets using Reynolds Averaged Navier Stokes (RANS) equation coupled with turbulence models such as the *k-ω* and *k-ε* models can provide better knowledge on the flow field. The calculations provide information on the turbulence characteristics of jet and hence act as the database for the assessment of jet mixing noise. More extensive investigations were happening on rectangular turbulent jets than any other non circular jets over the past few decades due to its superior jet mixing and velocity decay rates. Numerical simulations of turbulent compressible subsonic jet from baseline rectangular nozzles with aspect ratios of 2:1, 4:1, 8:1 and its beveled nozzles (both long and short) were carried out using a commercial CFD software. The Mach number at exit for the above nozzles was 0.9. The simulations were performed in a three dimensional computational domain using steady RANS equations and SST *k-ω* turbulence model. The computational domain was discretized using hexahedral / tetrahedral mesh with approximately 2.5 million cells. The flow was investigated for the velocity fields, mean and variance of axial velocity. The impact of aspect ratio and bevel length on these parameters was also analyzed.

7.2.   RESULTS AND DISCUSSION

7.2.1.   Mean and Variance of Axial Velocity

A series of contour plots are presented for the rectangular plain and bevelled nozzle configurations for three aspects ratios of 2:1, 4:1 and 8:1 to acquire an insight into the velocity field.

7.2.1.1 Plain Rectangular Nozzle

The mean and variance of axial velocity are plotted on two axial stream wise planes, one containing the minor axis (x, y) and other containing the major axis (x, z). The same are also plotted on 11 cross stream planes at axial locations where $x/D_j=$ 0.1, 0.7, 1.1, 1.4, 2, 3.5, 5, 6.5, 8, 10 and 15. Both the stream wise and cross stream plane contours are presented side by side in Figures 7.1 to 7.6.

The predictions are compared with the experimental data reported by Bridges and Wernet (2015). The distinction in the flow fields with respect to aspect ratio of rectangular nozzles are well evident from these contours and it is reasonably matching with the experimetal data too. It is obvious from the contour of mean axial velocity that the potential core gets shortened with increase in aspect ratio. However, this fact cannot be quantified from these plots. The contours of variance of axial velocity give an indication of the turbulence intensity of the jets and the variation of which with respect to the aspect ratio is obvious from Figures 7.2, 7.4 and 7.6.
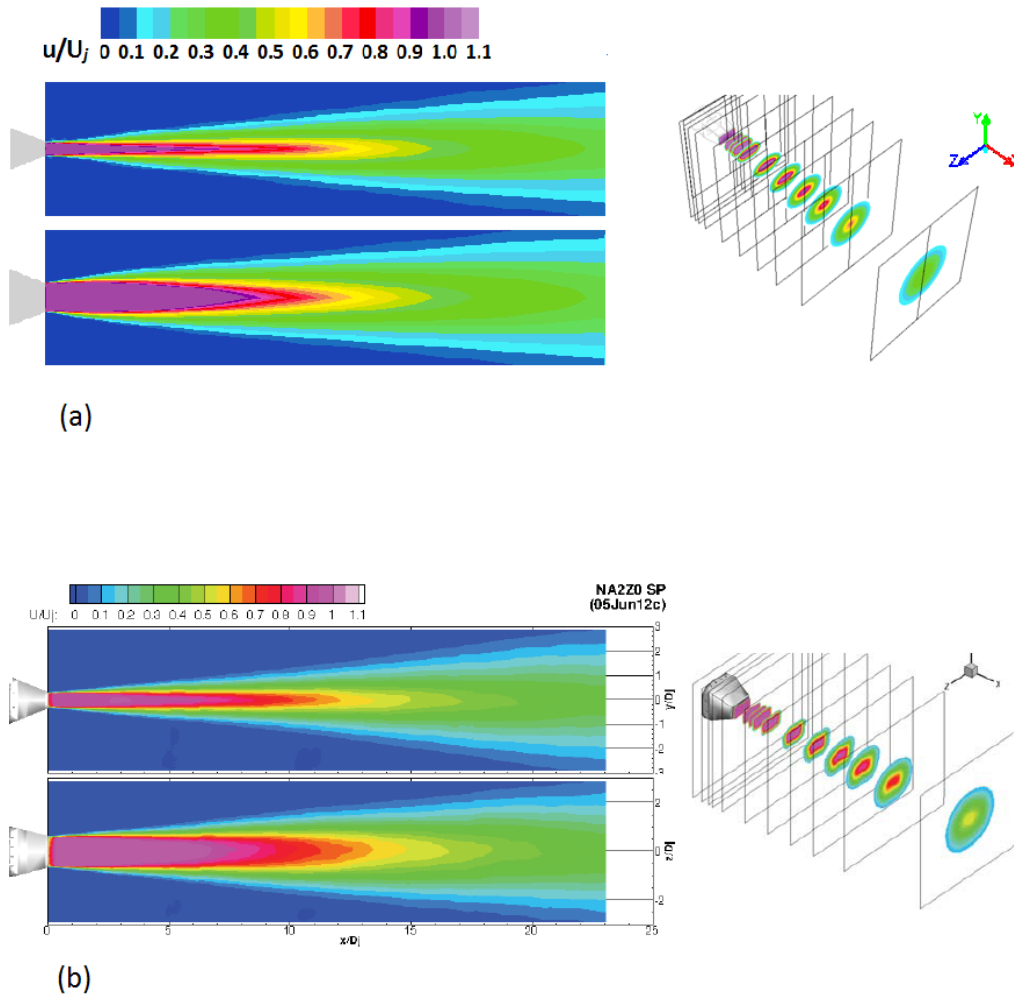
Fig.7.1   Mean axial velocity contour along the streamwise planes (left) and cross stream planes (right) for rectangular nozzle with aspect ratio 2:1 in (a) the present simulation and (b) experimental data reported by Bridges and Wernet (2015)

Fig. 7.2   Variance of axial velocity contour along the streamwise planes (left) and cross stream planes (right) for rectangular nozzle with aspect ratio 2:1 in (a) the present simulation and (b) experimental data reported by Bridges and Wernet (2015)

(a)

(b)

Fig. 7.3 Mean axial velocity contour along the streamwise planes (left) and cross stream planes (right) for rectangular nozzle with aspect ratio 4:1 in (a) the present simulation and (b) experimental data reported by Bridges and Wernet (2015)
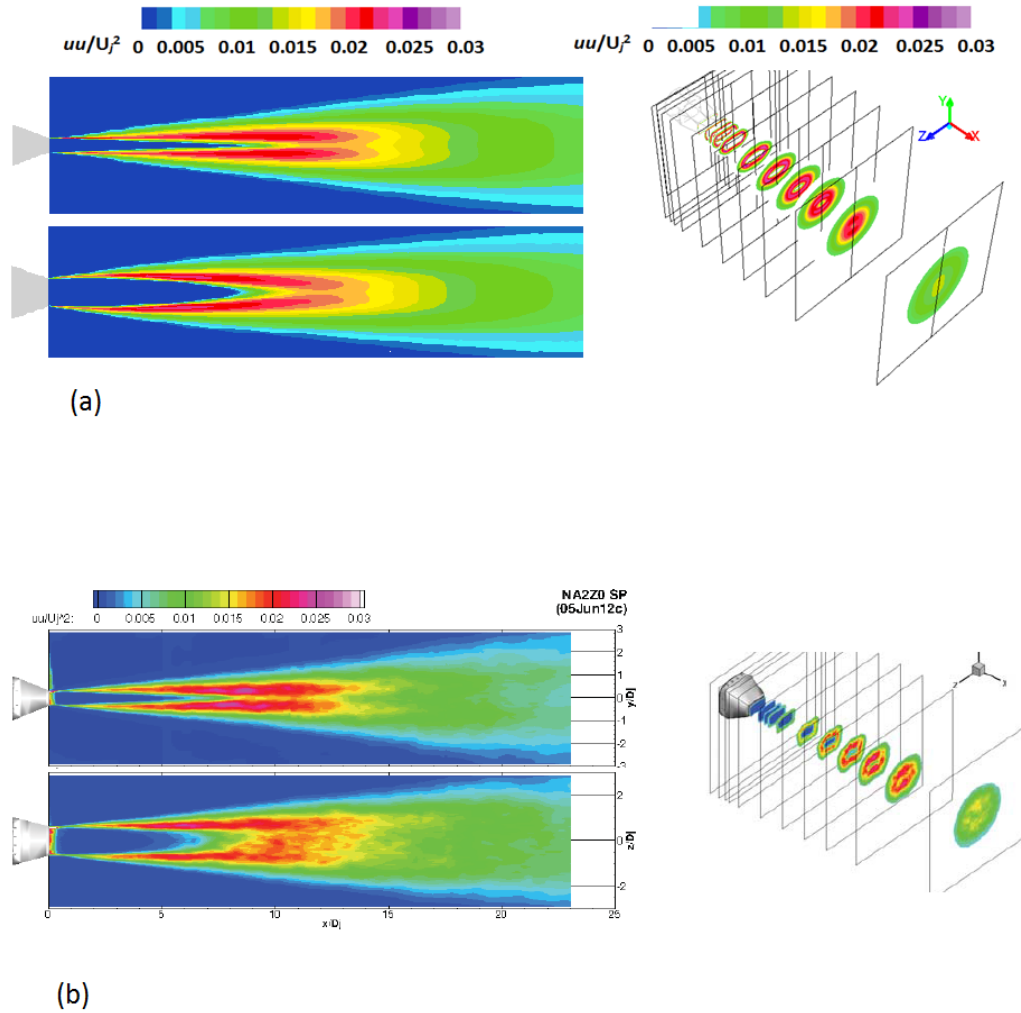
Fig. 7.4 Variance of axial velocity contour along the streamwise planes (left) and cross stream planes (right) for rectangular nozzle with aspect ratio 4:1 in (a) the present simulation and (b) experimental data reported by Bridges and Wernet (2015)
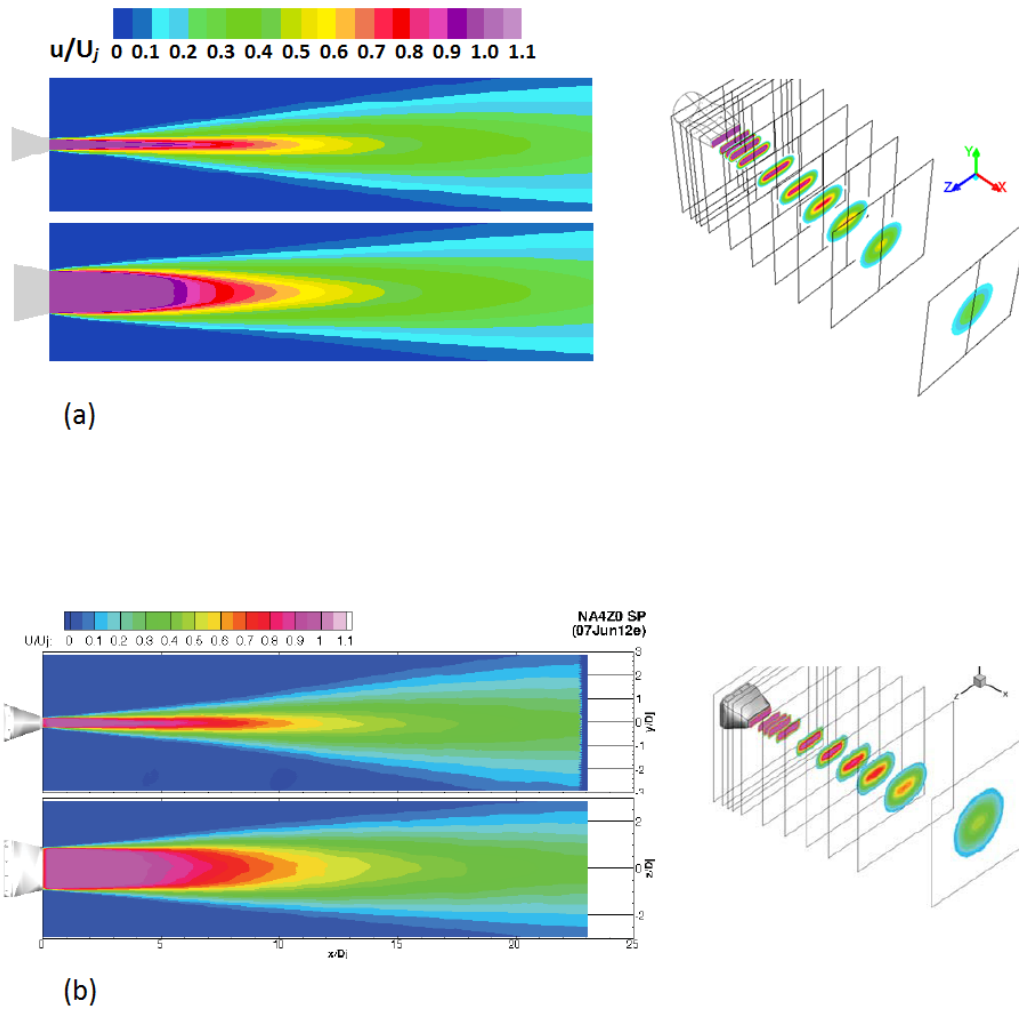
Fig. 7.5   Mean axial velocity contour along the streamwise planes (left) and cross stream planes (right) for rectangular nozzle with aspect ratio 8:1 in (a) the present simulation and (b) experimental data reported by Bridges and Wernet (2015)
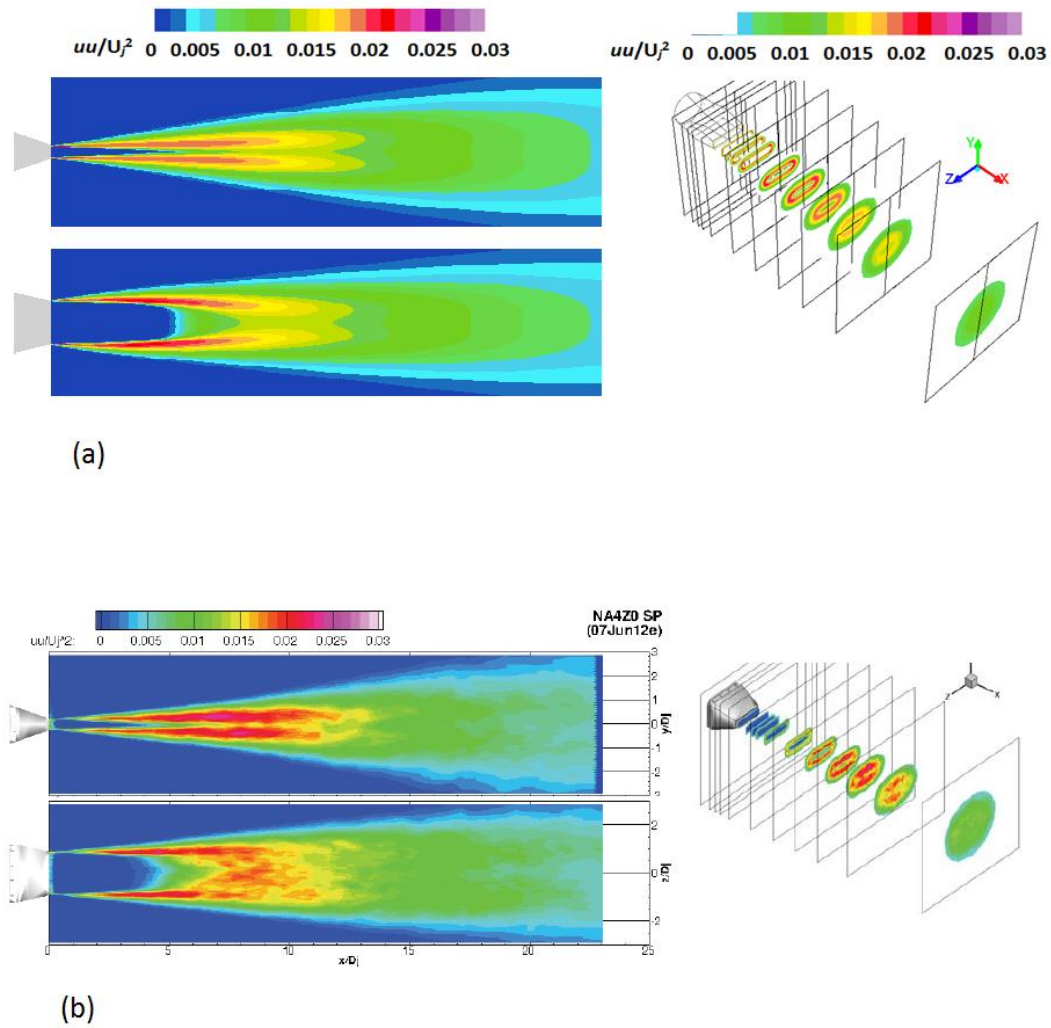
Fig. 7.6 Variance of axial velocity contour along the streamwise planes (left) and cross stream planes (right) for rectangular nozzle with aspect ratio 8:1 in (a) the present simulation and (b) experimental data reported by Bridges and Wernet (2015)
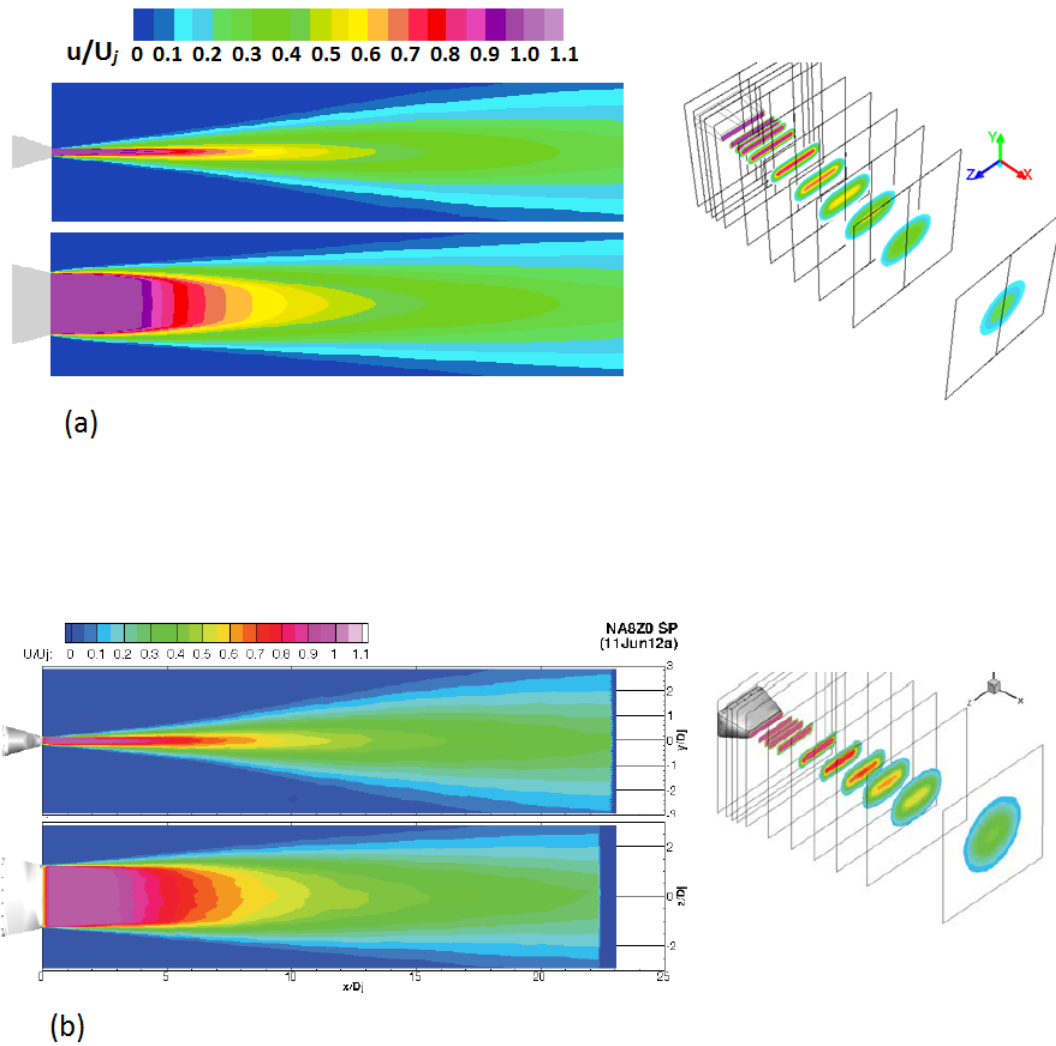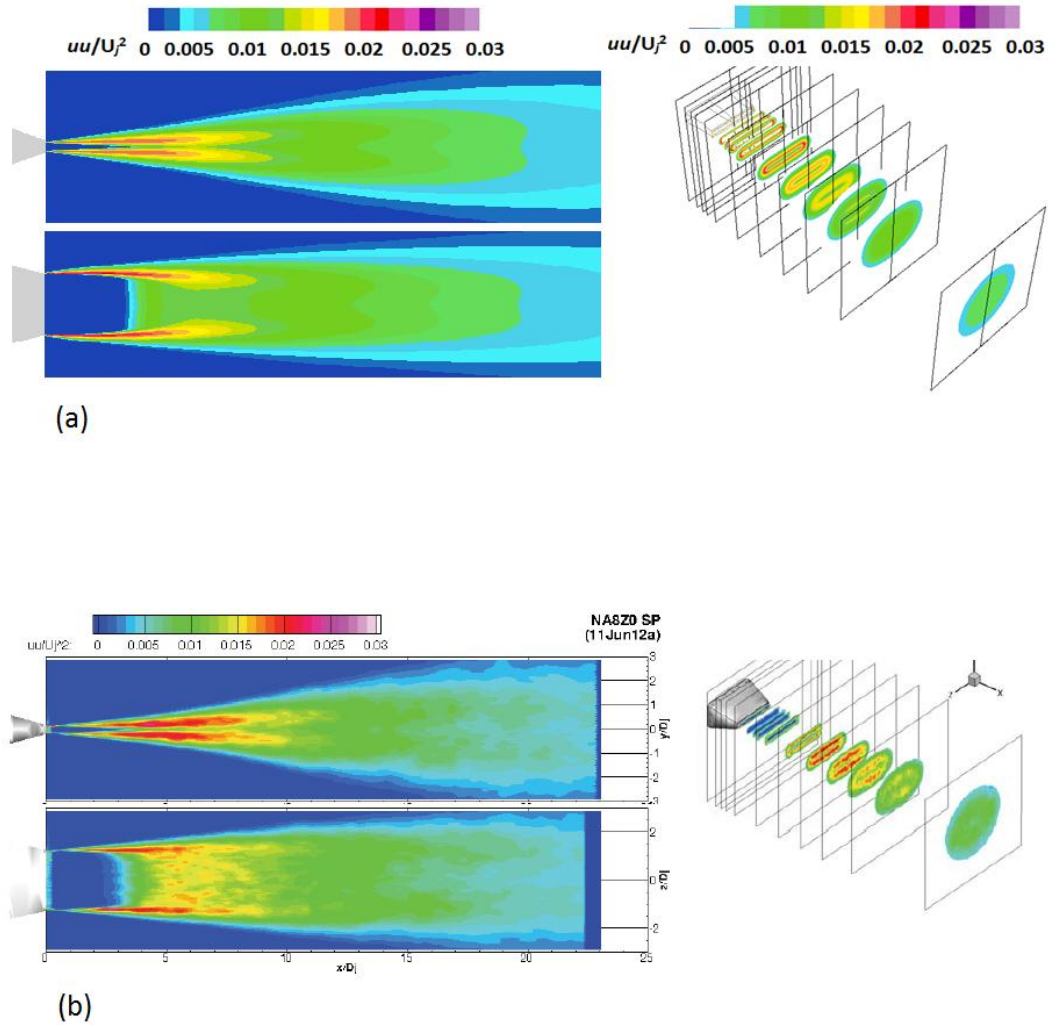
The position of jet centreline, major axis and minor axis liplines for the rectangular nozzles along which the variation of mean and variance axial velocity are plotted is shown schematically in figure 7.7. For rectangular nozzles with aspect ratio 2, 4, and 8 the variation of mean axial velocity along the centreline, and along both the major and the minor axis lip lines are plotted in Figures 7.8 to 7.16. The numerical predictions are also compared with the experimental data reported by Bridges and Wernet (2015). It is obvious from the centre line variation of axial velocity that the potential core gets shortened with increase in aspect ratio. Potential core length (axial location where the average axial velocity is 0.95 times the jet velocity at nozzle exit U_j) for the three rectangular nozzles is obtained as 6.0 4.0 and 3.0 for aspect ratios 2:1, 4:1 and 8:1 respectively. The predictions are matching well with the experimental values reported by Bridges and Wernet (2015). However, the decay of velocity is predicted well only for a certain length beyond which overprediction is observed in all the cases. The reduction in potential core length indicates that better turbulent mixing has taken place in high aspect ratio nozzles. The magnitude of axial velocity along the minor axis is overpredicted for all the nozzle configurations. The error is minimum within the potential core for nozzles with AR 2 and 8 with a variation of less than 10%. For the nozzle with AR of 4, the error in magnitude of axial velocity is found to be slightly higher than the other two and uniform throughout. In the case of velocity profiles along the major axis lip the diagreement is maximum for the nozzle with AR = 8 alone. In the variation of mean axial velocity along the the lip lines, the region of constant velocity and velocity decay as measured by the experiments are captured well in the numerical predictions also.
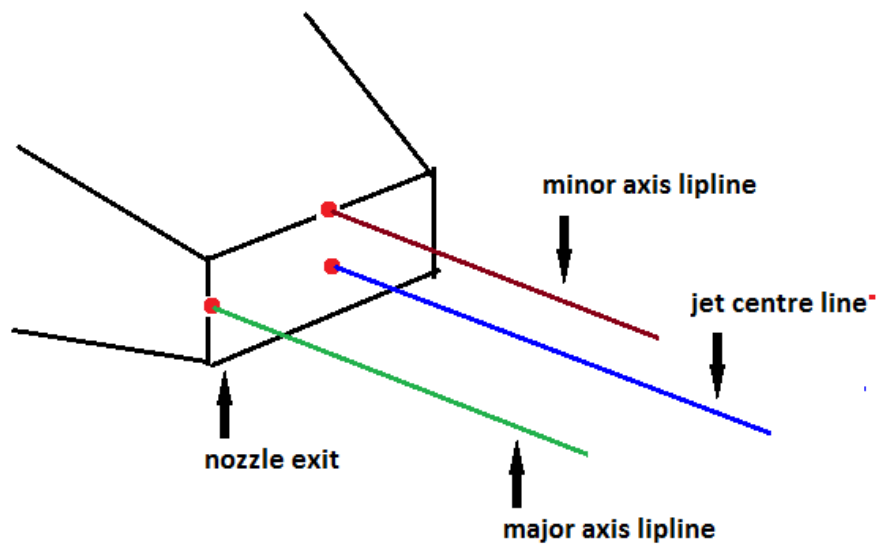
Fig. 7.7 Position of centre line, major and minor axis liplines for a rectangular nozzle

Fig. 7.8 Mean axial velocity along the centreline of rectangular nozzles with aspect
      ratio 2:1

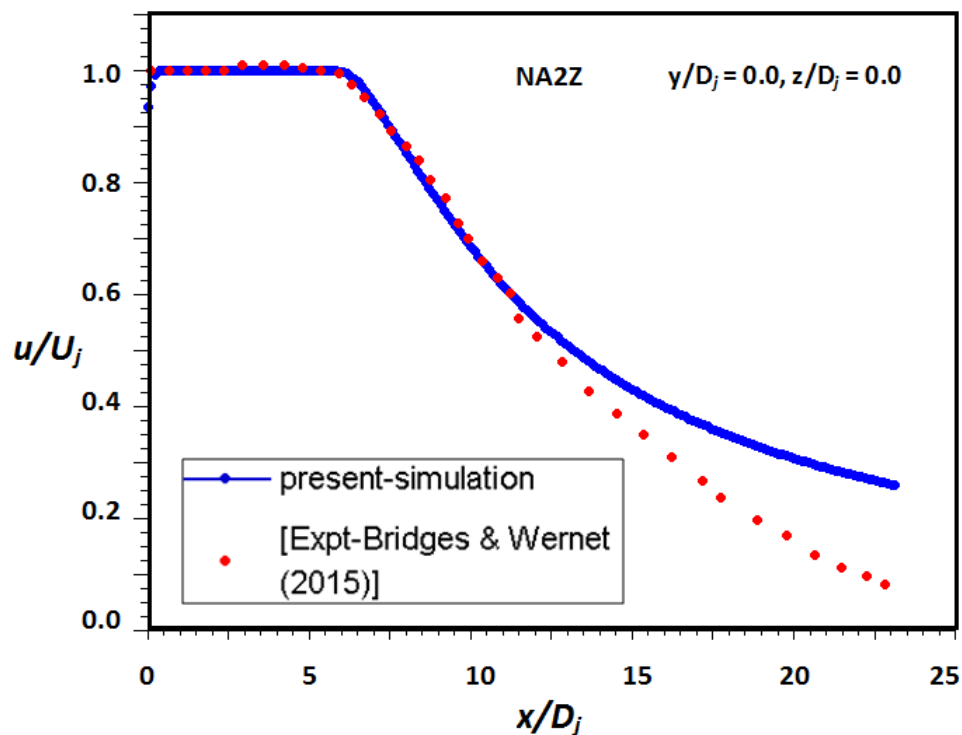Fig. 7.9 Mean axial velocity along the centreline of rectangular nozzles with aspect ratio 4:1

Fig. 7.10 Mean axial velocity along the centreline of rectangular nozzles with aspect ratio 8:1

Fig. 7.11   Mean axial velocity along the minor axis lipline of rectangular nozzles with aspect ratio 2:1

Fig. 7.12 Mean axial velocity along the minor axis lipline of rectangular nozzles with aspect ratio 4:1

Fig. 7.13 Mean axial velocity along the minor axis lipline of rectangular nozzles with aspect ratio 8:1

Fig. 7.14 Mean axial velocity along the major axis lipline of rectangular nozzles with aspect ratio 2:1
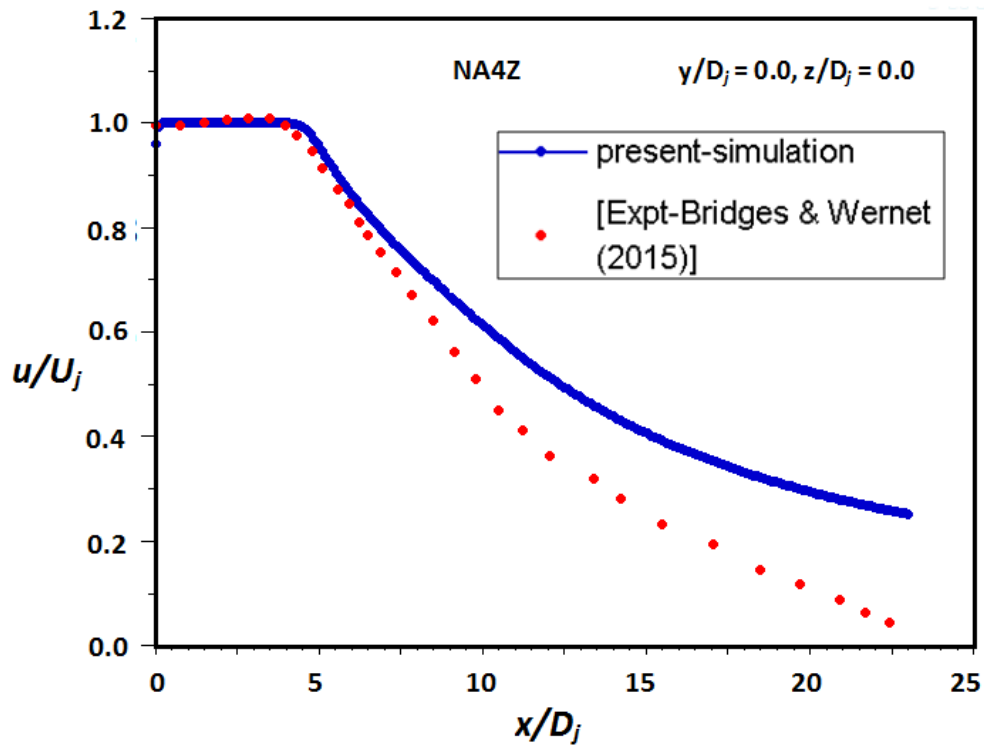
Fig. 7.15 Mean axial velocity along the major axis lipline of rectangular nozzles with
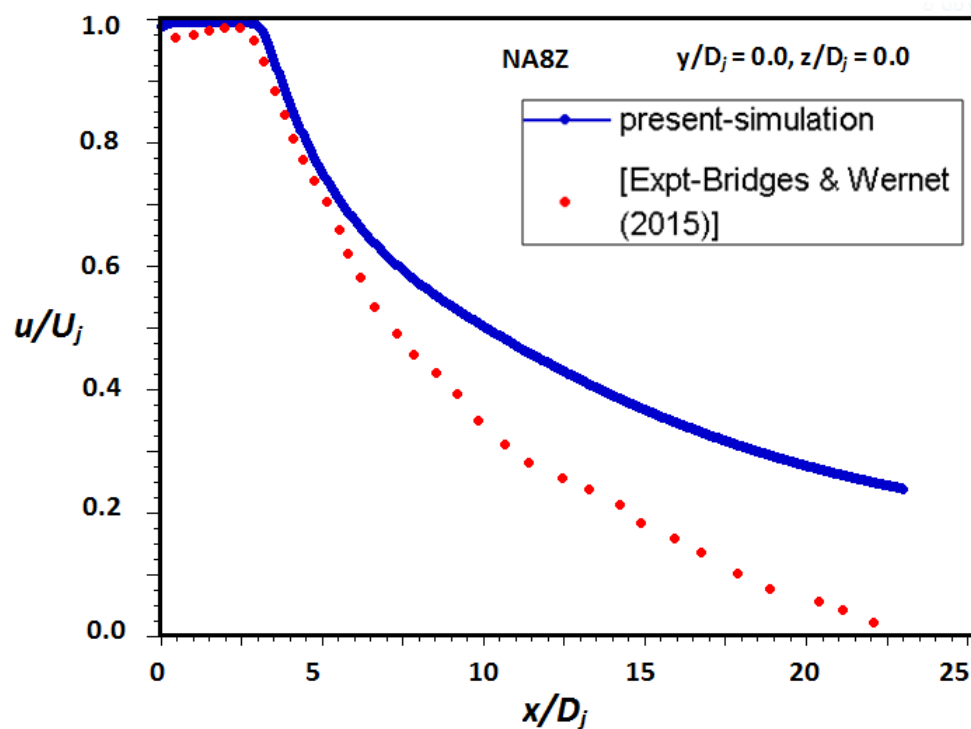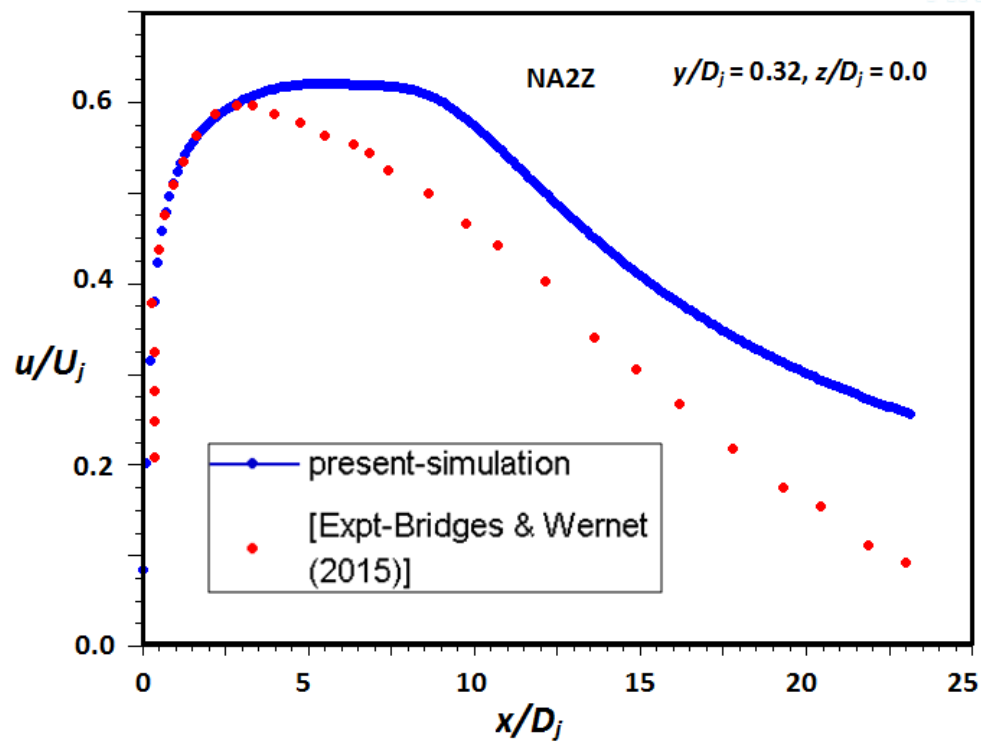aspect ratio 4:1

Fig. 7.16   Mean axial velocity along the major axis lipline of rectangular nozzles
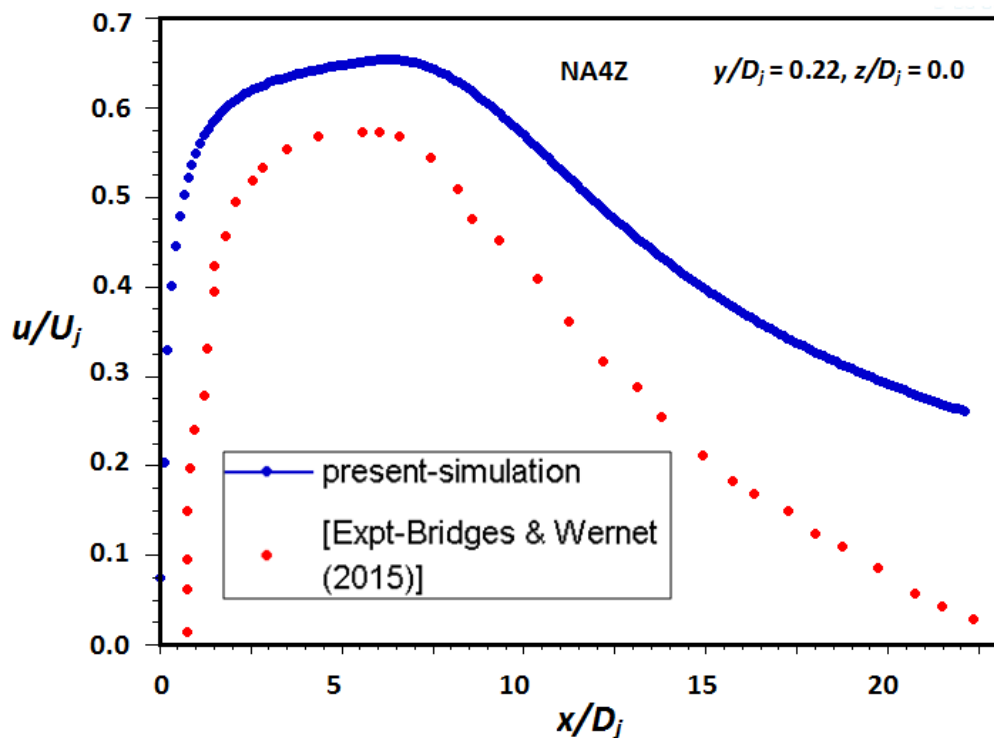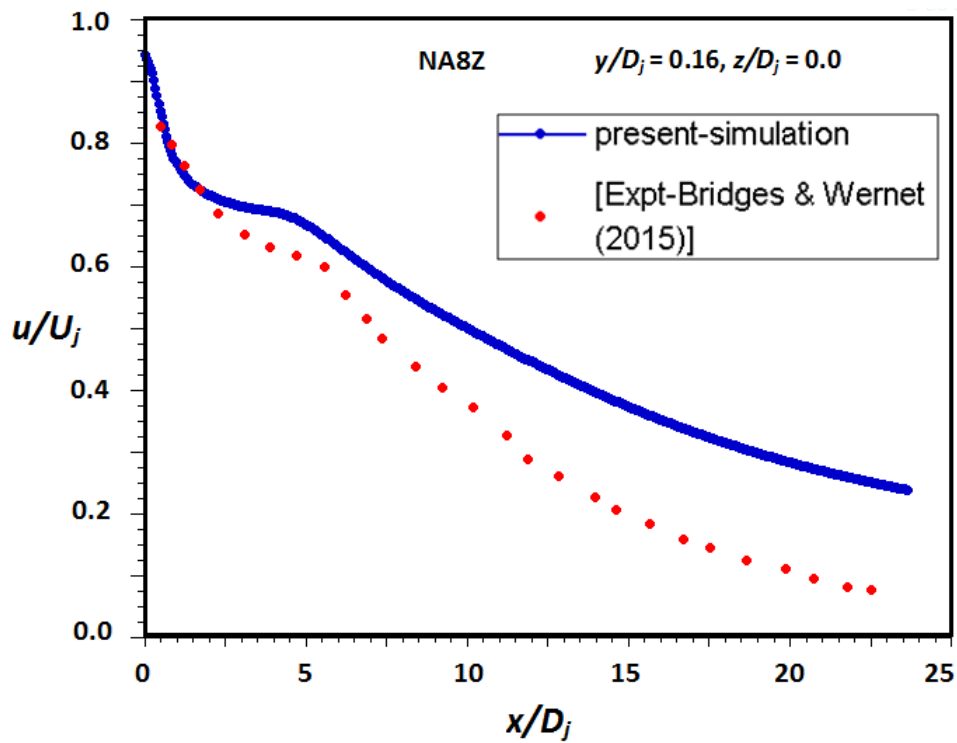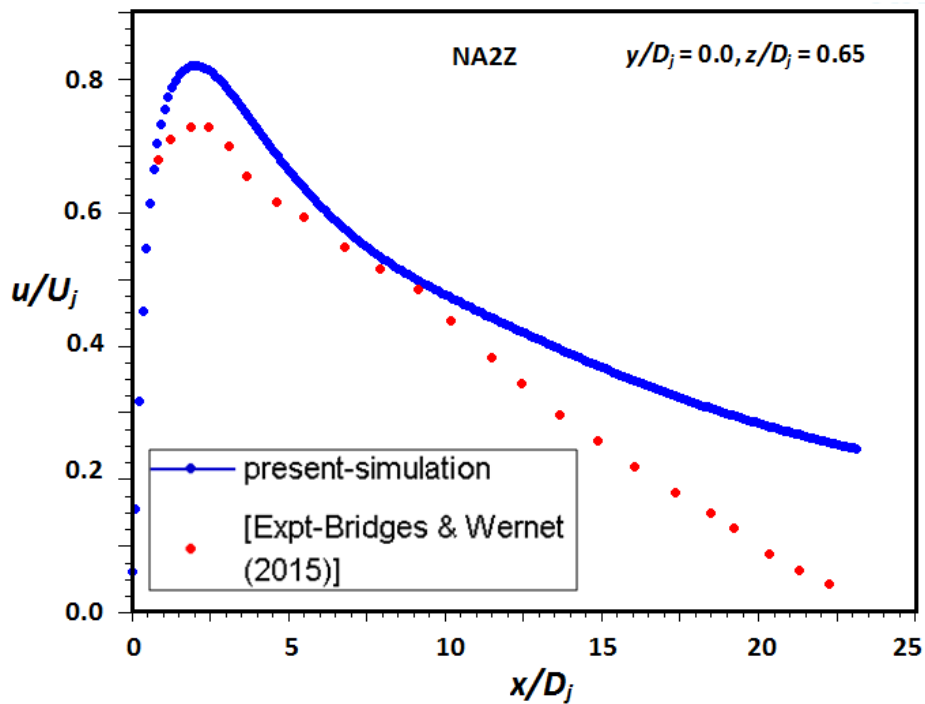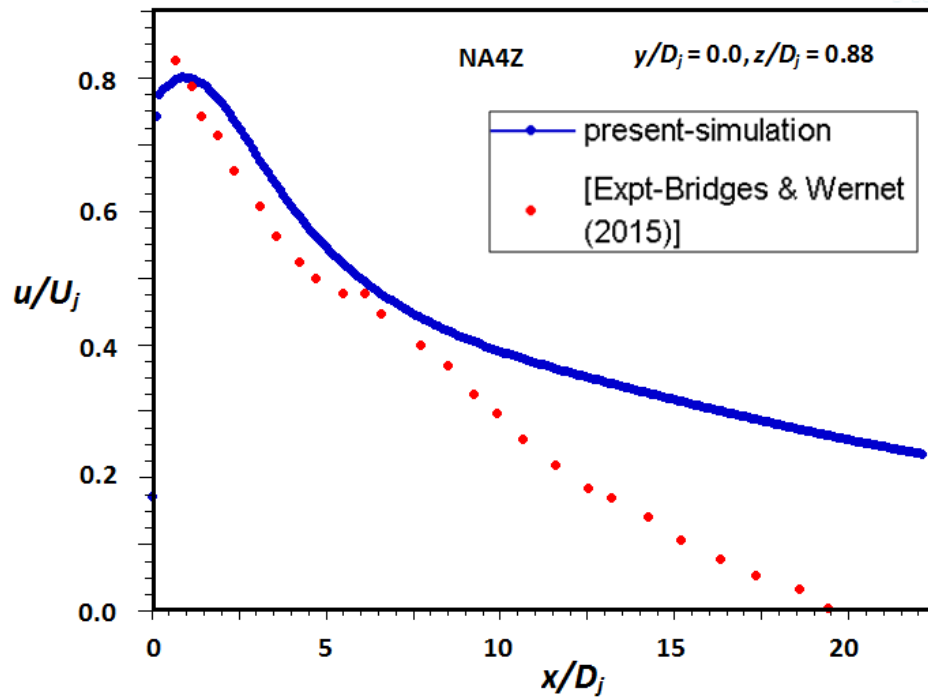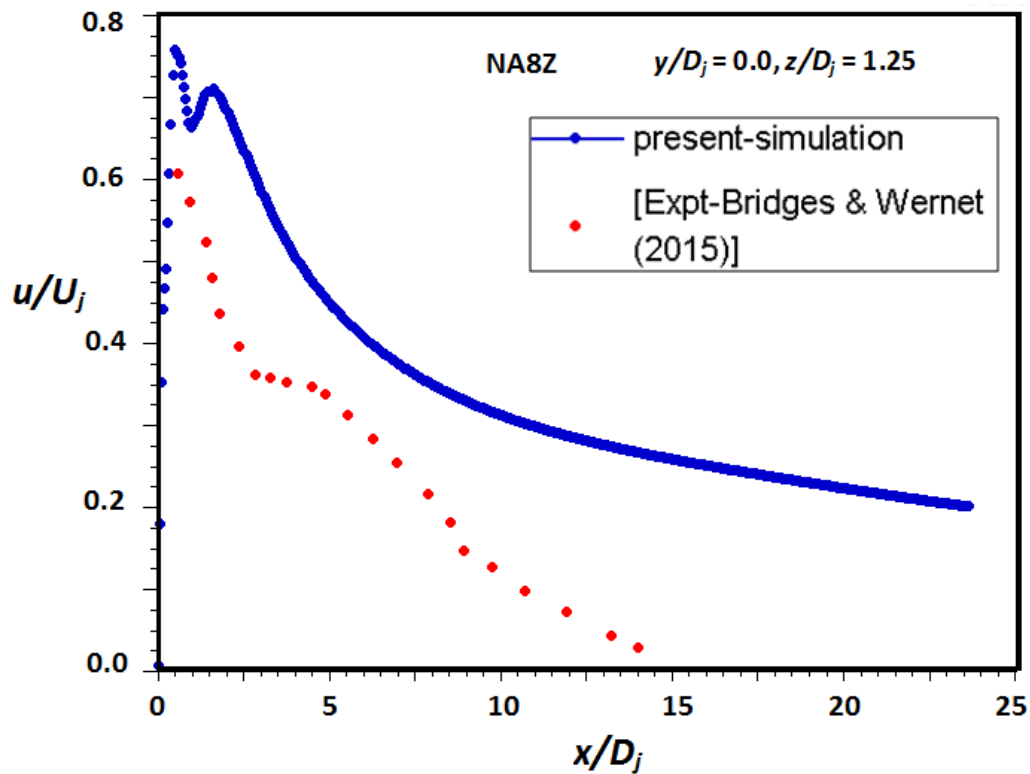with aspect ratio 8:1

Figures 7.17 to 7.25   shows the comparison of the variance profile of axial velocity along the centre line and also along the major and minor axis lip lines. The trend in variation of the axial variance is predicted correctly in all cases but the peak values of axial variance along the centrelines are slightly under predicted in the present calculations when compared with the experimental values reported by Bridges and Wernet (2015). The range of peak values of axial variance for the rectangular nozzles were predicted as 0.013-0.016 where as the experimental values measured were in the range 0.016-0.019. The postion of peak of axial variance are predicted well and agrees with the potential core length reported by the experiments.

The peakvalues of axial varaince along the minor axis lip are underpredicted. However, the variation in values with respect to the aspect ratio of the nozzle agrees well with the experimental results. The axial variance profile along the major axis lip is found to be in good conformity with the experimental values for all the three nozzle configurations. Bridges and Wernet (2015) reported that the position of axial variance peak along the major axis lip are closer to the nozzle compared to the minor axis and the peak of turbulence along major axis indicates the end of potential core. The above locations were captured well in the present numerical calculations. The variance profile of cross stream velocity along the centreline is shown in Figure 7.26. The comparison with respect to the aspect ratio of the nozzle shows that the peak value of variance is maximum for the nozzle with aspect ratio 2. The variation of turbulent viscosity shown in Figure 7.27 indicate that there is a drastic dropdown of turbulent viscoisity within a distance equal to 12 times the diameter of the jet for all the nozzles. But the distance where this dropdown starts are found closer to the nozzle exit with increase of aspect ratio. The turbulent kinetic energy variation along the

centreline is shown in Figure 7.28 and the peak value of kinetic energy is maximum

for the nozzle with aspect ratio 2.

Fig. 7.17   Variance profile of mean axial velocity along the centreline of rectangular
           nozzles with aspect ratio 2:1

Fig. 7.18   Variance profile of mean axial velocity along the centreline of rectangular
           nozzles with aspect ratio 4:1

Fig. 7.19   Variance profile of mean axial velocity along the centreline of rectangular nozzles with aspect ratio 8:1
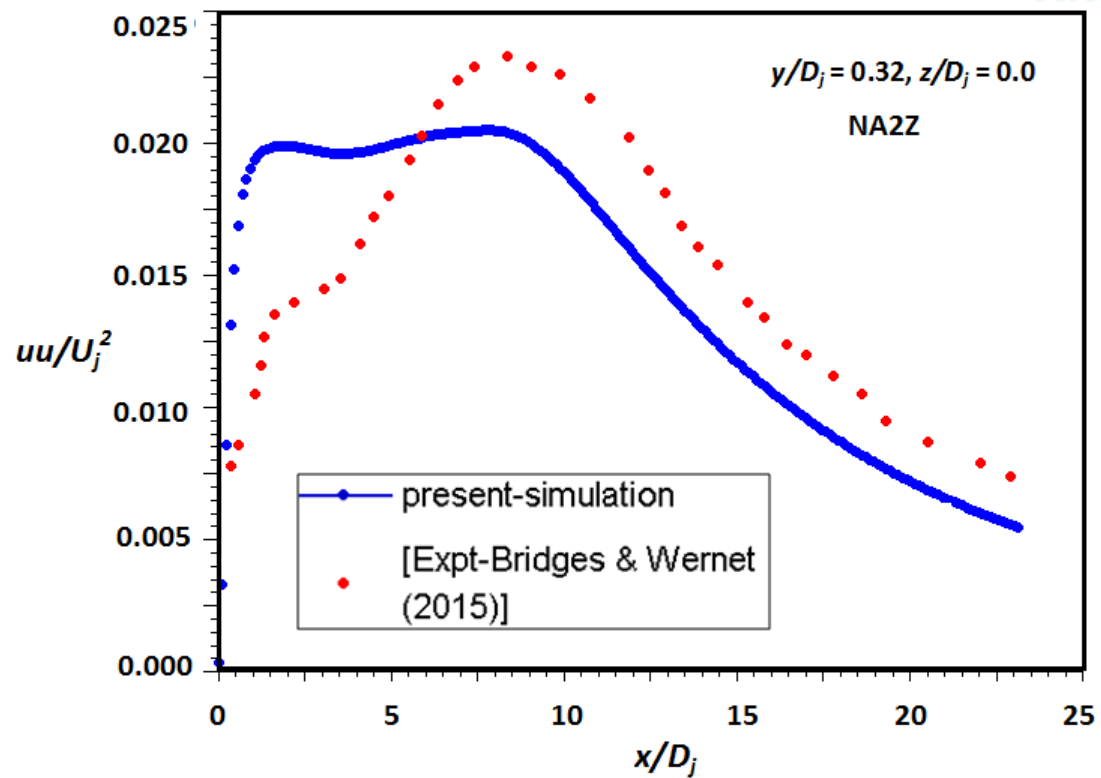
Fig.7.20   Variance profile of mean axial velocity along minor axis lipline of rectangular nozzles with aspect ratio 2:1
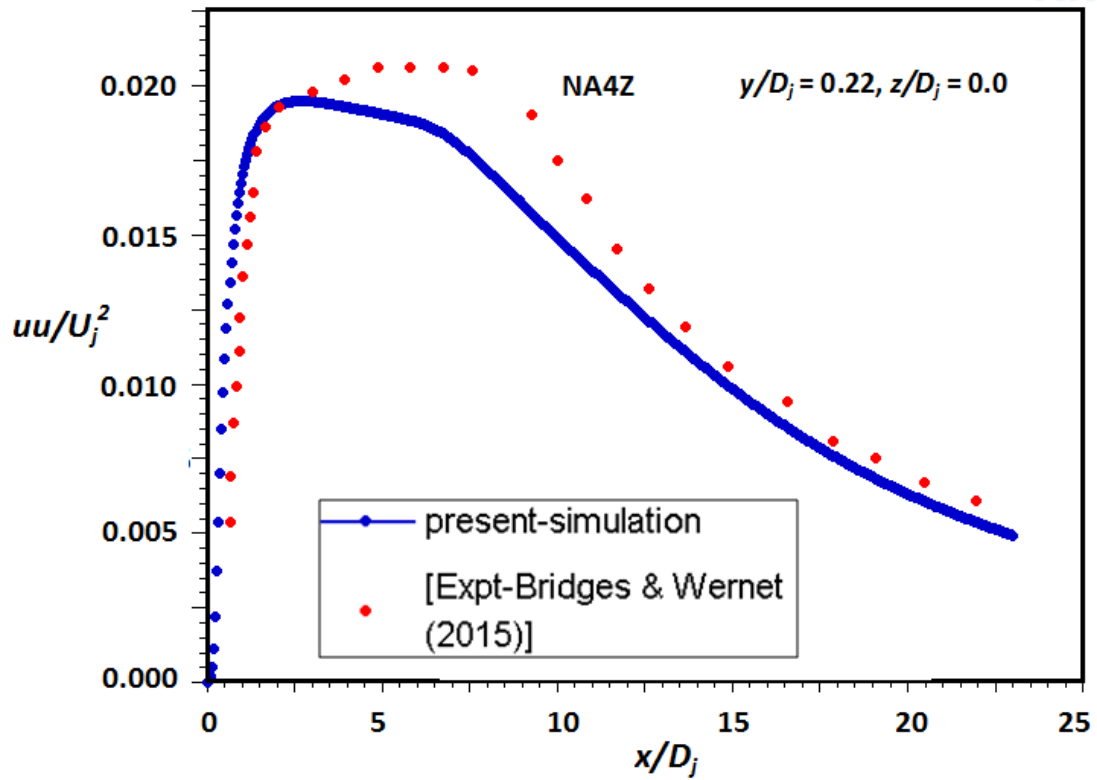
Fig. 7.21 Variance profile of mean axial velocity along minor axis lipline of
rectangular nozzles with aspect ratio 4:1
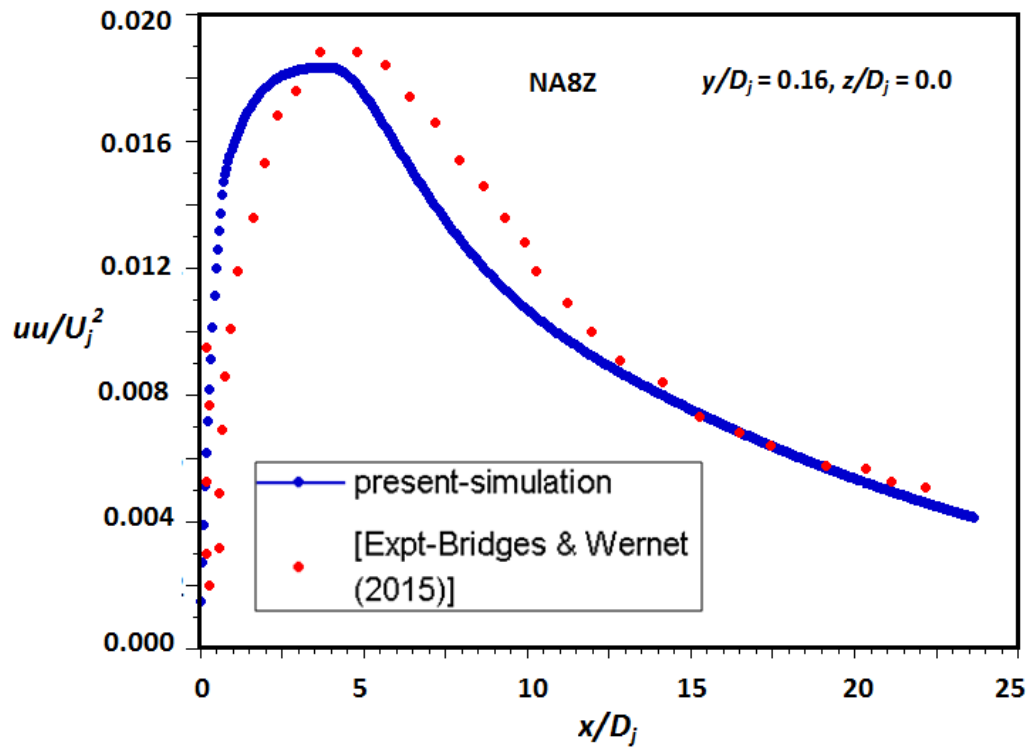
Fig. 7.22 Variance profile of mean axial velocity along minor axis lipline of
rectangular nozzles with aspect ratio 8:1
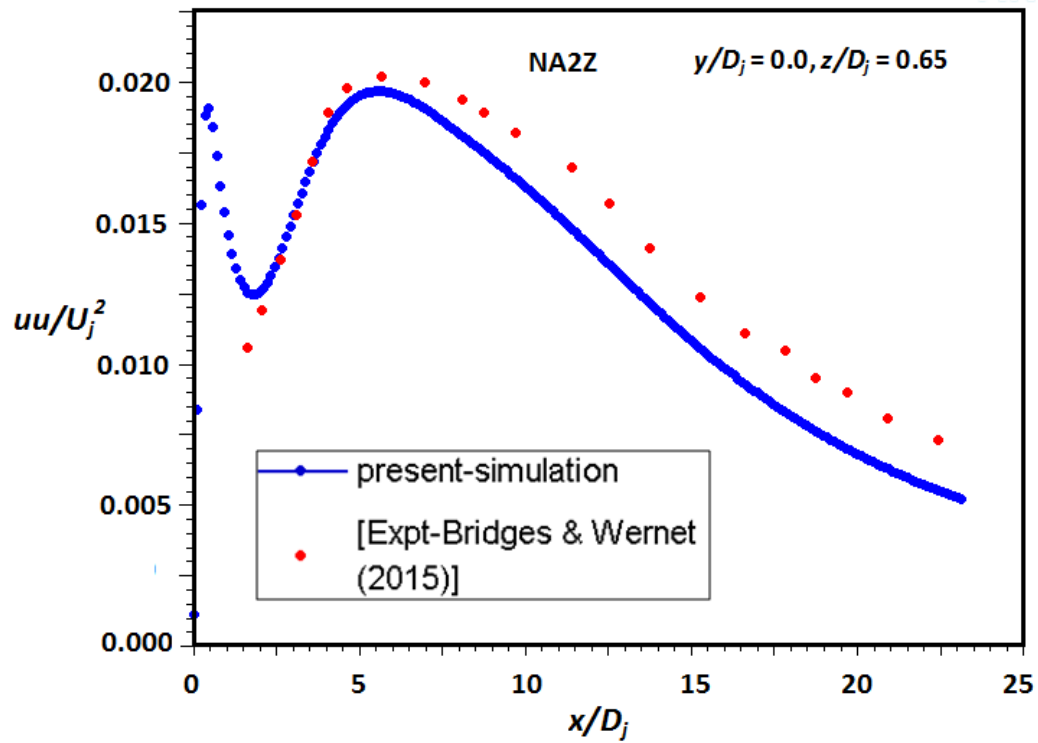
Fig. 7. 23 Variance profile of mean axial velocity along the major axis lipline of rectangular nozzles with aspect ratio 2:1

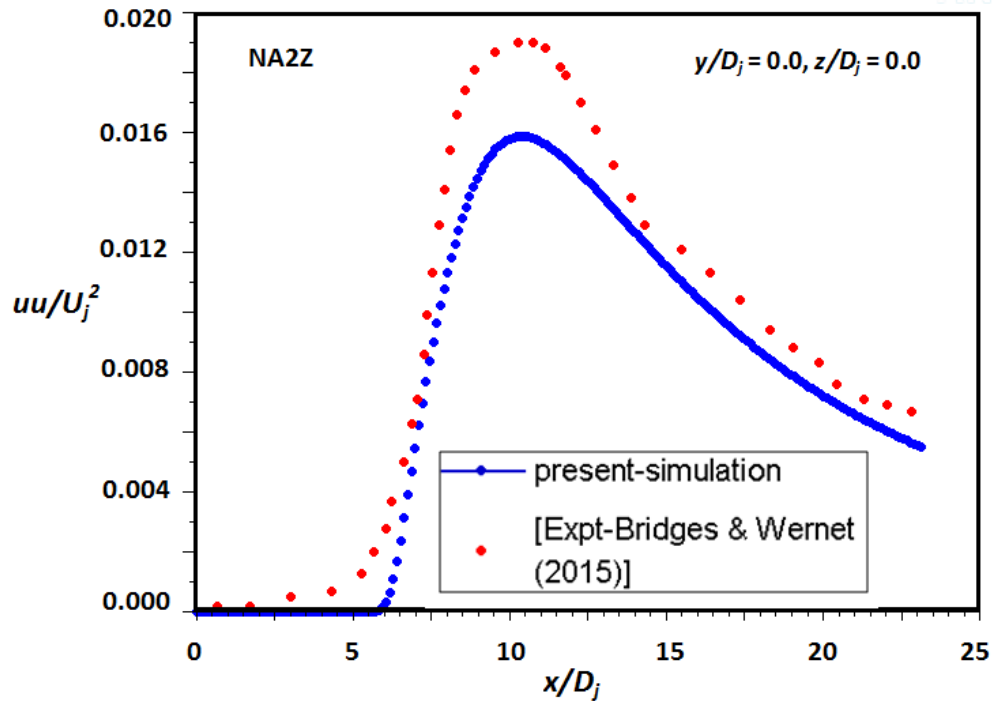Fig.7.24 Variance profile of mean axial velocity along the major axis lipline of rectangular nozzles with aspect ratio 4:1

Fig.7.25 Variance profile of mean axial velocity along the major axis lipline of
rectangular nozzles with aspect ratio 8:1
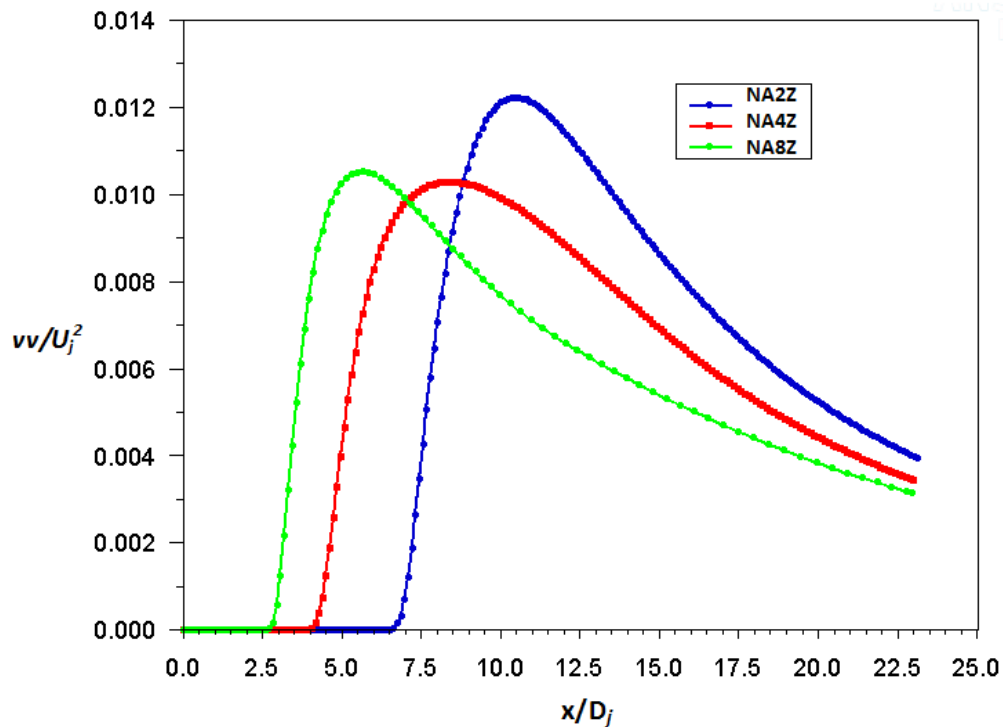
Fig.7.26 Variance profile of mean cross stream velocity along the centre line of
rectangular nozzles with aspect ratio 2:1, 4:1, and 8:1
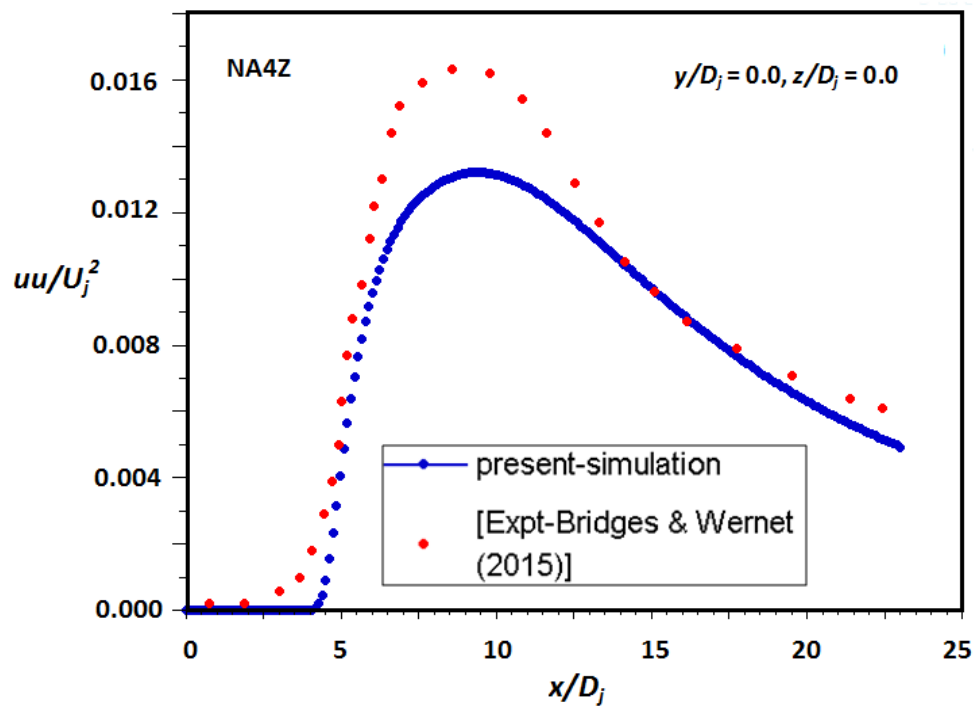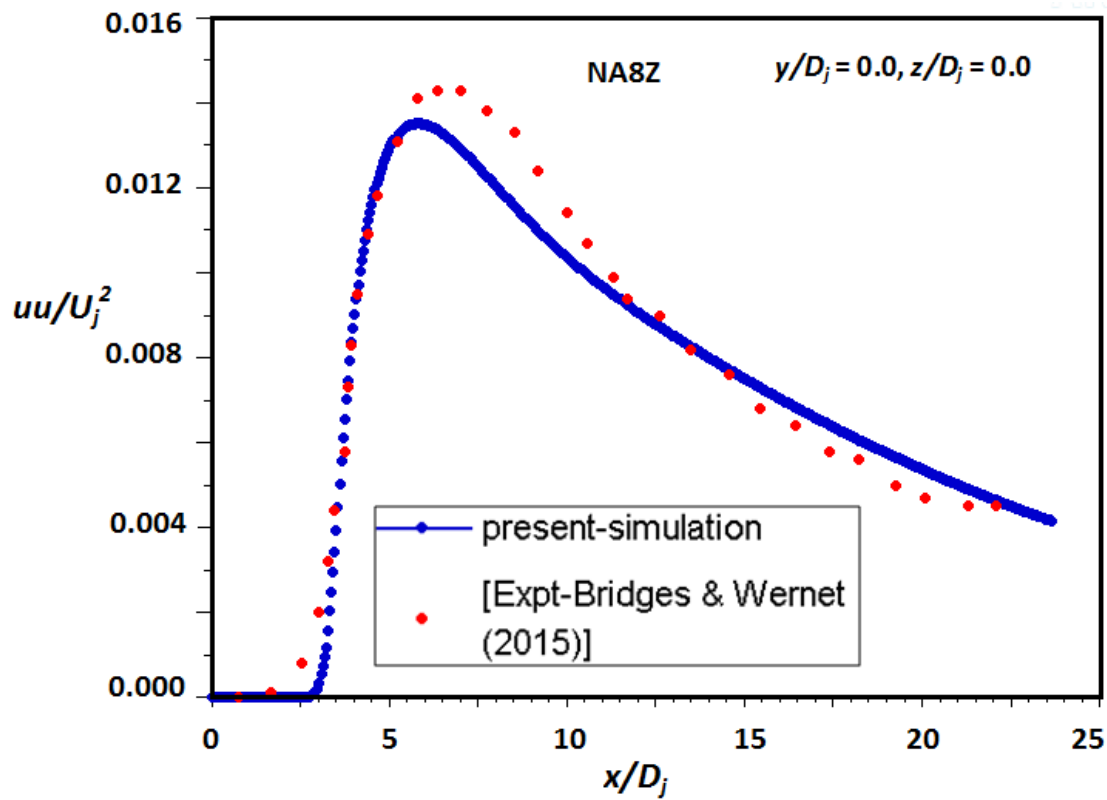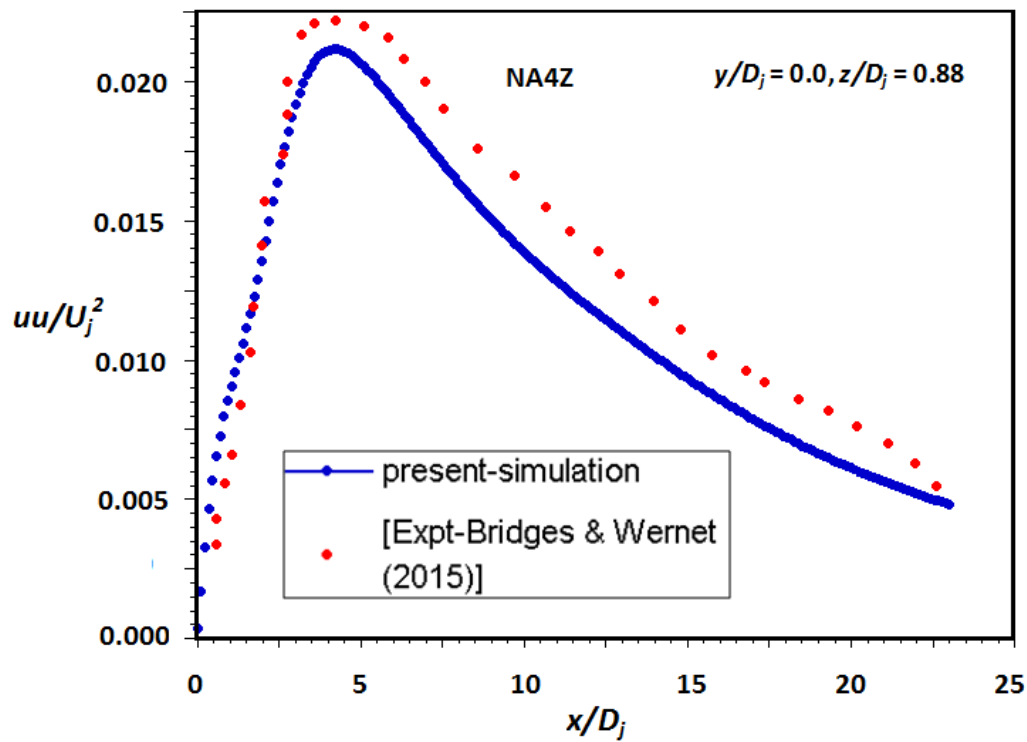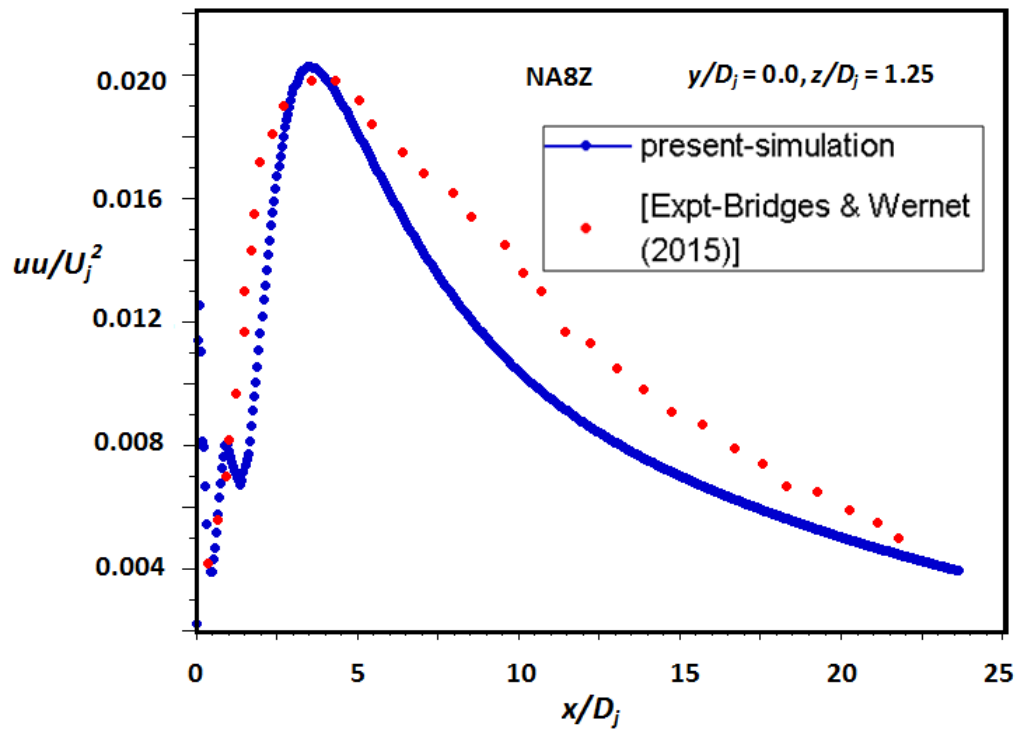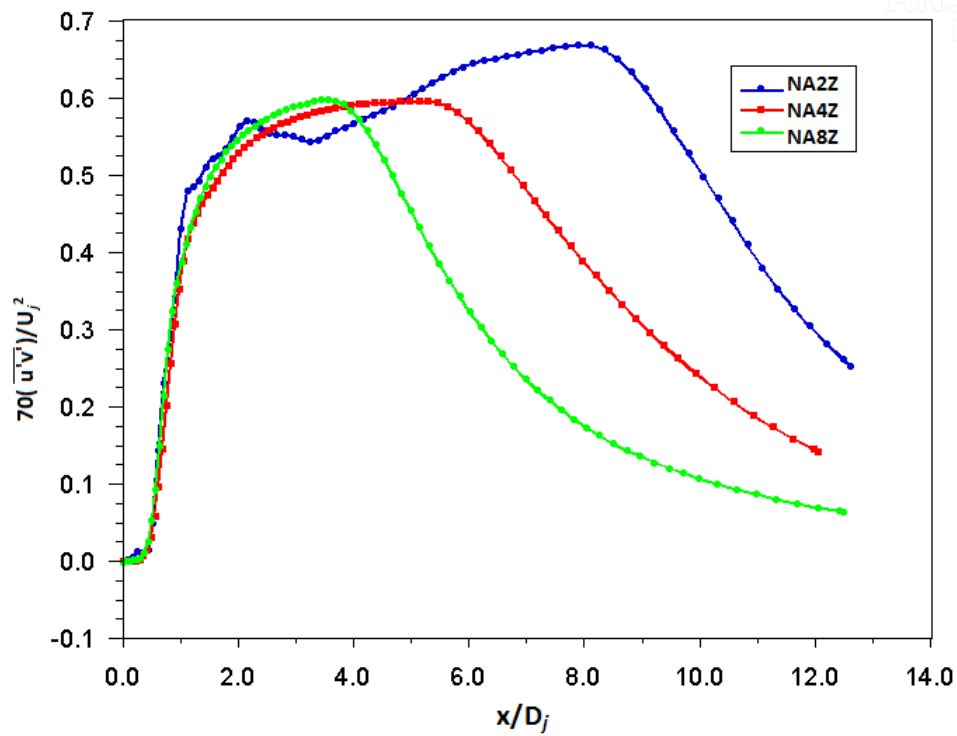
Fig.7. 27 Turbulence viscosity along the centre line of rectangular nozzles with aspect ratio 2:1, 4:1, and 8:1
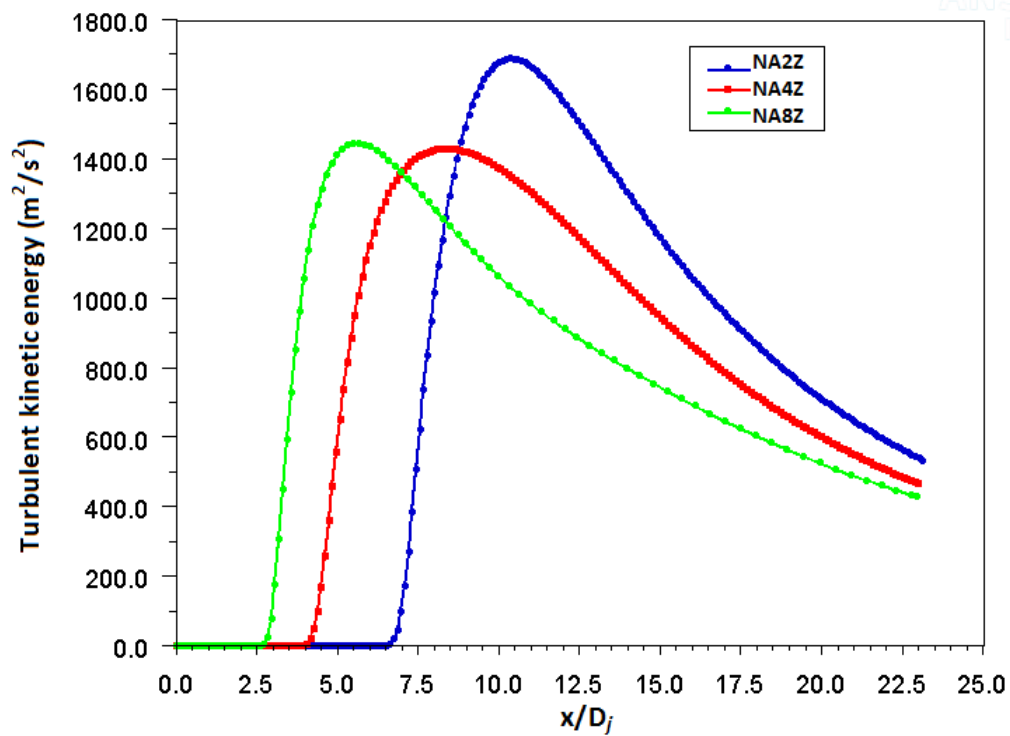
Fig. 7.28 Turbulence kinetic energy along the centre line of rectangular   nozzles with aspect ratio 2:1, 4:1, and 8:1

7.2.1.2 Bevelled Rectangular Nozzles

Bevelled rectangular nozzles are characterised by triangular side walls formed by extending the lower lip of the rectangular nozzles and the sides aligned by the minor axis meeting this lip. The extension length (*L*) of the lower edge of the bevelled nozzle was made in increments to the shorter dimension (*h*) of the rectangular nozzle. Mean and variance of axial velocity for rectangular bevel nozzles with aspect ratio 2:1 and bevel lengths 1.3" (short bevel NA2B1) and 2.7" (long bevel NA2B2) are shown in Figures 7.29 to 7.31. The results are compared with that of rectangular nozzle without bevel. The centre line mean and variance of axial velocity appears to be in line with the published experimental data. The delay in the onset of turbulence on the longer side (y/D_j = -0.31) of the bevel is clearly visible and agrees well with the experimental data of variance along short and long lip lines of bevel nozzle. The peak value of variance is also under predicted and similar to the predictions of the base rectangular nozzle.

Mean and variance of axial velocity for rectangular bevel nozzles with aspect ratio 4:1 and bevel lengths 1.3"(short bevel NA4B1) and 2.7"(long bevel NA4B2) are shown in Figures 7.32 to 7.34. The profiles along the centre line do not show any difference from the same base rectangular nozzle profiles and agrees well with the experimental data. The impact of both bevel on rectangular nozzle and length of the bevel is evident in the lip line profiles of turbulence. The position of the peak turbulence is predicted well particularly for the long bevel with slight under prediction in the magnitude.

The mean and turbulent velocity field along the centre line and the lip lines for rectangular bevel nozzles with aspect ratio 8:1 (short bevel NA8B1 and long bevel NA8B2 with bevel lengths of 1.3" and 2.7" respectively) is shown in Figures 7.35 to

7.37. Similar to the other two bevel nozzles with aspect ratio 2 and 4, mean axial velocity along the centreline shows negligible variation from the base rectangular nozzles. However, the variance along the centre line and along the liplines have certain effect on beveling of the nozzle. The increase in turbulence is maximum for the higher aspect ratio and longer bevel nozzle.

Fig. 7.29 Mean axial velocity of the rectangular bevel nozzles with aspect ratio 2:1 (a) short bevel and (b) long bevel.

Fig. 7.30 Variance of axial velocity along the centreline of the rectangular bevel nozzles with aspect ratio 2:1 (a) short bevel and (b) long bevel.
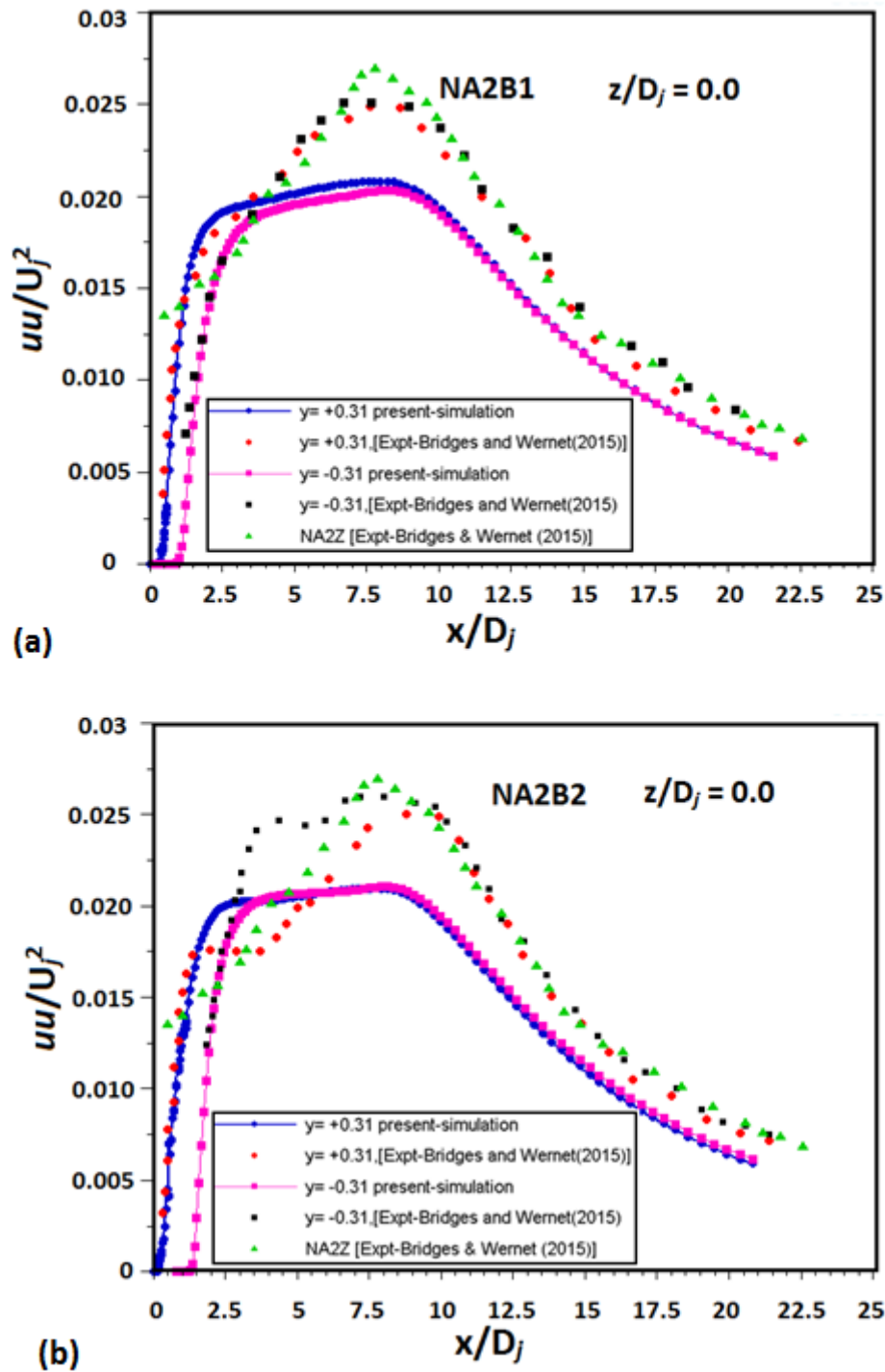
Fig. 7.31 Variance along the lipline of the short and long sides of the rectangular
bevel nozzles with aspect ratio 2:1 (a) short bevel and (b) long bevel.
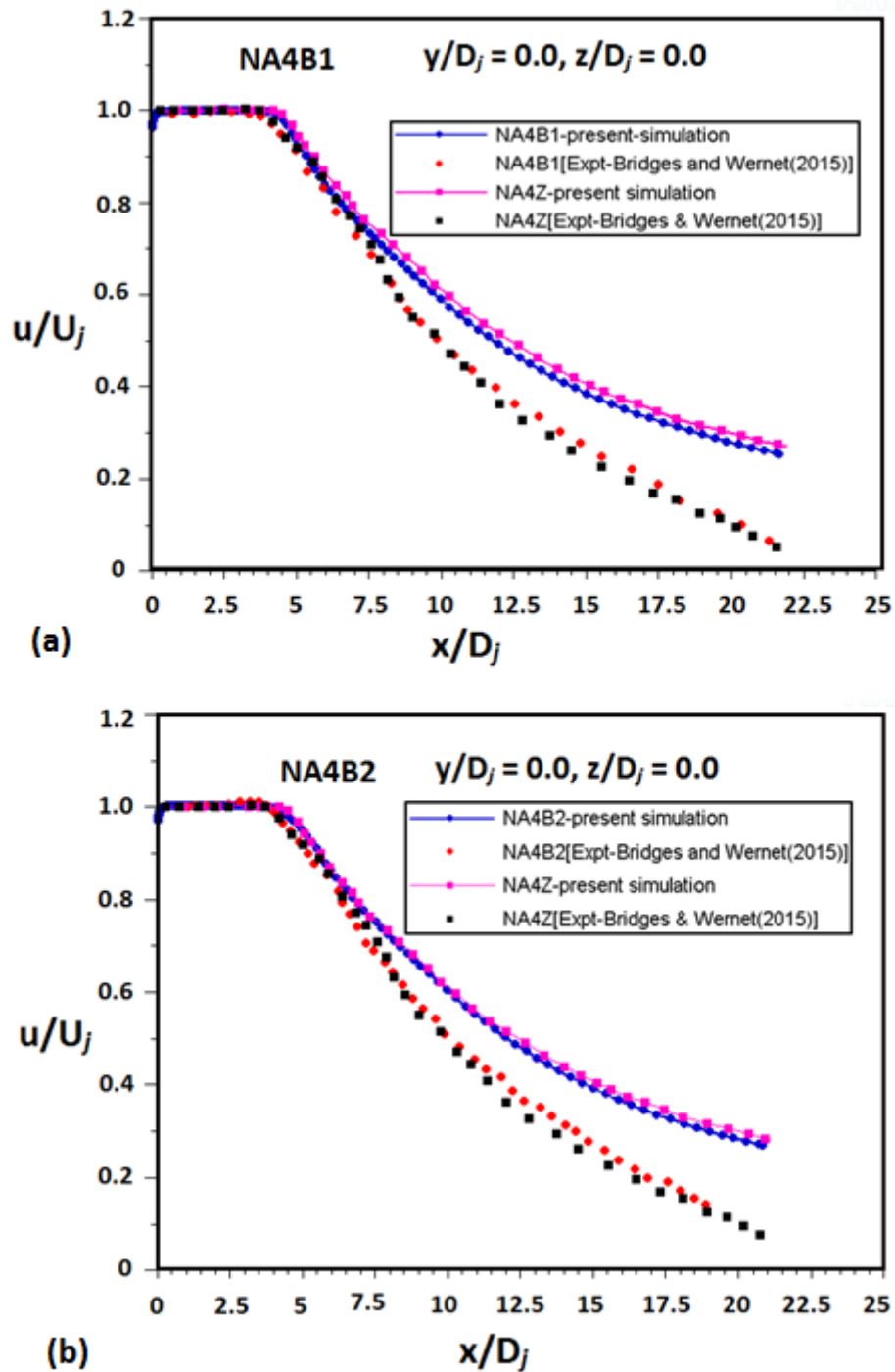
Fig. 7.32 Mean axial velocity of the rectangular bevel nozzles with aspect ratio 4:1
(a) short bevel and (b) long bevel.
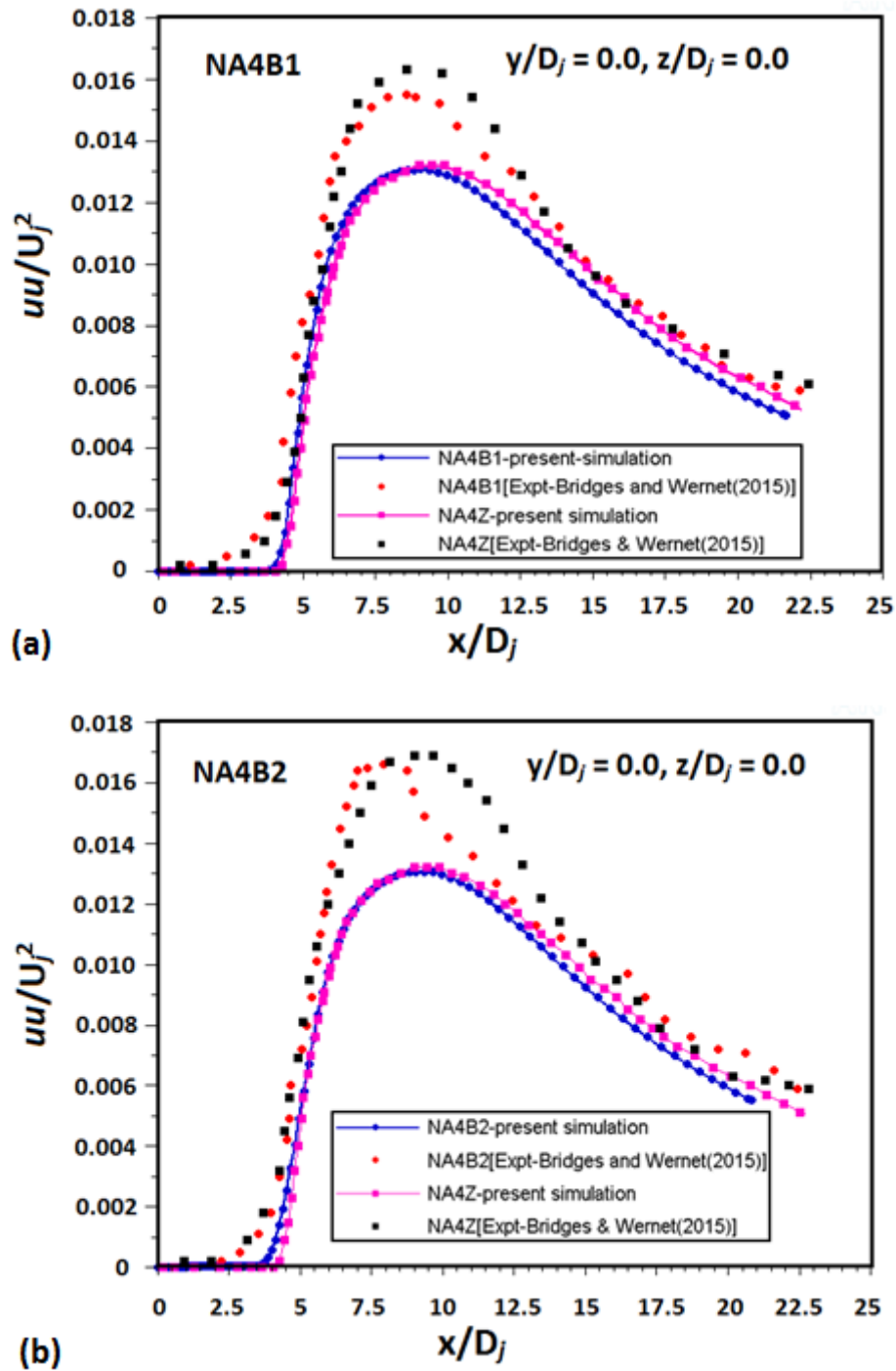
Fig. 7.33 Variance of axial velocity along the centreline of the rectangular bevel
nozzles with aspect ratio 4:1 (a) short bevel and (b) long bevel.
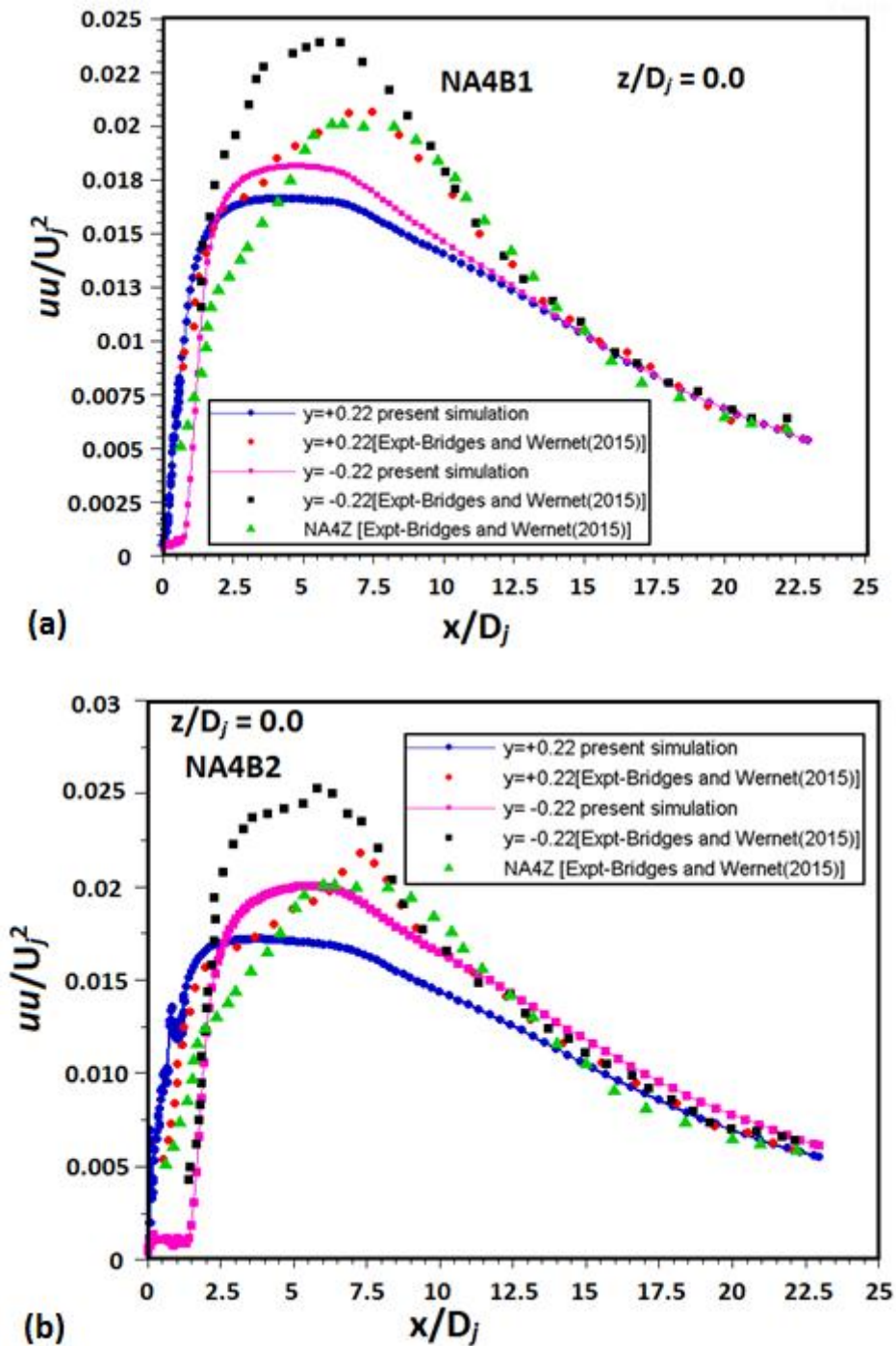
Fig. 7.34 Variance along the lipline of the short and long sides of the rectangular bevel nozzles with aspect ratio 4:1 (a) short bevel and (b) long bevel.
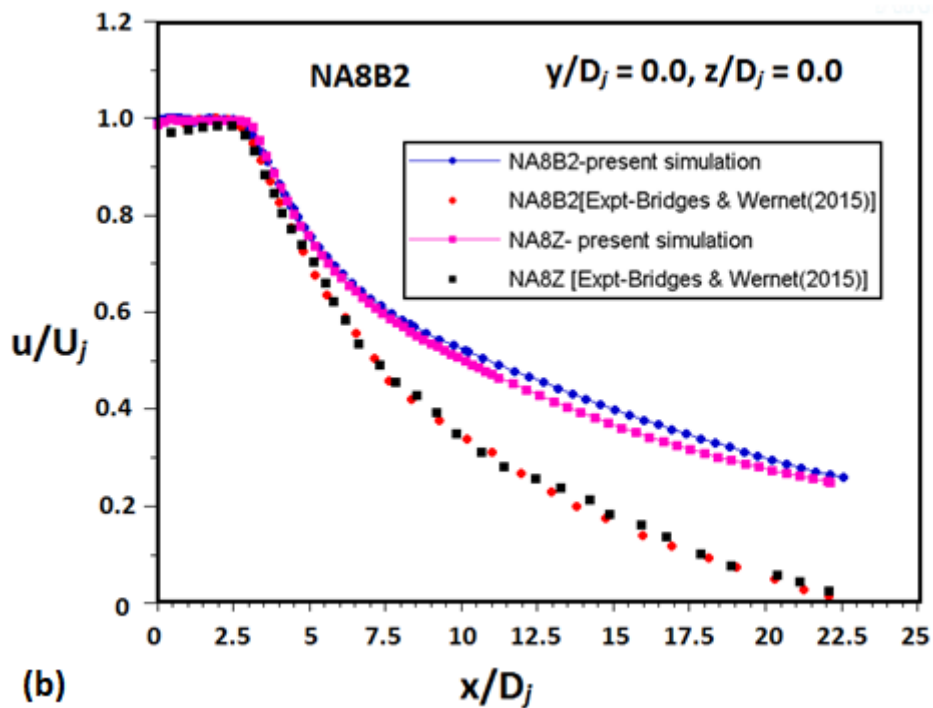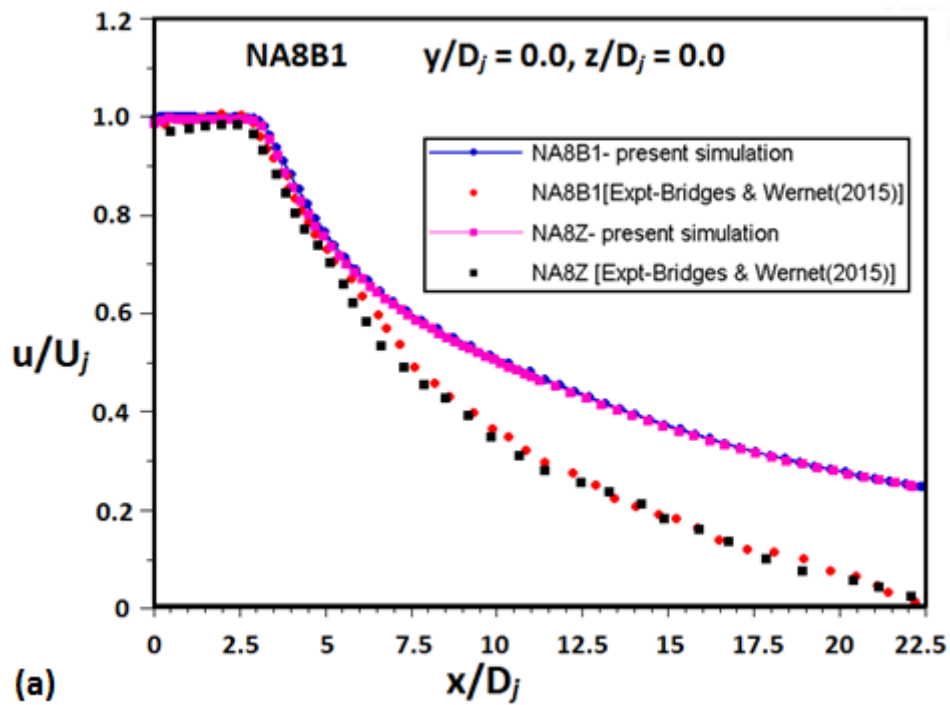
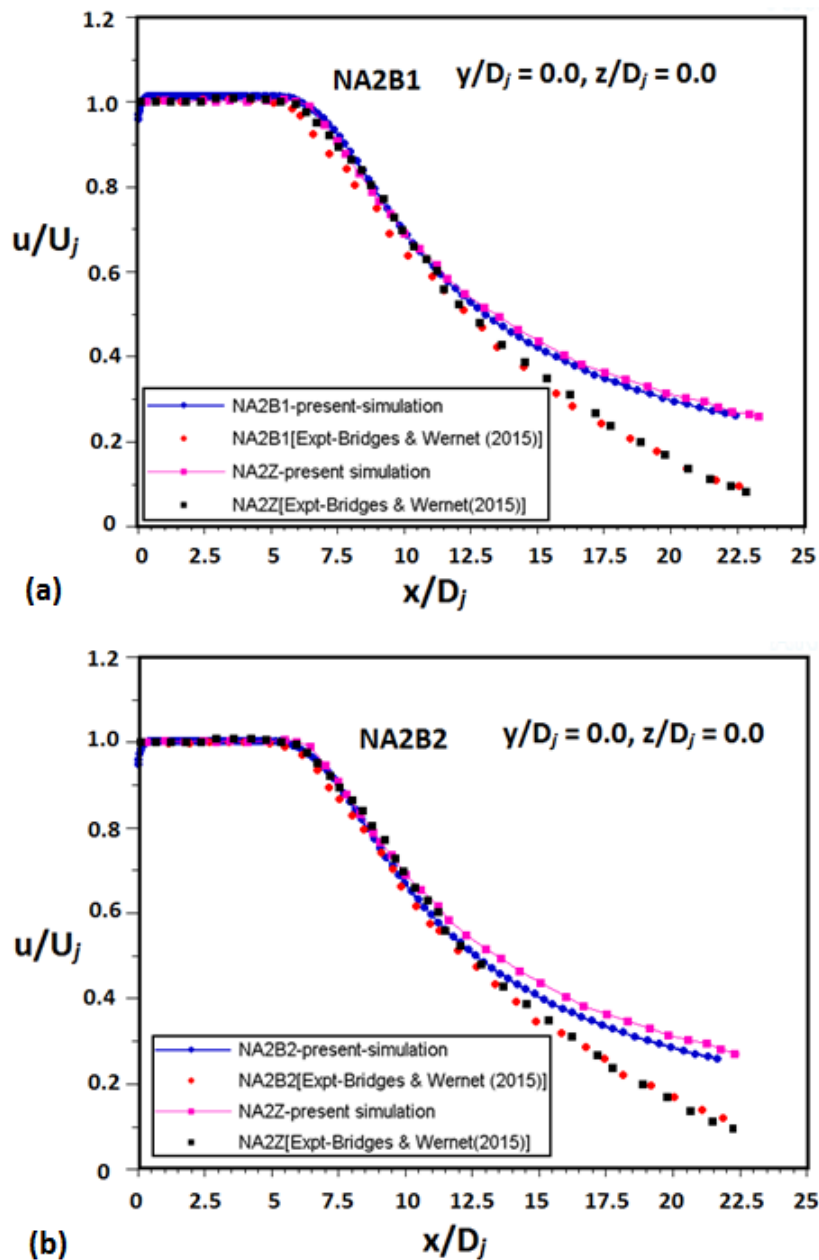Fig. 7.35 Mean axial velocity of the rectangular bevel nozzles with aspect ratio 8:1
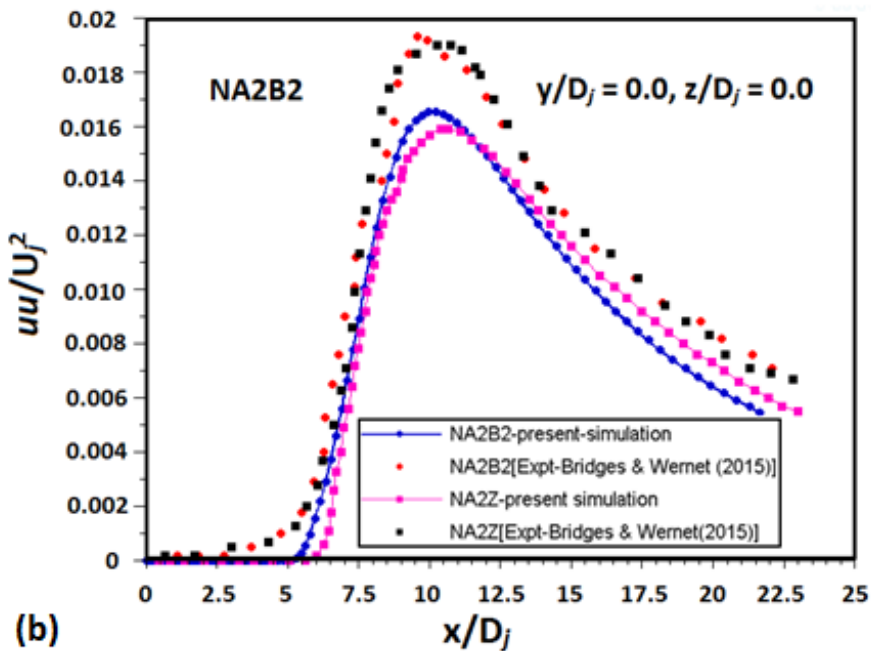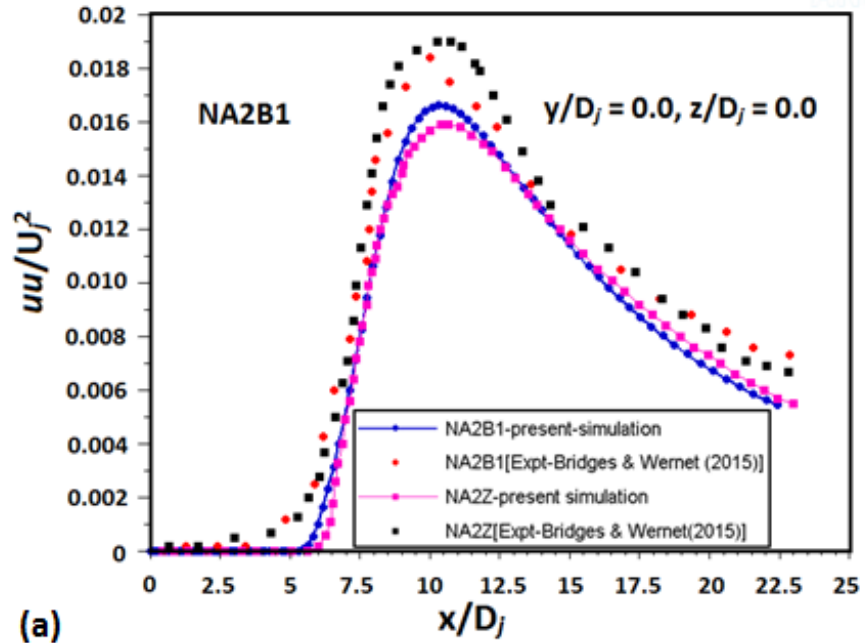(a) short bevel and (b) long bevel.
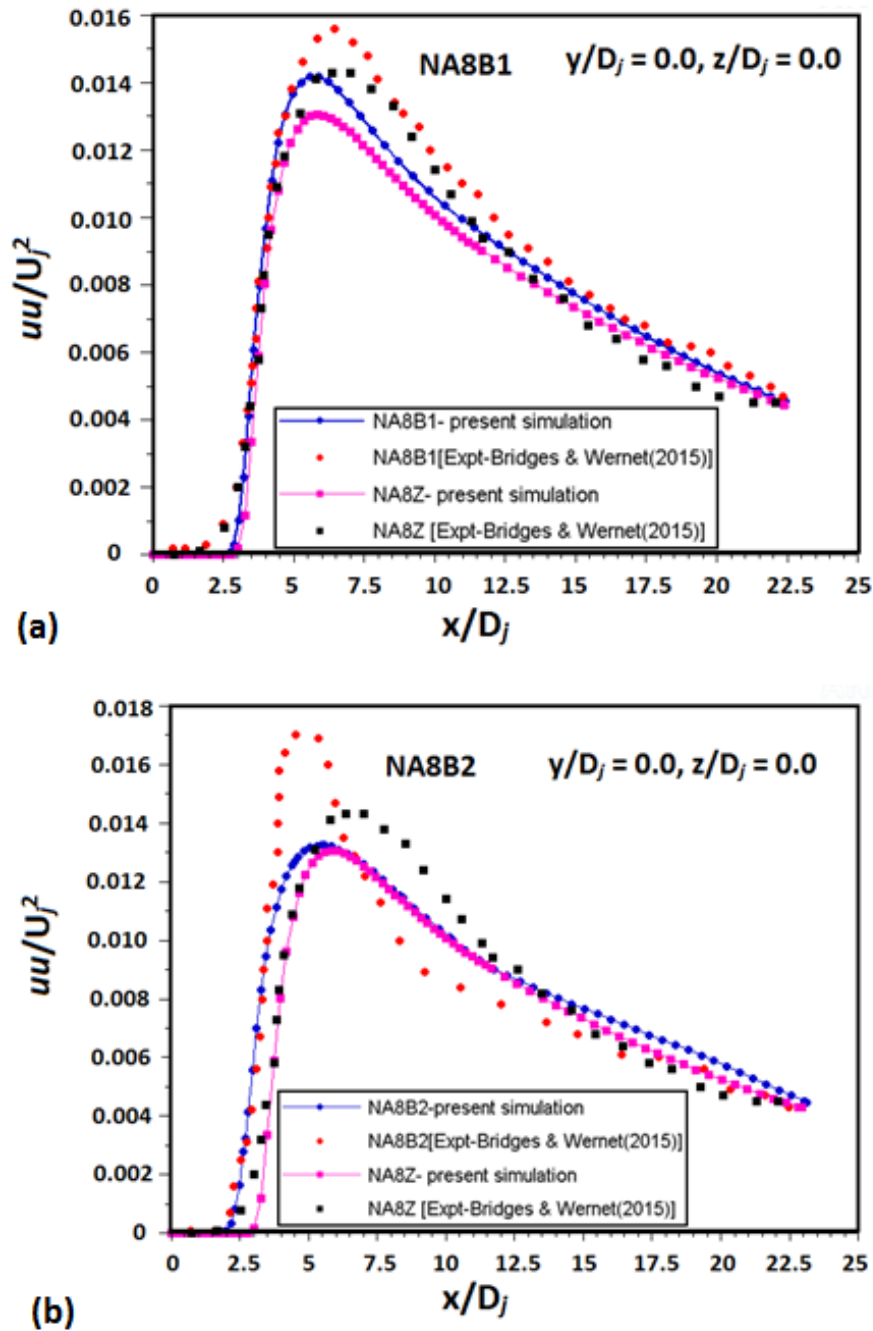
Fig. 7.36 Variance of axial velocity along the centreline of the rectangular bevel
nozzles with aspect ratio 8:1 (a) short bevel and (b) long bevel.
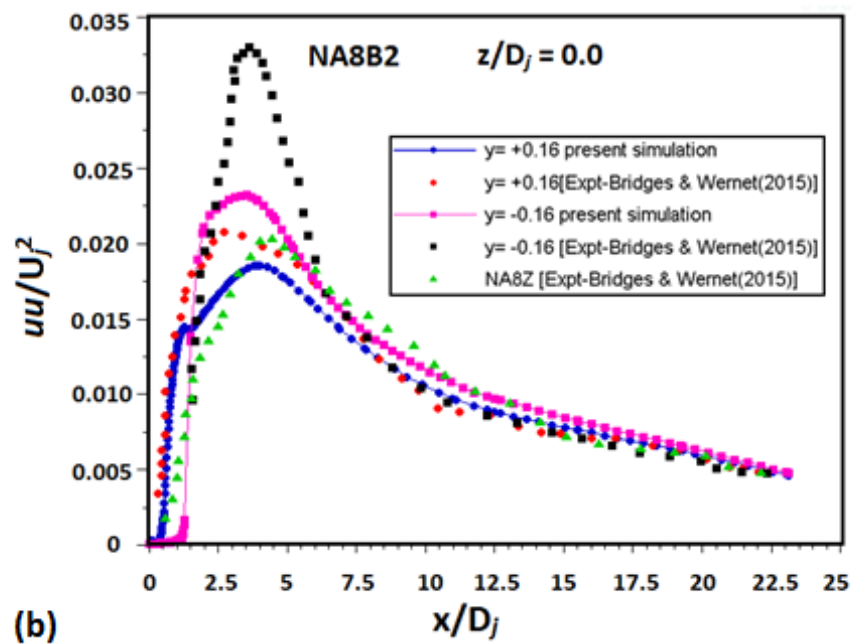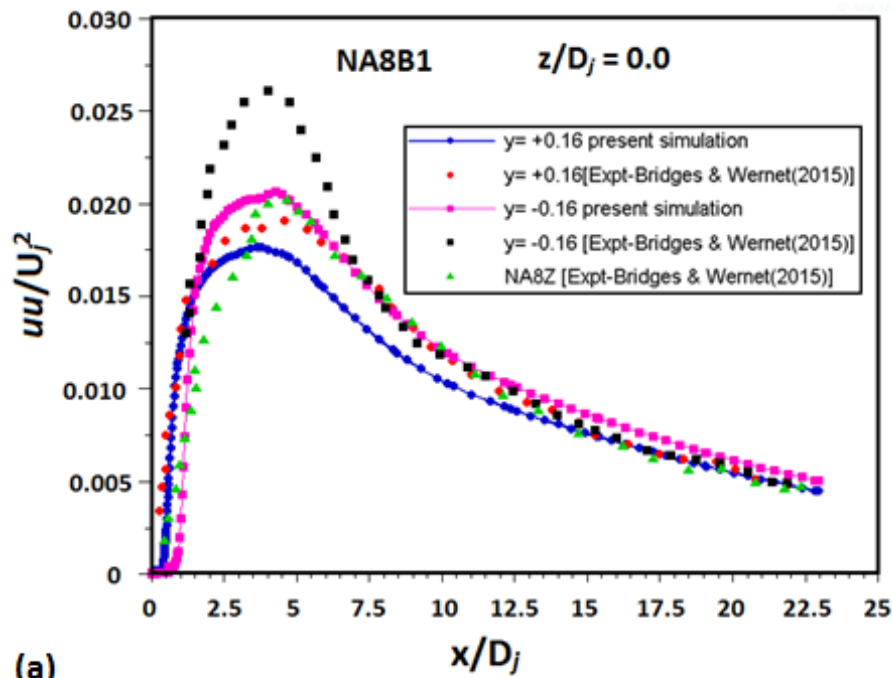
Fig. 7.37   Variance along the lipline of the short and long sides of the rectangular bevel nozzles with aspect ratio 8:1 (a) short bevel and (b) long bevel.

7.2.2 Jet Spread Rate

The procedure for calculating the jet spread rate is already explained in section 3.2.3.2. The variation of jet half width in the *XY* plane, $Y_{1/2}$ with the downstream distance *X* is indicated in the Figures 7.38 to 7.41. The jet in the *XY* plane spreads linearly and jet spread rate is defined as the slope of the half width line. For the rectangular plain nozzles with aspect ratio 2, 4 and 8, the jet spread rate slightly increases from 0.113 to 0.115 with increase in aspect ratio and depicted in Figure 7.38.

The effect of bevelling and bevel length ratio on the jet spread rate was also studied for aspect ratio 2, 4 and 8. For the rectangular bevel nozzle with aspect ratio 2, bevelling has no effect on the spread rate for the short bevel configuration (NA2B1) as shown in Figure 7.39. But with increase in bevel length ratio, the long bevel configuration (NA2B2) shows a considerable change in the spread rate with respect to plain nozzle from 0.113 to 0.120.

For rectangular nozzle with aspect ratio 4 bevelling causes a slight increase in jet spread rate whereas change in bevel length ratio has negligible effect and can be visualised in Figure 7.40. In the case of rectangular nozzle (Fig. 7.41) with aspect ratio 8, there is a significant change in the jet spread rate with increase in bevel length ratio for both short (0.121) and long (0.127) bevel from its base (0.115) rectangular nozzle.

The variation of jet half width in the XZ plane, $Z_{1/2}$ and in the XY plane, $Y_{1/2}$ are plotted with the downstream distance X as shown in Figures 7.42 to 7.50. The variation of the half-width in the XZ plane is neither linear nor it increases

monotonically. At some intermediate location the half-widths in the central planes cross over which indicate the locations of axis switching. Axis switching is a phenomenon in which the cross-section of an asymmetric jet evolves in such a manner that, after a certain distance from the nozzle, the major and the minor axes are interchanged. A 90^0 switch takes place after a certain downstream distance due to the expansion of the jet cross-section in the direction of the minor axis and contraction in the direction of the major axis (Tsuchiya and Horikoshi (1986), Ho and Gutmark (1987)). Nan Chen and Huidan Yu. (2014) explained the mechanism of axis switching in the following way. As the jet develops, it spreads through mixing and entrainment with the surroundings. When the flow in the major axis approaches the boundary, the entrainment in the major axis is weakened while the mixing along the minor axis becomes competitive to the major axis. As the jet further develops, the flow along minor axis exceeds that along the major axis, which is how the 90° axis-switching occurs. From the obtained results it is seen that bevelling of the rectangular nozzle causes the axis switching to take place in close proximity to the nozzle exit than the plain nozzle.

For the rectangular nozzle with aspect ratio 2 (*AR = 2)* no cross over point is seen for the plain nozzle, but for the bevel nozzles (NA2B1 and NA2B2) the cross over point is seen in close proximity to the nozzle exit (around 15D_j) as shown in Figures 7.42 to 7.44. The cross over point is seen at roughly 25D_j for plain rectangular nozzle (NA4Z) for an aspect ratio of 4 (Fig. 7.45). However, no cross over point is observed within the axial range of jet development for rectangular plain nozzle with *AR*=8 (Fig. 7.48). Krothapalli *et al.* (1981) reported that the distance from the nozzle

exit to the cross over point (*Xc*) increases with increase in aspect ratio and hence the above predictions are acceptable.

Multiple cross over point can be seen for both short and long bevel nozzles with *AR* = 4 and 8 as shown in Figures 7.46, 7.47, 7.49, and 7.50, which may be due to the effect of bevelling and bevel length ratio. The cross over point is found to be shifting towards the nozzle exit with increase in bevel length ratio.
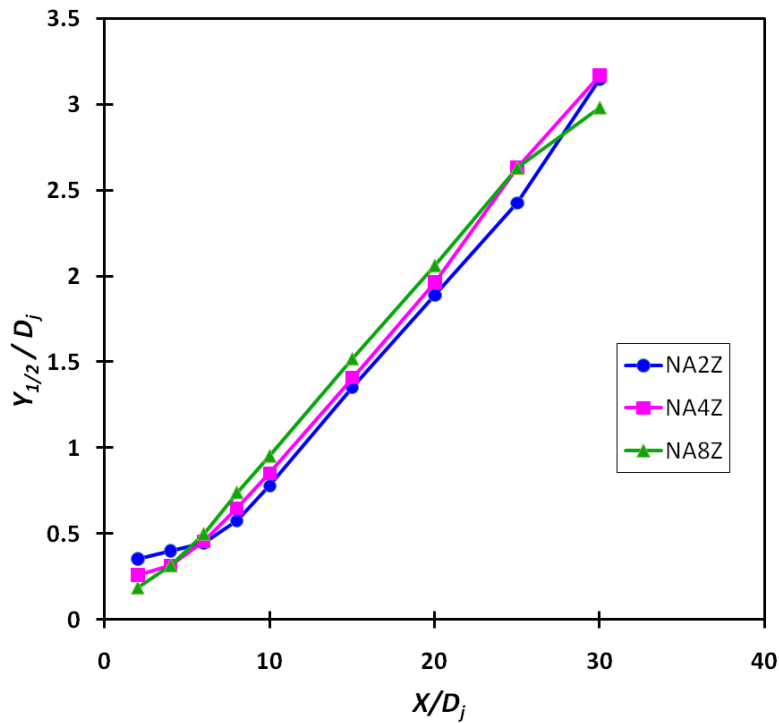
Fig. 7.38 Growth of rectangular jet with aspect ratio 2, 4, and 8 in the *XY* plane
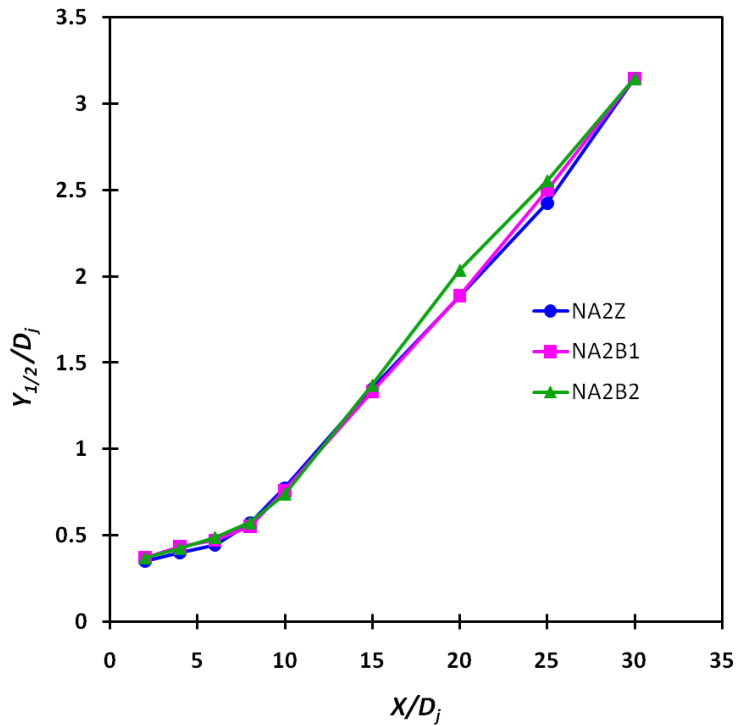
Fig. 7.39   Comparison of growth of rectangular bevel jets with aspect ratio 2 (NA2B1 and NA2B2) with the plain nozzle (NA2Z) in the *XY* plane
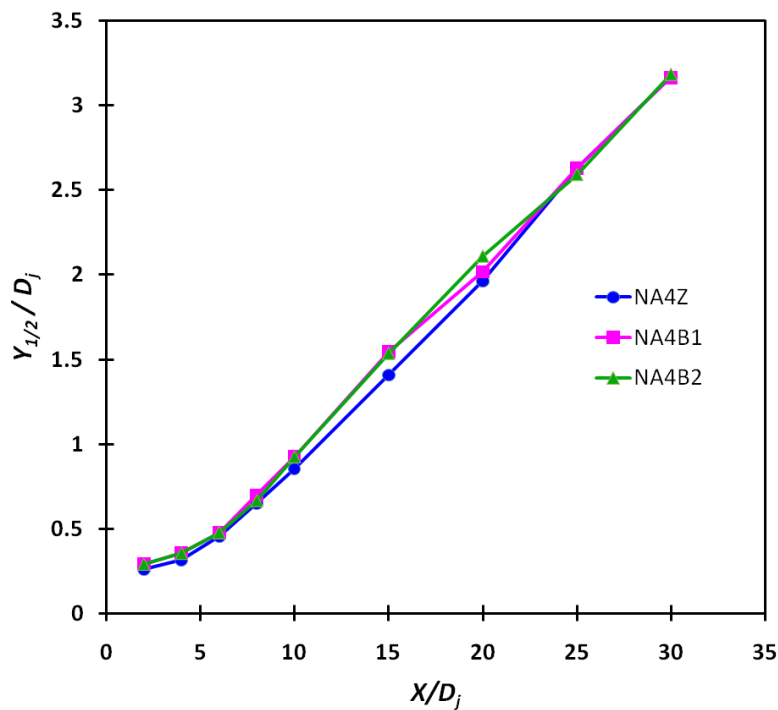
Fig. 7.40   Comparison of growth of rectangular bevel jets with aspect ratio 4 (NA4B1 and NA4B2) with the plain nozzle (NA4Z) in the *XY* plane
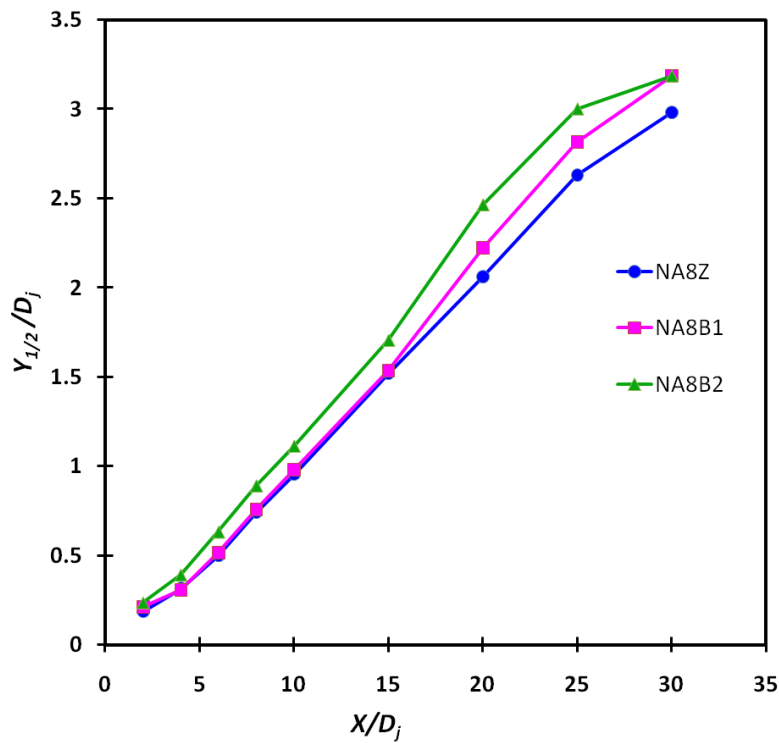
Fig. 7.41   Comparison of growth of rectangular bevel jets with aspect ratio 8
            (NA8B1 and NA8B2) with the plain nozzle (NA8Z) in the *XY* planes
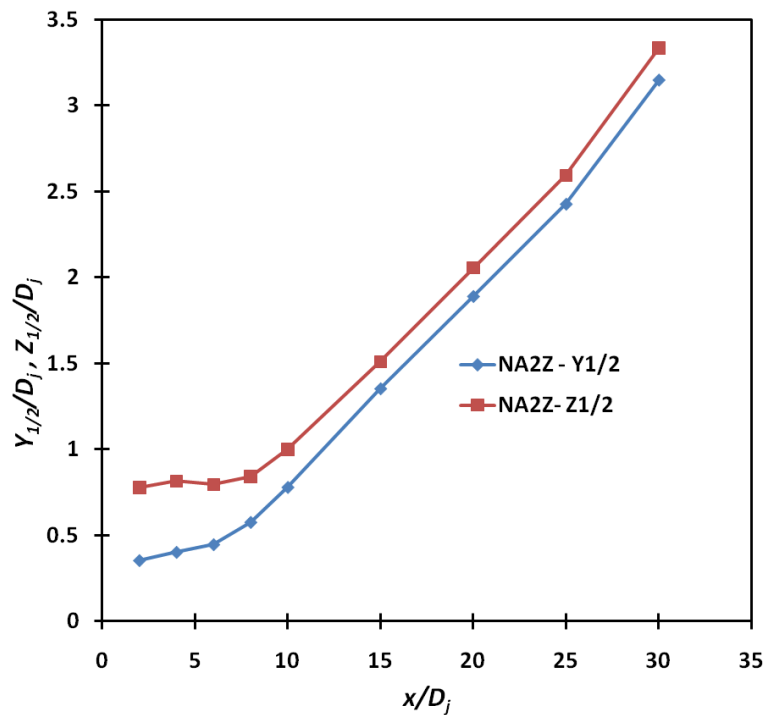
Fig. 7.42 Growth of rectangular jet with aspect ratio 2 in the *XY* and *XZ* planes
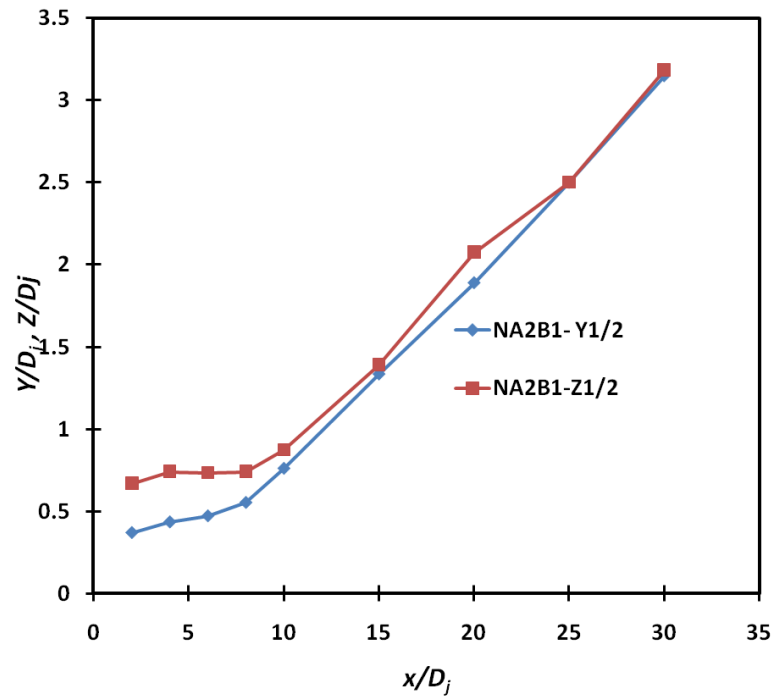
Fig. 7.43 Growth of rectangular short bevel jet with aspect ratio 2 in the *XY* and *XZ* planes
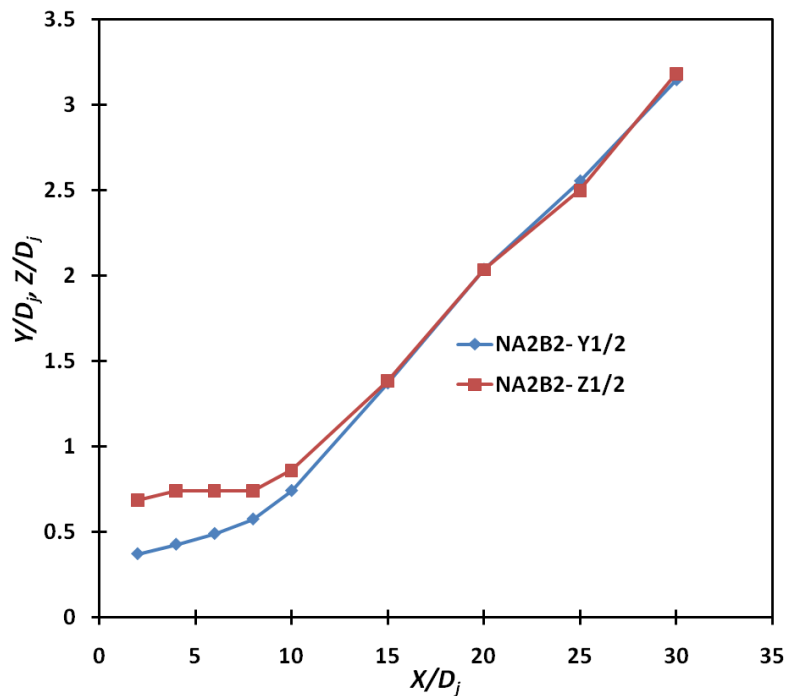
Fig. 7.44 Growth of rectangular long bevel jet with aspect ratio 2 in the *XY* and *XZ* planes
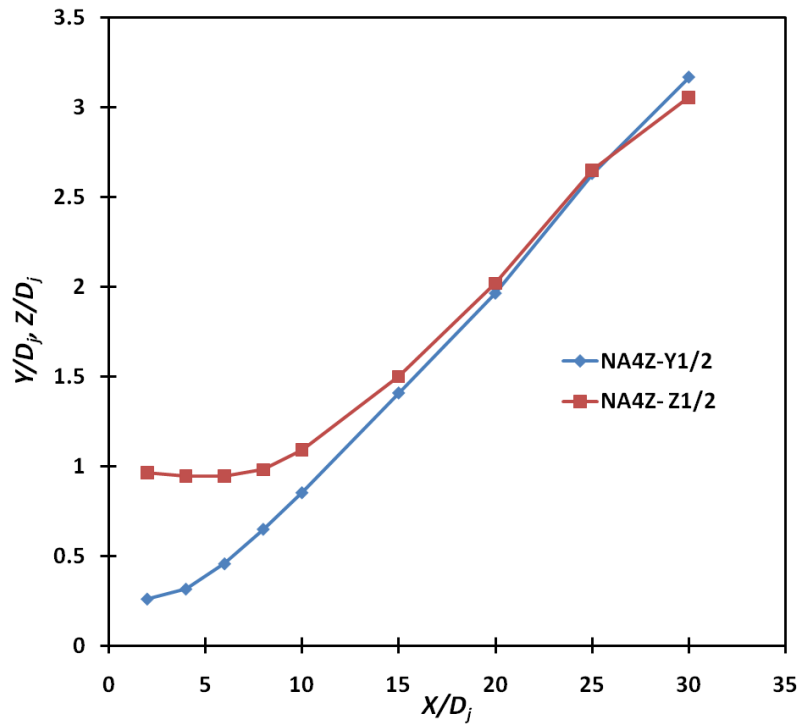
Fig. 7.45 Growth of rectangular jet with aspect ratio 4 in the *XY* and *XZ* planes
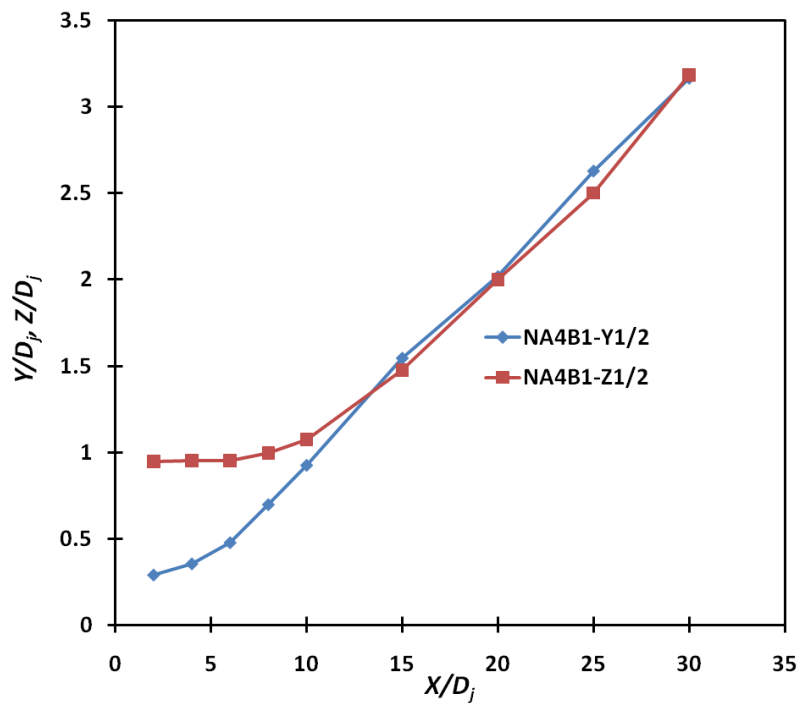
Fig. 7.46 Growth of rectangular short bevel jet with aspect ratio 4 in the *XY* and *XZ* planes
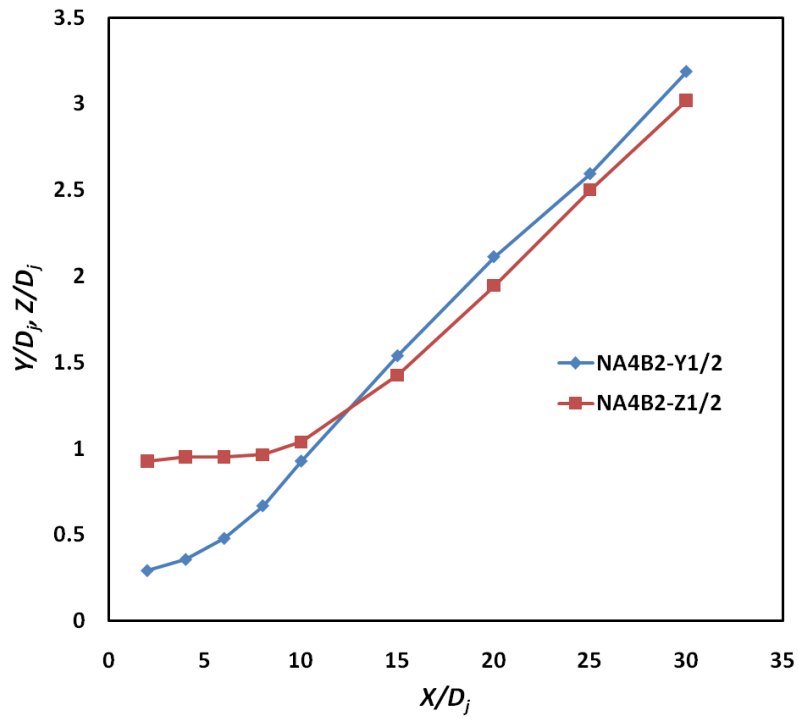
Fig. 7.47 Growth of rectangular long bevel jet with aspect ratio 4 in the *XY* and *XZ* planes
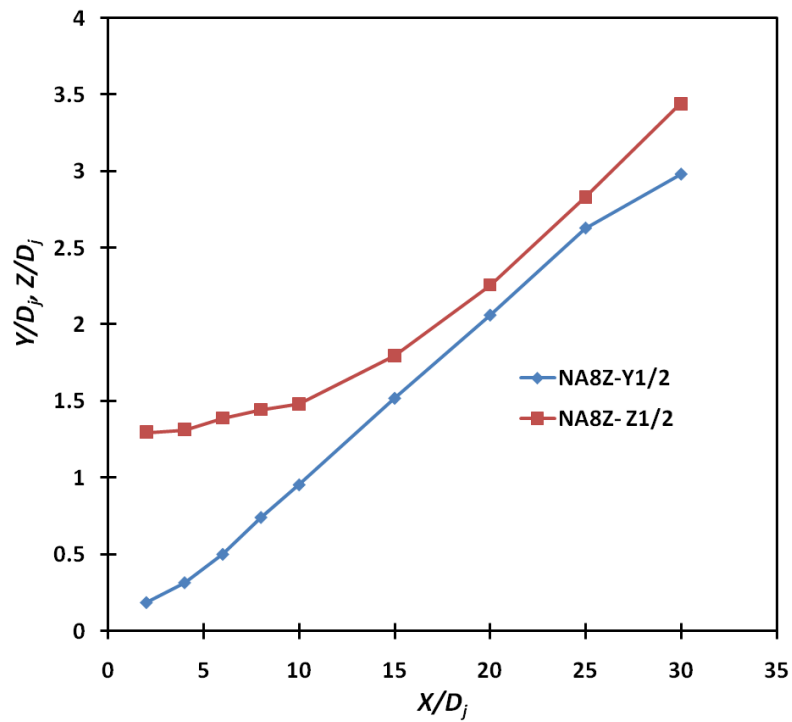
Fig. 7.48 Growth of rectangular jet with aspect ratio 8 in the *XY* and *XZ* planes
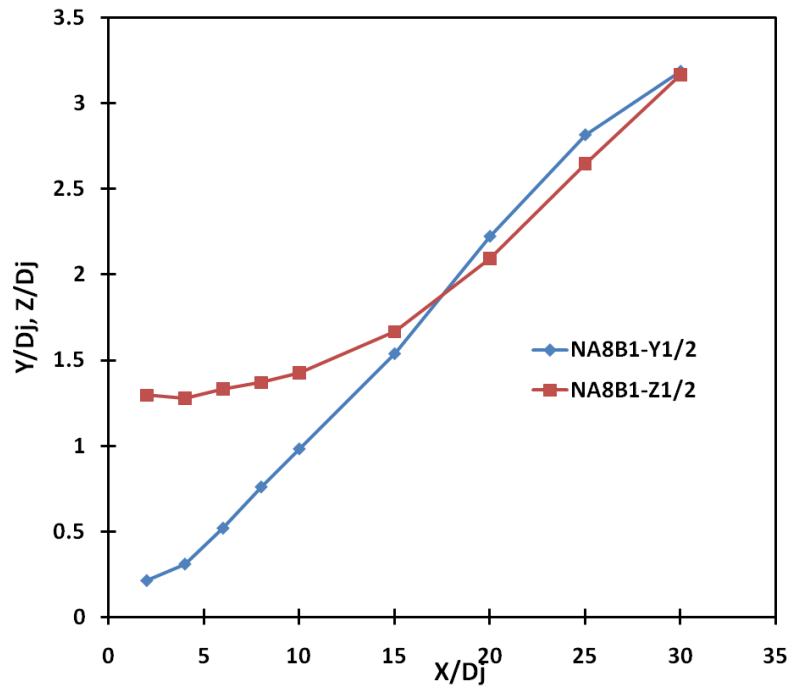
Fig. 7.49 Growth of rectangular short bevel jet with aspect ratio 8 in the *XY* and *XZ* planes
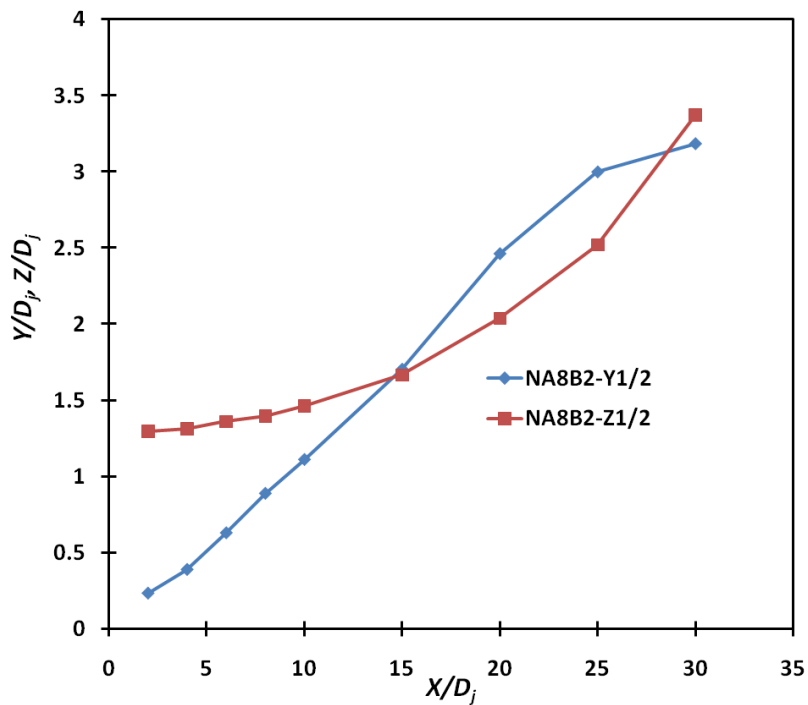
Fig. 7.50 Growth of rectangular long bevel jet with aspect ratio 8 in the *XY* and *XZ* planes

7.2.3 Exit Boundary Layer Characteristics

The condition of the boundary layer at the nozzle exit is an important parameter which has a significant impact on the jet noise. For a nozzle, this state can be characterized by the profiles of mean velocity (u) and turbulence intensity (u') along a radial line at the exit plane Zaman (1985, 2012). At high-subsonic conditions the ratio $\rho u/\rho_j U_j$ and $\rho u'/\rho_j U_j$ are considered for plotting mean velocity profile and turbulence intensity profile respectively where ρ is the density of flow and ρ_j is the density along centerline at nozzle exit. Both the profiles are plotted against $(y\text{-}y_w)/D_j$ where y is the radial distance and y_w is the location of the nozzle wall measured from the centre of nozzle exit. Radial profiles of mean velocity and turbulence intensity for the rectangular and rectangular bevel nozzles are shown in Figures 7.51 to 7.54. Even though the mean velocity profile appears to be nominally laminar, the turbulent intensity is seen to be higher, for all cases. This higher magnitude of turbulent intensity (i.e. greater than or equal to 0.05 times the exit velocity, U_j, along the core of the jet) makes the condition within exit boundary layer to be nominally turbulent. Nozzles with a nominally laminar boundary layer were found to be noisier compared to nozzles which were characterized by a nominally turbulent boundary layer state (Zaman, 1985). Figure 7.51 shows the comparison of nozzle exit boundary layer characteristics for plain rectangular nozzles with aspect ratio 2:1, 4:1 and 8:1. On increasing aspect ratio there is a transition of boundary layer towards turbulent region and the peak value of turbulent intensity within the boundary layer was also found to decrease. Therefore, nozzle with aspect ratio 8:1 will be quieter compared to the other two and this observation was consistent with the experiment results (Bridges, 2012). Figures 7.52 to 7. 54 show the nozzle exit boundary layer characteristics of beveled rectangular nozzles with the above aspect ratios and their comparison with the

respective plain rectangular nozzles. Rectangular bevel nozzle with shorter bevel length shows a sharp drop in the peak turbulence intensity in boundary layer for all the three aspect ratios making them quieter compared to the plain nozzle. However, increasing the bevel length causes a sudden jump in the turbulence intensity peak for nozzles of high aspect ratio (4:1 and 8:1) causing increase in jet noise and these results are also consistent with the available experimental data (Bridges, 2012) for rectangular bevel with aspect ratio 4:1 .
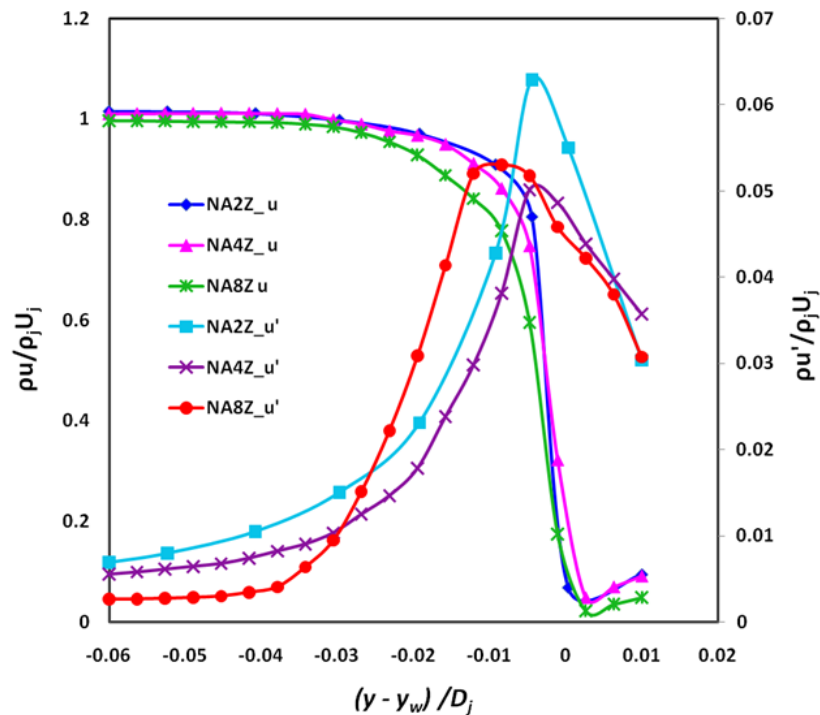
Fig. 7.51 Comparison of exit boundary layer profiles for plain rectangular nozzle with aspect ratio 2, 4 and 8
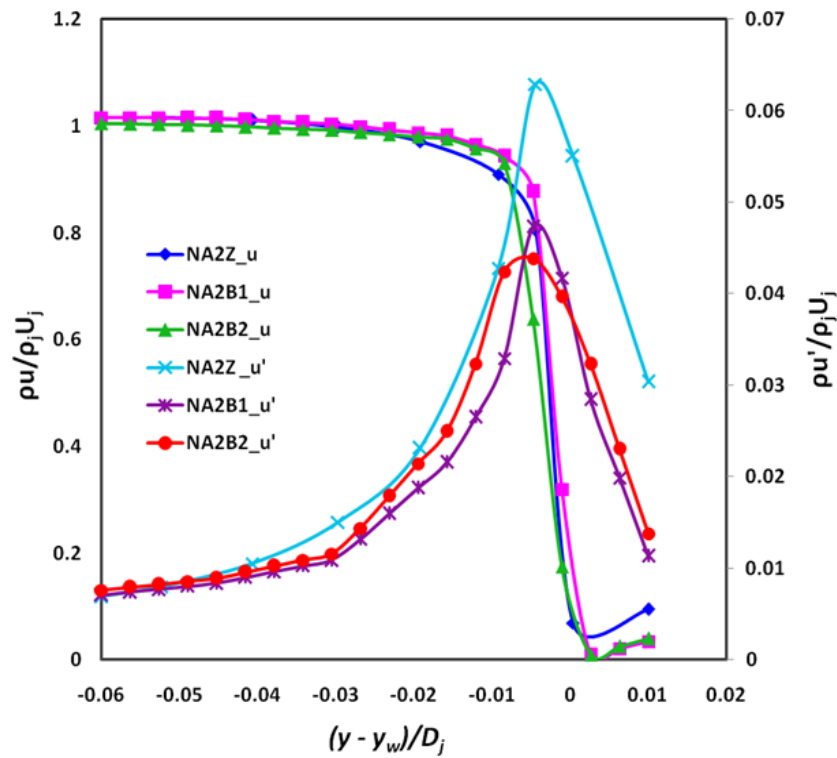
Fig. 7.52 Comparison of exit boundary layer profiles for plain rectangular and rectangular bevel nozzles with aspect ratio 2:1
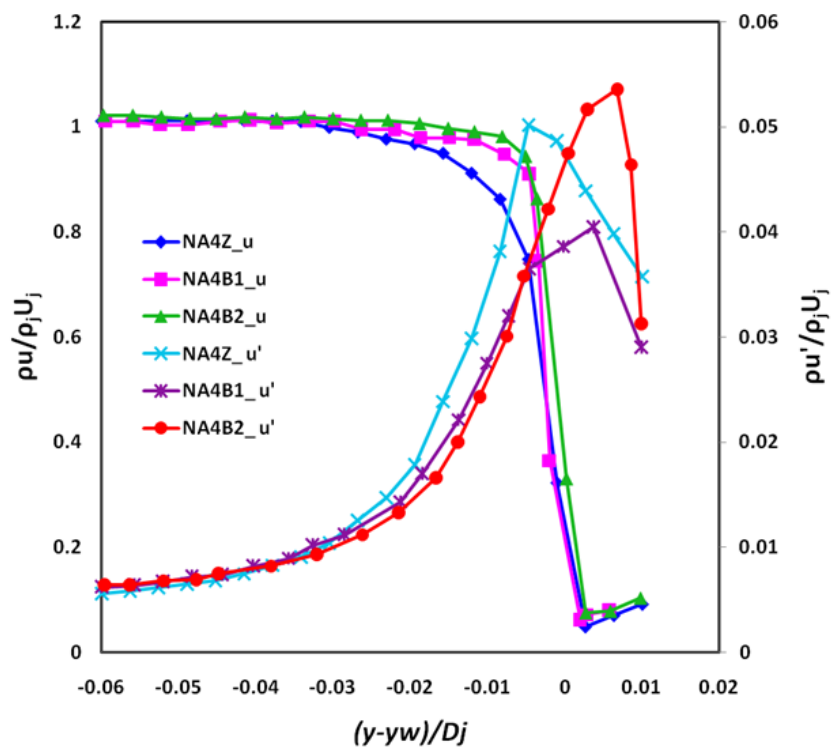
Fig. 7.53 Comparison of exit boundary layer profiles for plain rectangular and rectangular bevel nozzles with aspect ratio 4:1
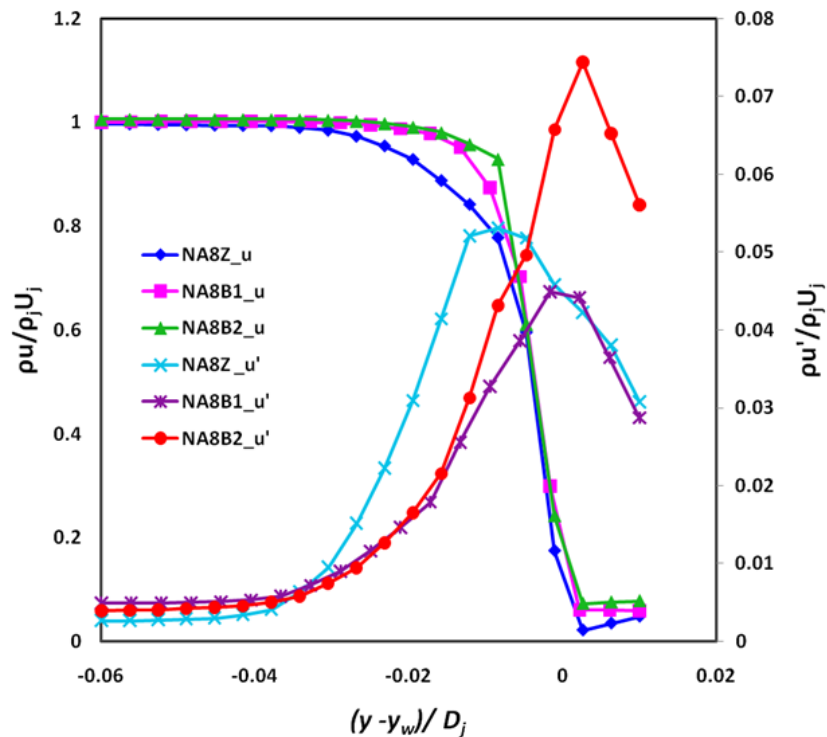
Fig. 7.54 Comparison of exit boundary layer profiles for plain rectangular and rectangular bevel nozzles with aspect ratio 8:1

7.2.4 Jet Core Turbulence

Velocity profile at the nozzle exit is drawn for the plain rectangular nozzle with the radial distance (y) nondimensionalised with the short side dimension (h) of the rectangular nozzle as shown in Figure 7.55. The corresponding turbulence intensity profiles are also shown in Figure 7.56. Shape factor for the three nozzles are estimated as 1.3 for nozzle with aspect ratios 2 or 4 and 1.6 for nozzle with aspect ratio 8. It is clear from the shape factor values and the turbulent intensity profiles that the boundary layer at the nozzle exit and the jet inflow condition is nominally turbulent in this region. However, the peak value of turbulence for high aspect ratio nozzle is approximately 5% and thereby the core turbulence and the radiated noise is less. In the numerical procedure, the finest grid is employed in the nozzle near wall region to resolve the turbulence boundary layer in a better manner.
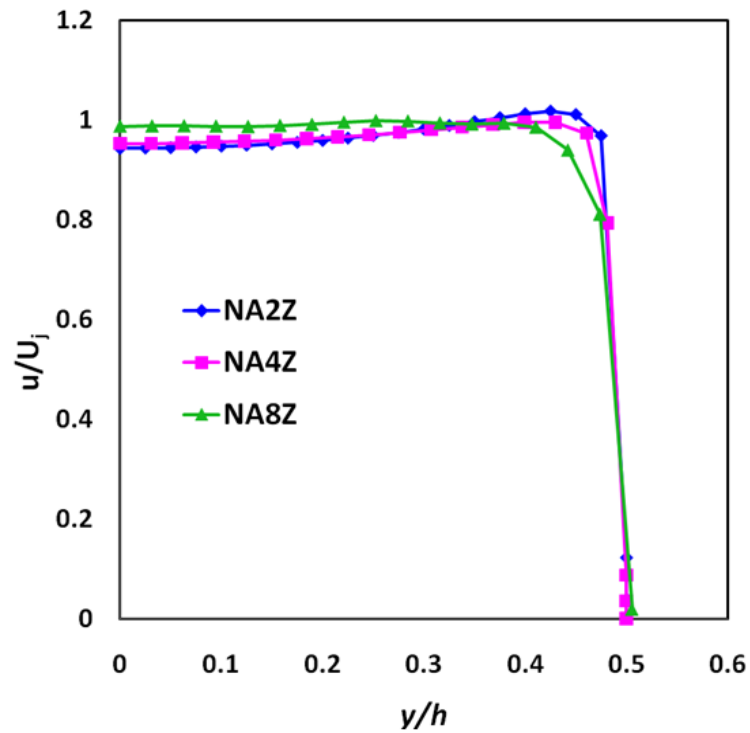
Fig. 7.55 Velocity profiles at nozzle exit for plain rectangular nozzles with aspect ratio 2, 4 and 8
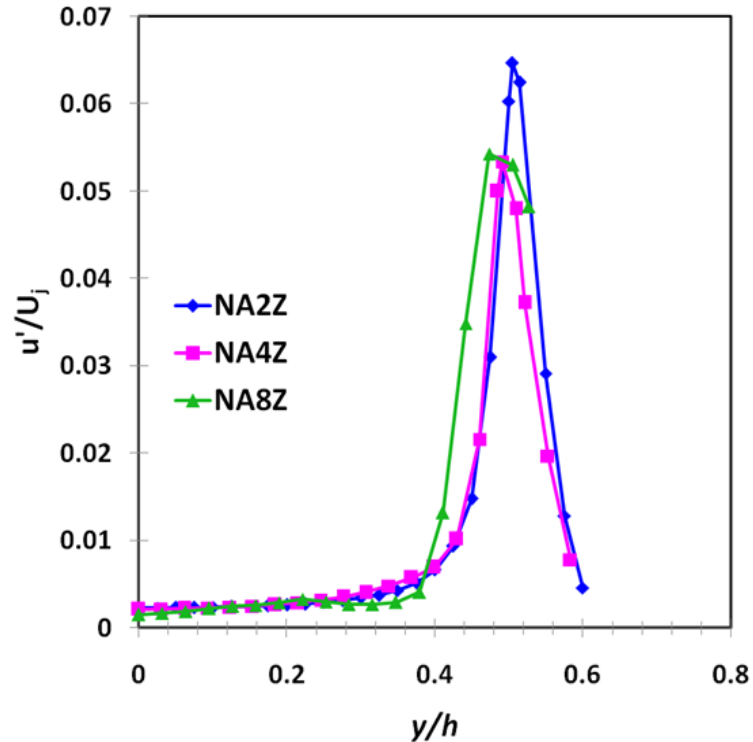
Fig. 7.56 Turbulent intensity at nozzle exit for plain rectangular nozzles with aspect ratio 2, 4 and 8

7.2.5   Comparison of Overall Sound Pressure Level

The overall sound pressure levels were calculated for plain and rectangular bevelled nozzles with an aspect ratio of 4 at different receiver locations from 30^0 to 150^0. The polar angles were measured from forward to the aft side as shown in Figure 5.12 (Chapter 5). The acoustic results in the polar plane (Fig. 7.57) illustrate that an acoustic benefit of approximately 3dB is achieved for the rectangular bevelled nozzle configurations.
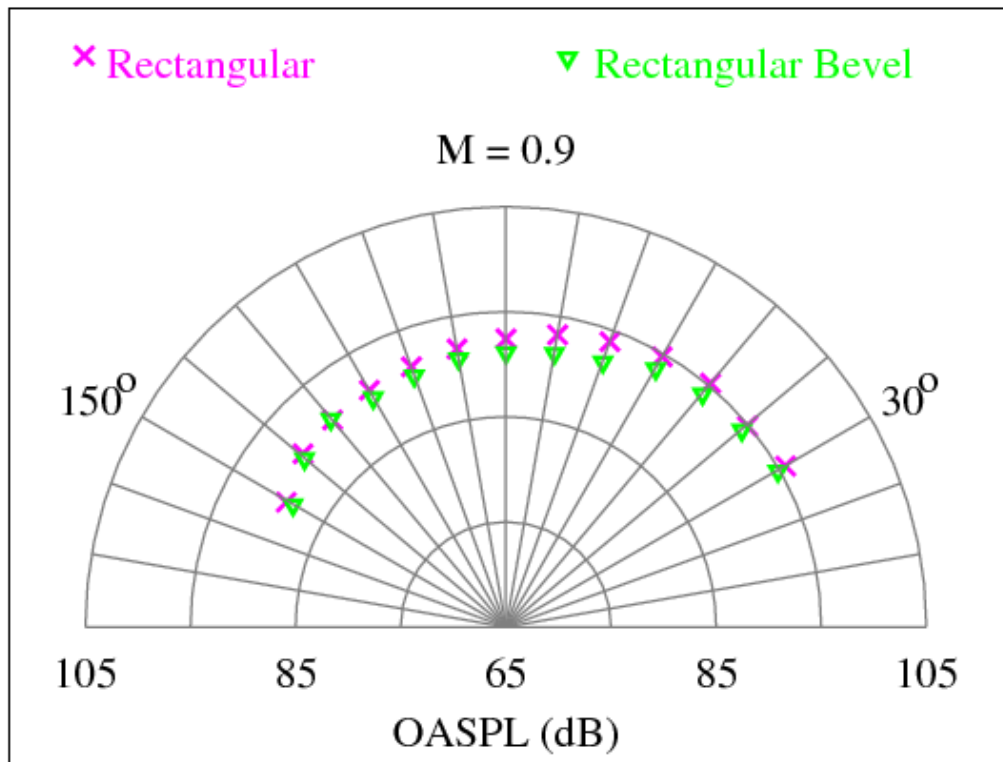
Fig. 7.57 Sound pressure levels for plain and rectangular bevelled nozzles (*AR=4*) at different polar angles

7.3   SUMMARY

A numerical analysis of unheated jets with Mach number 0.9 from rectangular nozzles with and without bevel for three aspect ratios and two bevel length ratios have been performed using RANS calculations employing SST k-ω turbulence model. The simulations were carried out on a grid with approximately 2.5 million cells. The

predictions seem to be reasonably good for the mean and variance of velocity when compared with available experimental data in the literature. The potential core length was predicted well for all configurations of plain and bevelled rectangular nozzles. It was observed that potential core gets shorter with nozzles of higher aspect ratios which signify enhanced spreading of jet. The positions of peak values of turbulence intensity together with the turbulence anisotropy were captured accurately. The bevelled nozzle considerably improves turbulent mixing and thereby modifies the turbulent characteristics of the jet. The impact of increased length of the bevel on enhanced turbulence characteristics is significant, especially with high aspect ratio nozzle. The overall sound pressure levels were calculated by acoustic analogy at various receiver locations. The acoustic predictions show that rectangular bevel nozzles have acoustic benefit when compared with plain round and rectangular nozzles.

CHAPTER - 8

CONCLUSIONS

A comprehensive computational investigation of compressible turbulent subsonic jets emanating from both round and rectangular nozzles with and without bevel has been carried out. The effect of bevelling of round nozzle on the mean and turbulent flow characteristics were analysed in detail. The dynamics of jet and its dependence on the rectangular nozzle parameters such as aspect ratio and bevel length ratio were also investigated. Acoustic benefits due to bevelling of the nozzle were evaluated for both round and rectangular nozzles.

8.1 DYNAMICS OF CIRCULAR JET ON BEVELLED GEOMETRY

Numerical investigation of Mach 0.75 jet from round and bevelled nozzles has been performed using RANS calculations with SST k-ω turbulence model. The simulations were carried out with a comparatively smaller grid size than that normally used for large eddy simulation. Potential core length and shear layer thickness were predicted well in both cases. It was observed that bevel nozzle had a shorter potential core with an enhanced spreading of jet when compared with a round nozzle. The evaluation of shear layer thickness of bevelled jets also confirmed better spreading rate. The virtual origin was determined and self similarity profiles were plotted. A lack of self similarity was observed for bevel nozzle close to the nozzle exit up to a downstream distance of four times the jet diameter. The predictions seem to be reasonably good for turbulent fluctuating quantities such as Reynolds stresses ($u'u'$, $v'v'$)and turbulence viscosity ($u'v'$) when compared with available experimental data in the literature. The peak values of turbulence intensity together with the turbulence

anisotropy were captured accurately. The bevelled nozzle considerably improves turbulent mixing and thereby modifies the turbulent characteristics of the jet. The radial profiles of velocities (both mean and fluctuating components), the contours of Mach number and turbulence intensity can provide better knowledge on the flow field that is essential for the calculation of jet noise. The Reynolds stresses which is supposed to be the major acoustic source for jet noise was found to have lower magnitude of $u_i'u_i'$ for a bevelled jet when compared to a circular jet. Moreover, a reduction of approximately 2 dB was predicted by the FW-H acoustic analogy for bevelled jets. The aerodynamic and aeroacoustic analysis give an insight into the alteration in turbulent characteristics of jets and in turn the noise benefit attained with comparatively lesser computational resources.

8.2 DYNAMICS OF RECTANGULAR JET ON BEVELLED GEOMETRY

A detailed numerical analysis of unheated jets with Mach number 0.9 emanating from rectangular nozzles and rectangular bevel nozzles with three aspect ratios, 2:1, 4:1, 8:1 and two bevel length ratios have been performed using RANS calculations with SST k-ω turbulence model. The predictions seem to be reasonably accurate for the mean and variance of velocity when compared with available experimental data in the literature. Potential core length was predicted well for all configurations of both plain rectangular nozzle and bevelled nozzles. It was found that potential core gets shorter with nozzles of higher aspect ratios which signify an enhanced spreading of jet. Even though the absolute value of peak turbulent intensity was under predicted in all cases, the position of peak values of turbulence intensity together with the turbulence anisotropy were captured accurately. The impact of

increasing the extension length of the bevel on turbulence characteristics enhancement was more significant in nozzle having larger aspect ratio (*AR=8*). The jet half width on *XY* and *XZ* planes were plotted and the spread rate for rectangular plain and bevel nozzles were calculated. It was observed that the jet spread rate along *XY* plane improved with increase in aspect and bevel length ratios. However, a considerable variation of spread rate with respect to the plain rectangular jet was recorded for the long bevel nozzle with aspect ratio 8:1. The jet entrainment and mixing were enhanced by bevelling the rectangular nozzle and also by increasing the bevel length ratio. This was indicated by the presence of multiple cross over points and shifting of axis switching closer to the nozzle exit in the jet half width plots. The condition of nozzle exit boundary layer was investigated and nominally turbulent boundary layer was found to be present for all cases of rectangular plain and bevel nozzles which make them quieter compared to other nozzles. However, in the case of rectangular bevel nozzle, a sudden jump observed in the turbulence intensity peak with increase in bevel length ratio may enhance the mixing noise. The jet core turbulence and boundary layer analysis were also performed for the three rectangular plain nozzles as well. The calculated shape factor indicates the jet core to be nominally turbulent and the decrease in turbulence peak with increase in aspect ratio signify a decrease in jet mixing noise.

One of the major application of bevelled nozzle lies in the reduction of noise as the axis of the jet is inclined to the nozzle axis. Hence the noise foot print towards the ground can be considerably reduced by properly aligning the nozzle. Acoustic calculations were also carried out using acoustic analogy and the overall sound pressure levels (OASPL) were calculated. The acoustic benefits attained for round and

rectangular nozzles with and without bevel were evaluated. The acoustic predictions confirm that bevel nozzles can achieve an average noise reduction of at least 3 dB when compared with baseline round and rectangular nozzles.

The flow and turbulent characteristics of the jet provides a data base for the computation of noise generation from jets. The determination of these quantities helps a great deal in the calculation of noise level from jets, which is presently a critical environmental concern. Computational aeroacoustic codes use the flow characteristics of jets for further acoustic calculations using Ffowcs Williams–Hawkings (FW-H) equations. Large Eddy Simulations (LES) or Direct Numerical Simulations (DNS) on finer grids can also be used to capture the peak values of turbulent characteristics of jets accurately. The acoustic calculations using LES yields better results if better grid resolutions are used. Although the acoustic predictions by DNS are accurate, the computational domain must enclose the receiver which poses limitation to the far field receivers. A powerful and faster computational facility (clusters) can only perform the LES/DNS calculations for far field acoustic receivers and predict noise within reasonable time. Experimental procedure for acquiring the aerodynamic and acoustic data from jets require high pressure storage receivers, compressors, settling chambers, pressure and velocity measuring instruments, microphones, data acquisition systems and anechoic chamber, which are highly expensive and the measurements are time consuming. Hence, innovative designs in the nozzle geometry intended to reduce the noise level from jets, can easily be evaluated using RANS model which was employed in the present work with lesser computational time and resources. The quick evaluation of designs will encourage the researchers to come up with novel concepts in nozzle profiles and geometries.

8.3   FUTURE WORK

The present analysis can be extended to complicated bevel geometries such as double bevelled nozzle, bevelled nozzle with tabs, bevelled chevron nozzle etc. The study on rectangular and bevel nozzles can also be extended to other rectangular nozzle configurations such as cut back nozzle, chevron nozzle etc., using Large Eddy Simulation (LES) or Direct Numerical Simulations (DNS) with the support of powerful computational resources. A reverse acoustic analysis can also be performed by making use of powerful computers to predict the Mach number of jet and its turbulent quantities, if the noise level generated by the jet alone (in decibels), is provided.

REFERENCES

Abdol-Hamid K.S., Pao S.P., Hunter C.A., Deere K.A., Massey S.J., Elmiligui A.(2006) PAB3D: Its history in the use of turbulence models in the simulation of jet and nozzle flows. *44th AIAA Aerospace Sciences Meeting and Exhibit,* 2006-489.

Abdol-Hamid K.S., Paul Pao, Steven J. Massey and AlaaElmiligui. (2004) Temperature Corrected Turbulence Model for High Temperature Jet Flow. *J. Fluids Eng,* 126(5), 844-850

Alnahhal M. and Panidis Th.(2009)Effect of sidewalls on rectangular jets. *Experimental Thermal and Fluid Science,* (33) 5,838-851.

AlnahhalM., Cavo A., RomeosA., Perrakis K., and Panidis Th. (2011) Experimental investigation of the effect of endplates and sidewalls on the near field development of a smooth contraction rectangular jet. *European Journal of Mechanics -B/Fluids*, 30,451-465.

Andersson N., Eriksson L.E. and Davidson L. (2003) Large-Eddy Simulation of a Mach 0.75 Jet. *AIAA*-2003-3312.

Andersson N., Eriksson L.E. and Davidson L. (2004) A Study of Mach 0.75 Jets and Their Radiated Sound Using Large-Eddy Simulation. *AIAA*-2004-3024.

Andersson N., Eriksson L.E. and Davidson L. (2005) Investigation of an isothermal Mach 0.75 jet and its radiated sound using large-eddy simulation and Kirchhoff surface integration. *International Journal of Heat and Fluid Flow*, 26(3), 393–410.

Arakeri V.H., Krothapalli A., Siddavaram V., Alkislar M.B. and Lourenco L.M. (2003) On the use of micro jets to suppress turbulence in a mach 0.9 axisymmetric jet. *Journal of Fluid Mechanics*, 490, 75–98.

Behrouzi P. and McGuirk J.J. (2015) Under expanded Jet Development from a Rectangular Nozzle with Aft-Deck. *AIAA Journal*, 53 (5), 1287 - 1298.

Bodony D.J and Lele S.K. (2004) Jet Noise Prediction of Cold and Hot Subsonic Jets Using Large-eddy Simulation. *10th AIAA/CEAS Aeroacoustics Conference* 2004, 2488-2504.

Bodony D.J and Lele S.K.(2005) On Using Large Eddy Simulation for the prediction of noise from cold and heated turbulent jets. *Physics of Fluids*17, 085-103.

Boersma B. J., Brethouwer G., Nieuwstadt F. T. M. (1998) A numerical investigation on the effect of the inflow conditions on the self-similar region of a round jet. *Physics of Fluids,*10, 899–909.

Boersma B. J. &Lele S. K.(1999)Large eddy simulation of compressible turbulent jets. *Center for Turbulence Research, Annual Research Briefs 1999*, 365-377.

Bogey C. and Bailly C. (2005) Effects of the inflow conditions on flow and noise. *AIAA Journal*, 43(5), 1000-1007.

Bogey C., Bailly C. and Juve D. (2001)Flow Field and Sound Radiation of a Mach 0.9 Jet Computed by LES.*RTO AVT Symposium on Ageing Mechanisms and Control: Part A – Developments in Computational Aero- and Hydro-Acoustics,* Manchester, UK, RTO-MP-079(I).

Bogey C., Bailly C. and Juve D. (2003) Noise investigation of a high subsonic, moderate Reynolds number jet using a compressible large eddy simulation. *Theoretical and Computational Fluid Dynamics*, 16(4), 273–297.

Bogey C., Barre S., Fleury V., Bailly C. and Juve D.(2007) Experimental study of the spectral properties of near-field and far-field jet noise. *International Journal of Aeroacoustics* , 6(2), 73 − 92.

Bridges J. (2012)Acoustic Measurements of Rectangular Nozzles with Bevel. *AIAA Paper,*2012-2252.

Bridges J.(2014)Noise from Aft Deck Exhaust Nozzles -Differences in Experimental Embodiments. *AIAA Paper*, 2014-0876.

Bridges J.(2015)Noise Measurements Of High Aspect Ratio Distributed Exhaust Systems. *AIAA Aviation 2015 Conference.*

Bridges J. and Wernet, M. P. (2015) Turbulence measurements of rectangular nozzles with bevel. *53rd AIAA Aerospace Sciences Meeting*, AIAA 2015-0228.

Carazzo G., Kaminski E. and Tait S. (2006) The route of self similarity in turbulent jets and plumes. *Journal of Fluid Mechanics*, 547, 137–148.

DeBonis J.R. (2006) Progress Towards Large-Eddy Simulations for Prediction of Realistic Nozzle Systems. *AIAA* 2006-487.

Deo R. C., Nathan G. J. and. Mi J. (2007) The influence of nozzle aspect ratio on a plane jet. *Experimental Thermal and Fluid Science*, 31, 825-838.

Deo R. C., Mi J., and Nathan G. J. (2008) The influence of Reynolds number on a plane jet. *Phys. Fluids*, (20), 075-108.

Di Francescantonio P.(1997) A new boundary integral formulation for the prediction of sound radiation. *Journal of Sound and Vibration*, 202(4), 491–509.

Ffowcs Williams J.E. and Hawkings D.L.(1969) Sound generated by turbulence and surfaces in arbitrary motion. *Proceedings of the Royal Society of London*, A 264, 321–342.

Frate F. C. and Bridges J.(2011) Extensible Rectangular Nozzle Model System. *AIAA Paper,* 2011-0975.

Freund J. B. (2001) Noise sources in a low Reynolds number turbulent jet at Mach 0.9.*Journal of Fluid Mechanics*, 438, 277–305.

George W. (2000) Introduction to turbulence. *Internal report. Dept. of Thermo and Fluid Dynamics,* Chalmers University of Technology, G¨oteborg, Sweden.

Georgiadis N. J., DeBonis J. R.(2006) Navier–Stokes analysis methods for turbulent jet flows with application to aircraft exhaust nozzles. *Progress in Aerospace Sciences*, 42 (2006), 377–418.

Gurunath K., Maniiarasan P., SenthilkumarS.andArulselvan K.(2014) Investigation on Low Speed Rectangular Jet. *The International Journal of Engineering and Science* 3 (01), 60-65.

Gutmark E., Schadow K.C., Parr T. P., Hanson-Parr D. M., Wilson K. J.(1989) Noncircular jets in combustion systems. *Exp Fluids*, 7, 248—258.

Gutmark E.J. and Grinstein E.F.(1999) Flow Control with Noncircular Jets. *Annu. Rev. Fluid Mech.,* 1999, 31, 239–72.

Ho C. M., Gutmark E. (1987) Vortex induction and mass entrainment in a small-aspect-ratio elliptic jet. *J Fluid Mechanics,* 179, 383—405.

Hunter C.A. and R. H. Thomas.(2003) Development of a jet noise prediction method for installed jet configurations. *AIAA Paper* 2003-3169.

Hussain F. and Husain H. S. (1989) Elliptic jets. Part 1. Characteristics of unexcited and excited jets. *J Fluid Mechanics*, 208, 257—320.

J. B. Freund, S. K. Lele, and P. Moin. (2000) Direct numerical simulation of a Mach 1.92 turbulent jet and its sound field .*AIAA Journal*, 38(11), 2023-2031.

J. L. Stromberg, D. K. McLaughlin, and T. R. Troutt. (1980) Flow field and acoustic properties of a Mach number 0.9 jet at a low Reynolds number. *Journal of Sound and Vibration*, 72(2),159-176.

Jordan P., Gervais Y., Valiére J.C. and Foulon H. (2002) Final results from single point measurements. *Project Deliverable D3.4, JEAN – EU 5th Framework Programme*,G4RD-CT2000-00313, Laboratoired'EtudeAeródynamiques, Poitiers.

Jordan P. and Gervais Y. (2003) Modeling Self and Shear Noise Mechanisms in Anisotropic Turbulence. *The 9th AIAA/CEAS Aeroacoustics Conference*, No. 8743 in AIAA 2003, Hilton Head, South Carolina.

Karabasov S. A., Afsar M. Z., Hynes T. P., Dowling A. P., McMullan W. A., Pokora C. D., Page G. J., and McGuirk J. J. (2010) Jet Noise: Acoustic Analogy informed by Large Eddy Simulation. *AIAA Journal*, 48(7), 1312-1325.

Khavaran A., Krejsa E. A., and Kim C. M. (1994) Computation of supersonic jet mixing noise for an axisymmetric convergent-divergent nozzle. *Journal of Aircraft*, 31(3), 603-609.

Kim W.H. and Park T.S.(2013) Effects of Noncircular Inlet on the Flow Structures in Turbulent Jets. *Journal of Applied Mathematics and Physics*, 1, 37-42.

Krothapalli A.(1980) Development and Structure of a Rectangular Jet in a Multiple Jet Configuration. *AIAA Journal,* 18(8), 945-950.

Krothapalli A., Baganoff D. and Karamcheti K. (1981) On the mixing of rectangular jet. *J. Fluid Mech*, 107, 201–220.

Kumaraswamy T., Santhiya C., Gupta M.S.(2015) Computational Analysis of Supersonic Jets from Rectangular Nozzles. *IJESMR*,2(9),5-19.

Lew P., Blaisdell G. A. and Lyrintzis A. S. (2005)Recent Progress of Hot Jet Aeroacoustics using 3-D Large-Eddy Simulation. *AIAA*-2005-3084.

Lighthill M. J.(1952) On sound generated aerodynamically, I. General Theory. *Proceedings of the Royal Society of London*, A211, 564–587.

Lighthill M. J. (1954) On sound generated aerodynamically II. Turbulence as a source of sound. *Proceedings of the Royal Society of London*, A222. 1–32.

Lyrintzis A. (1994)Review: The use of Kirchhoff's method in computational aeroacoustics. *ASME: Journal of Fluids Engineering,* 116, 665-676.

Lyrintzis A.(2003) Surface integral methods in computational aeroacoustics – from the (CFD) near-field to the (acoustic) far-field. *Int J Aeroacoustics*, 2(2), 95–128.

Mankbadi R. R., Hayder M. E., and Povinelli L. A.(1994) Structure of supersonic jet flow and its radiated sound. *AIAA Journal*, 32(5), 897-906

Menter F. R. (1993) Zonal Two Equation k-ω Turbulence Models for Aerodynamic Flows. *AIAA Paper,* 93-2906.

Menter F. R. (1994)Two-Equation Eddy-Viscosity Turbulence Models for Engineering Applications. *AIAA Journal*, 32(8), 1598-1605.

Mi J., Deo R. C. and Nathan G. J. (2005) Characterization of turbulent jets from high-aspect-ratio rectangular nozzles. *Physics of Fluids* 17(6), 068-102.

Mi J., Nathan G. J. and Luxton R. E. (2000) Centerline mixing characteristics of jets from nine differently shaped nozzles. *Exp. Fluids,* 28, 93–94.

Mi J., Kalt P. and Nathan G.J.(2004)Mixing Characteristics of a Notched-Rectangular Jet and a Circular Jet. *Proceedings of 15th Australasian Fluid Mechanics Conference,* Sydney, Australia- 2004.

Miller R. S., Madnia C. K., Givi P.(1995) Numerical simulation of non-circular jets. *Computers & Fluids*, 24, 1—25.

Moore C. J. (1977) The role of shear-layer instability waves in jet exhaust noise. *Journal of Fluid Mechanics*, 80, 321–367.

Moore P., Slot H. J and Boersma B. (2007) Simulation and measurement of flow generated noise. *Journal of Computational Physics*, 224, 449–463.

Nallasamy M.(1999) Survey of Turbulence Models for the Computation of Turbulent Jet Flow and Noise. *NASA/CR*—1999-206592.

Nan Chen and Huidan Yu (2014) Mechanism of axis switching in low aspect-ratio rectangular jets, *Computers & Mathematics with applications*, 67(2), 437-444.

Paliyath U. and Morris P. J. (2005) Prediction of Jet Noise From Circular Beveled Nozzles.*26th AIAA Aeroacoustics Conference*, AIAA 2005-3096.

Paul Pao S.and Abdol-Hamid K. S. (1996) Numerical Simulation of Jet aerodynamics Using the Three-Dimensional Navier-Stokes Code PAB3D. *NASA Technical Paper* 3596 (1996).

Pope S. B. (2002) Turbulent Flows, Cambridge University Press, UK.

Quinn W. R.(1989) On mixing in an elliptic turbulent free jet. *Physics of Fluids*, A1, 1716—1722.

Quinn W. R. (1992) Turbulent free jet flows issuing from sharp-edged rectangular slots: The influence of slot aspect ratio. *Experimental Thermal and Fluid Science*, 5,203–215.

Rembold B. and Kleiser L. (2004) Noise Prediction of a Rectangular Jet Using Large-Eddy Simulation. *AIAA Journal*, 42(9), 1823-1831.

Rice E.J. and Raman G. (1993) Supersonic Jets From Bevelled Rectangular Nozzles. *Winter Annual Meeting of the ASME Symposium on Flow Acoustics Interaction and Fluid Control.*

Sfeir A.A. (1979) Investigation of Three-Dimensional Turbulent Rectangular Jets. *AIAA Journal,* 17(10), 1055–1060.

Shur M. L., Spalart P. R., Strelets M. K. and Garbaruk A.V.(2007) Analysis of jet-noise-reduction concepts by large-eddy simulation. *International Journal of Aeroacoustics*, 6(3), 243–285.

Sundararaj M. and Elangovan S. (2013) Computational Analysis of Mixing Characteristics of Jets from Rectangular Nozzle with Internal Grooves. *Indian Journal of Science and Technology*, 6(5), 4543-4548.

Suresh P. R., Srinivasan K., Sundararajan T., and Das K. (2008) Reynolds number dependant of a plane jet development in the transition regime. *Phy. Fluids*, 20, 044105.

Tam C. (1998) Jet noise: Since 1952. *Theoret. Comput. Fluid Dynamics*, 10, 393-405.

Tide P.S. and Babu V. (2009*a*) Improved noise predictions from subsonic jets at mach 0.75 using URANS calculations. *Progress in Computational Fluid Dynamics*, 9(8), 460–474.

Tide P.S. and Babu V. (2009*b*) Numerical predictions of noise due to subsonic jets from nozzles with and without chevrons. *Applied Acoustics*, 70(2), 321–332.

Tide P.S. and Srinivasan K. (2009*c*) Aeroacoustic Studies of Beveled and Asymmetric-Chevron Nozzles. *American Institute of Aeronautics and Astronautics Paper*, AIAA-2009-3404.

Tsuchiya Y., Horikoshi C.(1986) On the Spread of Rectangular Jets. *Experiments in Fluids*, 4, 197-204.

Tucker P. (2008) The LES model's role in jet noise. *Progress in Aerospace Sciences*, 44, 427–436.

Uchiyama T., Kobayashi M., Iio S. and Ikeda T.(2013) Direct Numerical Simulation of a Jet Issuing from Rectangular Nozzle by the Vortex in Cell Method. *Open Journal of Fluid Dynamics*, 3, 321-330.

Uzun A., Blaisdell G.A. and Lyrintzis A.S. (2003) 3-D Large Eddy Simulation for Jet Aeroacoustics. *AIAA*-2003-3322.

Uzun A. and Hussaini M.Y. (2010) High-fidelity numerical simulations of a round nozzle jet. *16th AIAA/CEAS Aero Acoustics Conference, AIAA 2010-4016*.

Versteeg H., and Malalasekra W. (1995) An Introduction to Computational Fluid Dynamics: The Finite Volume Method, Second Edition, *Pearson Education Ltd*.

Viswanathan K. and Czech M. J. (2011) Adaptation of Beveled Nozzle for High Speed Jet Noise Reduction. *AIAA Journal,* 49(5), 932-944.

Viswanathan K., Shur M., Strelets M. and Spalart P. R. (2005) Numerical prediction of noise from round and beveled nozzles. *Euromech Colloquium 467: Turbulent Flow and Noise Generation*.

Viswanathan K., Shur M., Strelets M. and Spalart P.R. (2008) Flow and noise predictions for single and dual-stream beveled nozzles. *AIAA Journal*, 46(3), 601–626.

Viswanathan K., Spalart P.R. and Czech M.J. (2012) Tailored nozzles for jet plume control and noise reduction. *AIAA Journal*, 50(10), 2115–2134.

Von Glahn U.H. (1989) Rectangular Nozzle Plume Velocity Modeling for Use in Jet Noise Prediction. *AIAA*-89-2357.

Vouros A.P., Panidis T., Pollard A., and Schwab R.R. (2014) Near field vorticity distributions from a sharp-edged rectangular jet. *International Journal of Heat and Fluid Flow*, 51(2015), 383–394.

White F. M. (1994) Fluid Mechanics. International edition, 3rd edition, McGraw-Hill companies, Inc. Printed in the United States of America.

Zaman K. B. M. Q. (1985) Effect of Initial Condition on Subsonic Jet Noise. *AIAA Journal*, 23(9) 1985, 1370–1373.

Zaman K. B. M. Q. (1996*a*) Spreading Characteristics and Thrust of Jets From Asymmetric Nozzles. *NASA Technical Memorandum 107132*, *AIAA*-96-0200.

Zaman K. B. M. Q. (1996*b*) Axis switching and spreading of an asymmetric jet: the role of coherent structure dynamics. *J. Fluid Mechanics*, 316, 1-27.

Zaman K. B. M. Q. (2012) Effect of Initial Boundary-Layer State on Subsonic Jet Noise. *AIAA Journal*, 50(8), 1784-1795.

LIST OF PUBLICATIONS

International Journals:

1. M. Sandhya, P. S. Tide "Computational analysis of subsonic jets from round and beveled nozzles", *Int. J. of Energy Technology and Policy*, Inderscience Publishers, 2017 Vol.13, No.1, pp.141 – 157.

2. M. Sandhya, P. S. Tide "Computational Analysis of Subsonic Jets from Rectangular Nozzles with and without Bevel", *Journal of Spacecraft and Rockets*, American Institute of Aeronautics and Astronautics (**AIAA**), 2018 Vol. 55, No. 3, pp.749-763.

International Conferences:

1. "Performance of Refractory Metal Composite as Nozzle Throat Material and Recent Trends in Fabrication", SandhyaM., MubarakA.K., TideP.S., Second International Conference on Materials for the Future ICMF 2011.

2. "Review on the application of ablative materials for solid rocket motor nozzles and their Fabrication", Mubarak A. K., Sandhya M., Tide P. S., Second International Conference on Materials for the Future ICMF 2011, pp. 205-209.

3. "Numerical Investigation of Flow characteristics of subsonic jets from round and beveled nozzles", Sandhya M., Tide P. S., International conference on Energy, Environment, Materials and Safety ICEEMS 2014, pp. 423-429.

CURRICULUM VITAE

1. Name   :   **SANDHYA M.**

2. Date of Birth   :   18.02.1974

3. <u>Educational Qualifications</u>

1995 Bachelor of Technology (B Tech)

Institution	:	T.K.M College of Engineering, Kollam, Kerala. University of Kerala
Specialization	:	Mechanical Engineering

2006 Master of Technology (M Tech)

Institution	:	National Institute of Technology, Calicut, Kerala
Specialization	:	Energy Management

Doctor of Philosophy (PhD)

Institution	:	Cochin University of Science and Technology Kochi, Kerala
Registration Date	:	12.10.2010